

Distribution Agreement

In presenting this thesis or dissertation as a partial fulfillment of the requirements for an advanced degree from Emory University, I hereby grant to Emory University and its agents the non-exclusive license to archive, make accessible, and display my thesis or dissertation in whole or in part in all forms of media, now or hereafter known, including display on the world wide web. I understand that I may select some access restrictions as part of the online submission of this thesis or dissertation. I retain all ownership rights to the copyright of the thesis or dissertation. I also retain the right to use in future works (such as articles or books) all or part of this thesis or dissertation.

Signature:

Christopher George Sinon

Date

Abnormal Recovery from Anesthesia: A Marker of Early Cognitive Dysfunction in Rodent
Models of Disease

By

Christopher George Sinon
Doctor of Philosophy

Graduate Division of Biological and Biomedical Science
Neuroscience

Paul S. García, MD, PhD
Advisor

Ihab M. Hajjar, MD, MS
Advisor

Jeffrey H. Boatright, PhD
Committee Member

Machelle T. Pardue, PhD
Committee Member

Nigel P. Pedersen, MD
Committee Member

Malú G. Tansey, PhD
Committee Member

Accepted:

Lisa A. Tedesco, Ph.D.
Dean of the James T. Laney School of Graduate Studies

Date

Abnormal Recovery from Anesthesia: A Marker of Early Cognitive Dysfunction in Rodent
Models of Disease

By

Christopher George Sinon
B.S., University of Illinois at Chicago, 2012

Advisor: Paul S. García, MD, PhD
Ihab M. Hajjar, MD, MS

An abstract of
A dissertation submitted to the Faculty of the
James T. Laney School of Graduate Studies of Emory University
in partial fulfillment of the requirements for the degree of
Doctor of Philosophy
Graduate Division of Biological and Biomedical Science
Neuroscience
2019

Abstract

Abnormal Recovery from Anesthesia: A Marker of Early Cognitive Dysfunction in Rodent Models of Disease

By Christopher George Sinon

The widespread adoption of general anesthetics in the 19th century led to rapid advancements in surgical practice. However, alongside this growth there has been concern about the appearance of cognitive disturbances in the postoperative period. Large clinical research projects have begun to elucidate some of the risk factors that can predispose patients to postoperative cognitive impairments and correlated the risk for later cognitive impairments with the appearance of earlier postoperative cognitive disturbances. Unfortunately, most published work on abnormal recoveries from anesthesia exists in the form of individual case studies or uses methods that are not currently practical for translation to everyday clinical use. Preclinical models represent a promising approach towards investigating biological underpinnings of abnormal emergence and recovery. This thesis contains our work characterizing the immediate emergence and recovery from anesthesia in preclinical models of conditions known to be risk factors for developing postoperative cognitive impairments. We characterized the behavioral phenotype and neuropathology of a transgenic rat model of Alzheimer's Disease (AD). At 12-months of age there is neuropathology consistent with the early phase of AD, but with no observed behavioral differences between wild type and transgenic rats. We compared the latency to display emergence and recovery behaviors following isoflurane exposure in 12-month wild type and transgenic rats. Recovery from isoflurane is significantly delayed in transgenic AD rats when compared to wild type. Despite this, transgenic AD rats are not more sensitive to anesthetic drugs as measured by EEG, suggesting that delayed recovery may be due to exacerbation of AD disease pathology. Additionally, we investigated how emergence and recovery behaviors are altered in a type 2 diabetes rat model. We found that these rats do not differ from wild type rats in their emergence or recovery, but prior treadmill exercise hastened recovery from anesthesia in both groups. Overall, we demonstrate the ability to identify changes in the behavioral response to anesthetics in the recovery from general anesthesia due to disease progression and prehabilitative interventions. Our results highlight the need to treat the emergence and recovery from anesthesia as distinct clinical endpoints.

Abnormal Recovery from Anesthesia: A Marker of Early Cognitive Dysfunction in Rodent
Models of Disease

By

Christopher George Sinon
B.S., University of Illinois at Chicago, 2012

Advisor: Paul S. García, MD, PhD
Ihab M. Hajjar, MD, MS

A dissertation submitted to the Faculty of the
James T. Laney School of Graduate Studies of Emory University
in partial fulfillment of the requirements for the degree of
Doctor of Philosophy
Graduate Division of Biological and Biomedical Science
Neuroscience
2019

Acknowledgements

To Paul, I have so much respect your drive and aspiration. Your creativity, empathy and understanding make you a terrific mentor and I'm thankful for the opportunity to have learned from you. I wish you good luck and continued success in New York.

To Ihab and Roy, thank you both for your support, your knowledge and the opportunity to work on a fantastic project. I've enjoyed our discussions and collaboration over the years.

To Mabelle, Jeff, Malu and Nigel, thank you for your expertise and guidance over the years. I really enjoyed our conversations, both together and individually. I appreciate that your feedback has always been fair, constructive and forward-thinking. Along with Ihab and Paul, this was a really great group and I'm lucky to have had all of you.

To the members of the García lab, especially Jon and Matthias, thank you for making the lab such a great place to spend my last 5 years. I'll miss our time together and hope the best for all of you in the future.

To Jing and Adam, thank you for joining me in the long hours and early mornings. This wouldn't have been possible without being able to work with responsible, patient and diligent scientists such as yourselves.

To Nick, Austin, Peter and Daniel, thank you for all of your help in the completion of these experiments. I am lucky to have worked with enthusiastic, hard-working, smart and reliable undergraduates during my time at Emory. You will all go on to great things and I hope any advice I gave you will be half as helpful as the time you gave me.

To the Emory Neuroscience Graduate Program, I'm still so grateful for being offered a spot in this program. I've met some lifelong friends, terrific mentors and fallen in love while at Emory. Thanks for keeping science fun and approachable.

To my family and friends, I couldn't have started this without your encouragement and I never would have finished without your support. Mom, Dad, David, Nick, Meghan, Greg, Matt & Helen, I love you all so much. Sorry that I moved to Atlanta but the weather really is so much better here.

To Arielle, I love you and this was all worth it if only to meet you. And to Alfie, thanks for taking me on walks when I was writing this.

Table of Contents

LIST OF FIGURES AND TABLES

LIST OF ABBREVIATIONS

CHAPTER 1 - GENERAL INTRODUCTION.....	1
1.1 HISTORY OF ANESTHESIA.....	3
1.1.1 <i>Early Anesthetics</i>	4
1.1.2 <i>The Beginnings of Modern Anesthesia</i>	6
1.1.3 <i>Improvements in Anesthesiology</i>	7
1.2 HISTORICAL PROBLEMS IN THE STUDY OF CONSCIOUSNESS.....	8
1.2.1 <i>The Hard Problem of Consciousness</i>	8
1.2.2 <i>Easy Problems of Consciousness</i>	9
1.2.3 <i>Animal Consciousness</i>	11
1.3 CHANGES IN STATES OF CONSCIOUSNESS.....	13
1.3.1 <i>When has conscious experience changed?</i>	13
1.4 EFFECTS OF GENERAL ANESTHESIA.....	14
1.4.1 <i>Pharmacology</i>	15
1.4.2 <i>Behavior</i>	18
1.4.3 <i>Neurophysiology</i>	20
1.5 EMERGENCE AND RECOVERY FROM ANESTHESIA.....	23
1.5.1 <i>Anesthetic Reversal</i>	23
1.5.2 <i>Canonical Sequence of Emergence and Recovery Behaviors in Rats</i>	24
1.6 COGNITIVE PROBLEMS ARISING AFTER SURGERY.....	25
1.6.1 <i>Emergence Agitation</i>	25
1.6.2 <i>PACU Delirium</i>	27
1.6.3 <i>Postoperative Delirium</i>	28
1.6.4 <i>Postoperative Cognitive Dysfunction</i>	30
1.6.5 <i>Anesthesia Awareness With Recall</i>	31
1.7 GENERAL ANESTHESIA AND POSTOPERATIVE COGNITIVE IMPAIRMENTS.....	33

1.7.1 General Anesthetics and Neurotoxicity.....	33
1.7.2 General Anesthetics and Neuroinflammation	34
1.7.3 General Anesthetics and Neurophysiology	35
1.9 GAP IN KNOWLEDGE	39
1.10 THESIS OUTLINE	40
CHAPTER 2 - ANGIOTENSIN RECEPTOR BLOCKERS AS A MEDIATOR OF AD-LIKE COGNITIVE DYSFUNCTION IN THE TGF344-AD RAT MODEL	41
2.1 ABSTRACT.....	41
2.2 INTRODUCTION	42
2.2.1 The Amyloid Cascade Hypothesis of Alzheimer’s Disease	42
2.2.2 The Vascular Hypothesis of Alzheimer’s Disease.....	43
2.2.3 The Renin Angiotensin System as a Therapeutic Target in Early Alzheimer’s Disease.....	44
2.2.4 Candesartan, An Angiotensin Receptor Blocker (ARB).....	45
2.2.5 The TgF344-AD Rat Model.....	46
2.2.6 Summary.....	46
2.3 EXPERIMENTAL DESIGN AND HYPOTHESES	47
2.4 METHODS.....	48
2.4.1 Animals.....	48
2.4.2 Continuous Spontaneous Alternation Behavior Test	49
2.4.3 Novel Object Recognition Test.....	49
2.4.4 ARB Treatment	50
2.4.5 Water Radial Arm Maze.....	51
2.4.6 Blood Pressure Readings	51
2.4.7 Tissue Collection	52
2.4.8 Tissue Sectioning and Immunohistochemistry	52
2.4.9 Quantification of Immunohistochemistry.....	53
2.4.10 Statistical Analysis	53
2.5 RESULTS	54

2.5.1 Amyloid- β and GFAP are increased in the hippocampus of 12-month old TgF344-AD rats	54
2.5.2 No differences in Continuous Spontaneous Alternation Test performance or Novel Object Recognition at 12-months in TgF344-AD or WT rats	56
2.5.3 Candesartan decreases mean arterial pressure for both WT and TgF344-AD rats	58
2.5.4 Amyloid- β and GFAP are increased in the hippocampus of 18-month old TgF344-AD rats	59
2.5.5 Candesartan preserves task learning on the WRAM for TgF344-AD rats	62
2.5.6 Working and Reference memory impairment in 18-month old TgF344-AD rats is partially rescued by treatment with candesartan	65
2.6 DISCUSSION	66
CHAPTER 3 - DELAYED ANESTHETIC RECOVERY IN 12-MONTH TGF344-AD RATS.....	69
3.1 ABSTRACT.....	69
3.2 INTRODUCTION	70
3.2.1 Alzheimer's Disease and Anesthesia.....	71
3.2.2 Alzheimer's Disease and anesthetic sensitivity.....	72
3.3 EXPERIMENTAL DESIGN AND HYPOTHESES	72
3.4 METHODS.....	74
3.4.1 Animals.....	74
3.4.2 Continuous Spontaneous Alternation Behavior Test	74
3.4.3 Novel Object Recognition Test.....	75
3.4.4 Isoflurane Anesthesia	76
3.4.5 Anesthetic Emergence & Recovery	76
3.4.6 Activity Monitoring	77
3.4.7 Wireless EEG Transmitter Implantation.....	77
3.4.8 EEG Recording	79
3.4.9 Tissue Collection	79
3.4.10 Tissue Sectioning and Immunohistochemistry	80
3.4.11 Quantification of Immunohistochemistry.....	80
3.4.12 Statistical Analysis	80

3.5 RESULTS	81
3.5.1 Cognitive Testing.....	81
3.5.2 Emergence and Recovery from Isoflurane	84
3.5.3 Burst Suppression.....	86
3.5.4 Increased amyloid- β and GFAP in TgF344-AD rats after burst suppression.....	89
3.6 DISCUSSION	90
CHAPTER 4 - PREHABILITATIVE EXERCISE HASTENS ANESTHETIC RECOVERY IN DIABETIC AND NON-DIABETIC RATS	94
4.1 ABSTRACT.....	94
4.2 INTRODUCTION	96
4.2.1 Diabetes and Surgery	96
4.2.2 General Anesthesia and Cognitive Dysfunction.....	96
4.2.3 The Effects of Exercise on Cognitive Reserve.....	97
4.3 EXPERIMENTAL DESIGN AND HYPOTHESES	98
4.4 METHODS.....	99
4.4.1 Animals.....	99
4.4.2 Glucose Tolerance Test (GTT).....	99
4.4.3 Treadmill Exercise	99
4.4.4 Continuous Spontaneous Alternation Behavior Test	100
4.4.5 Isoflurane Anesthesia	101
4.4.6 Anesthetic Emergence & Recovery.....	101
4.4.7 Western Blot	102
4.4.8 Statistical Analysis	103
4.5 RESULTS	103
4.5.1 Glucose Tolerance Test.....	103
4.5.2 Y-maze Continuous Spontaneous Alternation Behavior Test Performance.....	104
4.5.3 Anesthetic Emergence and Recovery	105
4.5.4 PSD-95 Levels in Hippocampus.....	106

4.6 DISCUSSION	108
CHAPTER 5 - GENERAL DISCUSSION	111
5.1 INTRODUCTION	112
5.2 STICKY DOT TEST	114
5.3 EMERGENCE FROM ANESTHESIA WITH AD	116
5.4 RECOVERY FROM ANESTHESIA WITH AD	118
5.5 EMERGENCE AND RECOVERY FROM ANESTHESIA WITH T2DM.....	120
5.6 RECOVERY FROM ANESTHESIA AFTER EXERCISE TRAINING	121
5.7 RELATIONSHIP BETWEEN T2DM AND AD	123
5.8 SUMMARY	124
5.9 PERSISTENT PERIOPERATIVE NEUROCOGNITIVE DISORDERS	129
5.10 FUTURE DIRECTIONS.....	130
CHAPTER 6 - APPENDIX.....	133
APPENDIX 1 – IMMUNOHISTOCHEMISTRY IMAGE ANALYSIS	133
<i>A1.1 Hue, Saturation and Value.....</i>	<i>133</i>
<i>A1.2 Positive Pixel Count Analysis</i>	<i>135</i>
APPENDIX 2 – EXTENDED BURST SUPPRESSION ANALYSIS METHODS	140
<i>A2.1 – EEG Acquisition</i>	<i>141</i>
<i>A2.2 – BSR Analysis</i>	<i>141</i>
APPENDIX 3 – EXTENDED EEG RECORDING DENOISING METHODS	145
<i>A3.1 – MWT Selection Methods</i>	<i>146</i>
CHAPTER 7 - REFERENCES.....	151

List of Figures and Tables

Figure 1.1 – Framework for organization of the neural activity underlying conscious behaviors.	11
Figure 1.2 – Graph of the hypothetical amounts of arousal (wakefulness) and awareness present in different states of consciousness.....	14
Figure 1.3 – Inhalation anesthetics used in modern Anesthesiology.....	17
Figure 1.4 – Intravenous anesthetics used in modern Anesthesiology.....	18
Figure 1.5 - EEG traces demonstrating characteristic EEG voltage changes under increasing concentrations of isoflurane anesthesia.	21
Figure 1.6 – Associations between different delirium subtypes.	27
Figure 1.7 – Timeframe for the presentation of perioperative and postoperative cognitive changes.....	32
Figure 1.8 – Patterns of EEG during end maintenance of sevoflurane anesthesia as determined by features from the EEG power spectrum.....	36
Figure 1.9 – Different emergence trajectories from surgical anesthesia are associated with increased risk for PACU delirium.....	37
Figure 2.1 – Timeline of behavioral experiments.....	48
Figure 2.2 – Changes in neuropathology at 12-months for TgF344-AD rats.....	55
Figure 2.3 – No difference in spontaneous alternation test performance between TgF344-AD rats and WT littermates at age 12 months.	56
Figure 2.4 – No difference in Novel Object Recognition test performance between TgF344-AD and WT littermates at age 12 months.	57
Figure 2.5 – Candesartan decreases mean arterial pressure for both WT and TgF344-AD rats. .	58
Figure 2.6 – Treatment with candesartan did not affect the accumulation of amyloid- β and GFAP in 18-month old TgF344-AD rats.	60
Figure 2.7 – Comparison of 12 & 18 month TgF344-AD rat amyloid- β and GFAP quantification.	62
Figure 2.8 – TgF344-AD rats learn to complete the WRAM faster with training but with no change in total errors committed.....	64
Figure 2.9 – WRAM performance on training days 11 & 12 for TgF344-AD and WT rats treated with Candesartan.....	66

Figure 3.1 – Experimental workflows for behavioral testing and EEG recordings in TgF344-AD rats.....	73
Figure 3.2 – There were no observed differences in test performance on the SAT or NOR at 12 months between WT and TgF344-AD rats.....	83
Figure 3.3 – Isoflurane emergence period is hastened and recovery is delayed in TgF344-AD rats.....	85
Figure 3.4 – Example EEG recordings of cortical burst suppression.....	88
Figure 3.5 – TgF344-AD rats do not display increased sensitivity to sevoflurane.....	89
Figure 3.6 – Amyloid- β and GFAP levels are increased following sevoflurane administration in TgF344-AD rats.....	90
Figure 4.1 – Illustration of experimental timeline and design.....	98
Table 4.1. Blood glucose levels as measured by test strip for GTT	103
Figure 4.2 – GK rats perform worse than Wistars on a test of spatial working memory.....	105
Figure 4.3 – Exercise hastens recovery from general anesthesia in both Wistar and GK rats but has no effect on anesthetic emergence.....	106
Figure 4.4 - Wistar and GK rats both demonstrate increased PSD-95 levels in hippocampus after 10-days of treadmill exercise.....	107
Figure 5.1 – Hypothetical EEG correlates of different postoperative emergence durations.....	127
Figure 5.2 – Factors influencing postoperative cognitive recovery.....	128
Figure A1-1: Comparison of the raw image with the RGB values from each color component	133
Figure A1-2: Representation of the complete reproducible color spectrum in 8-bit depth, RGB color	134
Figure A1-3: Comparison of the raw image with the channels for stain identification within Qupath.....	136
Table A1-1: Qupath Positive Pixel Count Analysis Inputs	136
Figure A1-4: Visualization of the light transmittance gradients for both the hematoxylin and DAB stains	138
Figure A1-5: A step-by-step visualization of the positive pixel count analysis within Qupath	139
Figure A2-1: Continuous Burst Suppression Ratios calculated from the cortical electrode	143
Figure A2-2: Continuous Burst Suppression Ratios calculated from the Hippocampal electrode	144

Figure A3-1: Comparison of denoised EEG with raw EEG trace	146
Figure A3-2: Selection of db10 wavelet for denoising of EEG recorded from the Cortical electrode.....	148
Figure A3-3: Selection of sym2 wavelet for denoising of EEG recorded from the Hippocampal electrode.....	149
Figure A3-4: Comparison of EEG denoising strategies	150

List of Abbreviations

5-HT receptor – Serotonin receptor

A β - Amyloid-beta

AD – Alzheimer’s Disease

ANOVA – Analysis of Variance

APOE4 – Apolipoprotein ϵ 4

APP – Amyloid Precursor Protein

APP_{SW} – Human Mutant Amyloid Precursor Protein Swedish Variant

ARB – Angiotensin Receptor Blocker

ASA – American Society of Anesthesiologists

AT1 – Angiotensin II Receptor Type 1

ATP – Adenosine Triphosphate

AWR – Anesthesia Awareness with Recall

BBB – Blood Brain Barrier

BCE – Before Common Era

BDNF – Brain Derived Neurotrophic Factor

BIS – Bispectral Index

BMDM – Bone Marrow Derived Monocytes

BSR – Burst Suppression Ratio

CE – Common Era

CICI – Cortical Integration of Complex Information

Cl⁻ – Chloride

CNS – Central Nervous System

CSF – Cerebrospinal Fluid

DAB – 3,3'-Diaminobenzidine

ddSWA – Delta-dominant Slow Wave Anesthesia

DFN – Default Mode Network

DI – Discrimination Index

DM – Diabetes Mellitus

DSM-5 – Diagnostic and Statistical Manual of Mental Disorders, Fifth Edition

EA – Emergence Agitation

EEG – Electroencephalography

EMG – Electromyography

FDA – Federal Drug Administration

GA – General Anesthesia

GABA – Gamma-aminobutyric Acid

GABA_AR – Gamma-aminobutyric Acid A Receptor

GFAP – Glial Fibrillary Acidic Protein

GK – Goto-Kakizaki Rat

GTT – Glucose Tolerance Test

ICU – Intensive Care Unit

ISPOCD/ISPOCD2 – International Study of Postoperative Cognitive Dysfunction 1 and 2

JAMA – Journal of the American Medical Association

LORR – Loss of Righting Reflex

MAC – Minimum Alveolar Concentration

MCI – Mild Cognitive Impairment

MRI – Magnetic Resonance Imaging

MWT – Mother Wavelet Function

NCD – Neurocognitive Disorder

NMDA – N-methyl-D-aspartate

NOR – Novel Object Recognition

NREM – Non-Rapid Eye Movement

-O- – Ether

-OH – Alcohol

PACU – Post-anesthesia Care Unit

PACU-D – Post-anesthesia Care Unit Delirium

PBC – Postoperative Behavioral Change

PET – Positron Emission Tomography

POCD – Postoperative Cognitive Dysfunction

POD – Postoperative Delirium

PPND – Persistent Perioperative Neurocognitive Disorders

PS1 Δ E9 – Presenilin 1 Exon 9 Deletion

PSD-95 – Post-synaptic Density Protein 95

PTSD – Post-traumatic Stress Disorder

RAS – Renin Angiotensin System

REM – Rapid Eye Movement

ROI – Region of Interest

RORR – Return of Righting Reflex

SAT – Spontaneous Alternation Test

sdSWA – Spindle-dominant Slow Wave Anesthesia

SURE – Stein's Unbiased Risk Estimator

SWA – Slow Wave Anesthesia

T2D – Type 2 Diabetes Mellitus

TPN – Task Positive Network

TREM2 – Triggering Receptor expressed on Myeloid Cells 2

TrkB – Tropomyosin receptor kinase B

TF – Familiar Object Observation Time

Tg3xAD Mouse – Triple Transgenic Alzheimer's disease mouse model

TgF344-AD Rat – Transgenic Fischer 344 Alzheimer's disease rat model

TN – Novel Object Observation Time

VTA – Ventral Tegmental Area

W – Wistar Rat

WRAM – Water Radial Arm Maze

WT – Wild Type

Chapter 1 - General Introduction

Selected sections are adapted from: Sinon CG, Arora SS, Rodriguez AD, Garcia PS (2019). 'Special Considerations: Alzheimer's Disease', in Prabhakar H, Mahajan C, Kapoor I (ed.) *Essentials of Geriatric Anesthesia*. CRC Press.^[1]

The widespread adoption of general anesthetics in the 19th century led to rapid advancements in surgical practice. The refinements of the field of anesthesiology include the development of inhalation anesthetics, intravenous anesthetics, neuromuscular blockade, airway management, and monitoring of heart rate & body temperature for drug titration. The complexity and success rate of surgical procedures grew alongside our growing knowledge of anesthetic practices. However, alongside this growth there has been concern about the appearance of cognitive disturbances in the postoperative period. Discussions of this topic in the literature, dating as far back as the late 1800's, have commonly hypothesized that general anesthetics may underlie cognitive disturbances^[2, 3]. Two classic works, a 1953 paper in JAMA Pediatrics by James Eckenhoff on postoperative personality changes in children^[4] and a 1955 paper by Philip Bedford on postoperative cognitive decline in patients over aged 65^[5], laid a foundation for the modern study of the effects of general anesthetics on cognition.

Unfortunately, progress in this field of research has been slow and often contentious. It is not common practice for cognitive assessments of patients to be performed prior to surgery, so many of the accounts available regarding problems of cognition following surgery are from case reports or anecdotal evidence. For instance, the data from Eckenhoff's 1953 paper was gathered from surveys of parents on their child's recovery from surgery and Bedford's 1955 paper consisted of case histories where there was no obvious documented surgical complication that could explain the observed cognitive impairments. Bedford was prophetic in two of his assessments of the future of research on postoperative cognitive impairments:

1. The occurrence of these cognitive impairments will likely be clinically underreported (as "neurosis" among the young and "senility" among the old).

2. There must be “individual susceptibility” that predisposes a patient to postoperative cognitive disturbances.

Large clinical research projects have begun to elucidate some of the risk factors that can predispose patients to postoperative cognitive impairments. There has largely been a subdivision of cognitive impairments into separate conditions based primarily on the timing of appearance. Emergence agitation describes an agitated and hyperactive emergence where patients can become confused and violent. Post-anesthesia Care Unit (PACU) Delirium and Postoperative Delirium (POD) are acute disturbances in attention and cognitive function diagnosed in the recovery room and the days following surgery, respectively. Postoperative Cognitive Dysfunction (POCD) describes declines in cognitive function lasting weeks to months. These conditions share some common risk factors (such as advanced age and prior cognitive impairments) and the risk for later cognitive impairments increases with the appearance of earlier cognitive disturbance.

Preclinical models have demonstrated learning and memory impairments in the days and weeks following both surgery and general anesthesia independent of surgery. However, no preclinical models of POD or POCD are currently available. This thesis contains our work characterizing the immediate emergence and recovery from anesthesia in preclinical models of conditions known to be risk factors for developing postoperative cognitive impairments. This chapter serves as a detailed introduction to the use of anesthesia in the study of consciousness and our understanding of cognitive impairments in the immediate postoperative period.

1.1 History of Anesthesia

Techniques for anesthesia and/or sedation with analgesia were first used for medicine in antiquity. However, modern anesthesiology was born primarily from the work of physicians and

chemists working in the late-18th and early-19th centuries. From historical records, it appears clear that protocols for anesthesia have been developed and abandoned by healers many times throughout human history. Changing religious practices and the upheaval of past civilizations may partially explain why different early anesthetics were abandoned or forgotten, although it is also clear from early writings that early attempts at anesthesia used substances that were dangerous and poorly controlled^[6]. As late as 1845, one year before William Morton's famous "discovery" of ether anesthesia at Massachusetts General Hospital, a failed demonstration of nitrous oxide anesthesia during a tooth extraction was attempted by Horace Wells. Despite records of multiple previous successful dental procedures using nitrous oxide by Wells, the failed demonstration along with fear from the wider medical community regarding the use of ether or nitrous oxide during surgery convinced Wells to abandon the technique^[7]. Since the adoption of anesthesia in medicine starting in the 1840's, development and improvements in the use of anesthesia have primarily focused on improving safety in administration of anesthetics and improving the anesthesiologist's control of the induction, maintenance and emergence from anesthesia.

1.1.1 Early Anesthetics

"Anaesthesia" comes from the Greek, *αν-* (an-, 'not' or 'without') and *αἴσθησις* (aesthesia, 'perception' or 'sensation')^[8]. The modern adoption of the word is credited to Oliver Wendell Holmes, who suggested the name in correspondence with William T.C. Morton after the successful demonstration of ether anesthesia in October 1846^[9]. However, the recorded pursuit of techniques to lessen pain and perception in medical practice date back as far as the Ancient Sumerians and Egyptians. Alcohol was popular in ancient Mesopotamia^[10, 11] and there is evidence the Sumerians cultivated opium poppies as early as 3400 BCE^[12]. They referred to the

poppies as *hul gil* ('joy plant'), suggesting that they knew that the plant could be used for its euphoric properties. References to beer, wine and poppies appear in the oldest recovered Sumerian cuneiform tablets on herbal medicines^[13].

The Egyptian medical papyri contain detailed descriptions of early surgery, with the use of hemp and poppies for patient sedation^[14, 15]. These texts also contain the first recorded reference to the brain and demonstrate knowledge of the brain's role in control of motor function through case reports on head trauma. Ancient Egyptians also administered the first recorded local anesthetic medication, a mixture of powdered marble and vinegar^[9, 16]. The reaction of the two compounds forms carbonic acid and was used as topical treatment for painful wounds. Wine, cannabis incense and wolfsbane were used in ancient China and India as forms of anesthesia^[17]. The earliest written depictions of surgery performed with a general anesthetic medication come from China around 200 CE^[18, 19]. A Chinese surgeon named Hua Tuo is credited with using a mixture of wine and a substance called "mafeisan" ('cannabis boiling powder') to induce anesthesia before performing surgery to remove gangrenous portions of the intestine. Hua Tuo's patients were reported to fall unconscious for extended periods of time after drinking the mixture, however the exact ingredients of mafeisan were lost to history when Hua Tuo was executed for refusing to treat the warlord, Cao Cao^[20].

The slow development of medical techniques for minimizing pain and perception for surgery can be partially blamed on the reluctance of many early civilizations to perform invasive medical procedures. The Hammurabi code punished doctors for failed attempts at surgery with the removal of a hand^[21]. Surgery was not popular in ancient China, especially after the death of Hua Tuo, because the practice was viewed as a form of body mutilation within the beliefs of Confucianism^[18]. Alternatively, in some areas surgical practice flourished, but without the use of

anesthesia. Al-Zahrawi's medical encyclopedia, *Kitab al-Tasrif*, was a foundational text for physicians throughout the Middle Ages and the final chapter on surgical practice remained influential in Europe into the 18th century^[22]. While techniques for inhalation anesthesia administered via a sponge soaked herbal sedatives are recorded to have existed at this time in Europe and Asia^[23], but the *Kitab al-Tasrif* itself only recommended the use of restraints for patients undergoing painful procedures^[24].

1.1.2 The Beginnings of Modern Anesthesia

The first widely used modern anesthetics were nitrous oxide, ether and chloroform. The stupefying effects of all three substances were well known when they were adopted as tools for surgery, due to their recreational use and from public exhibitions of their effects. Credit for the discovery of anesthesia has been disputed amongst a number of scientists and physicians from the early 19th century. Humphry Davy suggested that the alleviation of pain caused by nitrous oxide could be useful for surgical operations in 1800^[6]. William Clarke of New York and Crawford Long of Georgia separately used ether anesthesia on patients in 1842. As mentioned, Horace Wells unsuccessfully attempted to demonstrate nitrous oxide anesthesia for medical students in Boston in 1845, following a year of successful use of the drug in his dental practice in Connecticut. Ether anesthesia was publicly demonstrated and internationally publicized by William Morton in 1846. The following year James Simpson published his experiments using chloroform as an anesthetic during childbirth, establishing the drug as an alternative to ether^[25].

Early attempts at explaining the anesthetic effects of these drugs led to confusion and disagreements regarding the usefulness of these drugs clinically. Nitrous oxide was characterized by some as being a “stimulant” at subanesthetic doses, because the drug “stimulated” a euphoric and dissociated state punctuated by giggling/laughter (hence the colloquialism “laughing gas”)^[7].

Morton disputed Wells' claims to be the inventor of general anesthesia by claiming ether as the first "non-stimulant" gas used for anesthesia and therefore sufficiently different from Wells' initial approach. In truth, both drugs depress CNS function and ironically ether appears to act as a stimulant of sympathetic function at low and moderate doses^[26, 27]. Gardner Quincy Colton reintroduced nitrous oxide in dental practice beginning in 1863^[28].

1.1.3 Improvements in Anesthesiology

During the late 19th and early 20th centuries, professional societies and training programs started to develop regarding the use of anesthesia. Techniques for patient airway management^[29], local anesthesia^[30] and the first neuromuscular blocks^[31] were all developed around this time. Since this period, advances in anesthesiology have traditionally focused on either improving patient safety during anesthesia or improving the pharmacodynamics and pharmacokinetics of anesthetic drugs. After halothane was synthesized in the 1950's, it replaced both diethyl ether and chloroform for use in surgical anesthesia. Halothane improved patient safety because it has fewer toxic side effects than chloroform^[32]. Halothane also improved occupational safety for anesthesiologists by reducing the likelihood of fires and explosions in operating rooms that had been supplied with highly flammable diethyl ether^[33]. The development of intravenous anesthetics removed the necessity for breathing masks during surgery, allowing for more complicated surgical procedures to be performed on the head and face of patients. The introduction of halogenated ethers further improved the safety and pharmacodynamics of inhalation anesthetics. For example, compared with the first inhalation anesthetics, sevoflurane is considerably safer for patients than diethyl ether and produces anesthesia significantly faster than nitrous oxide.

The minimum alveolar concentration (MAC) of an anesthetic drug is the concentration needed to cause immobility in 50% of patients^[34]. The description of MACs for common anesthetics and the discovery that MAC values are additive between anesthetics have led to new anesthesia protocols that reduce the individual drug concentrations necessary to produce general anesthesia^[35]. Today, anesthesia is often administered using drug cocktails that may contain an induction agent, neuromuscular blockade, a maintenance anesthetic and additional analgesics.

1.2 Historical Problems in the Study of Consciousness

The use of anesthesia has turned surgery into a task more similar to medical dissection, by reducing the patient to being just “a body” during operation^[36]. Anesthesia has also produced possibilities for better understanding how the brain produces consciousness (by virtue of understanding how anesthetics produce unconsciousness). Debate about the genesis, nature and purpose of consciousness is well established in philosophy and has proved to be a difficult subject for empirical research. While aspects of consciousness are certainly assessable by third party observers, there is concern that there is an individual, fundamentally subjective component to consciousness that is incompatible with a reductionist scientific explanation. This section explores three unanswered “problems” in the study of consciousness that are important considerations for study of mechanisms of general anesthesia.

1.2.1 The Hard Problem of Consciousness

*“The really hard problem of consciousness is the problem of **experience**. When we think and perceive, there is a whirl of information-processing, but there is also a subjective aspect. As Nagel (1974^[37]) has put it, there is **something it is like** to be a conscious organism.” -David Chalmers, *Facing Up to the Problem of Consciousness**

The modern conception of the Hard Problem of Consciousness was stated in a 1995 article by David Chalmers^[38]. Chalmers assesses the modern attempts to rigorously understand the basis of

consciousness as focusing on explanations of cognitive functions and abilities. He views the combined efforts of all consciousness researchers as attempting to segment consciousness into a collection of cognitive functions and abilities, which when explained will equal the sum total of what is consciousness. In Chalmers' assessment, this method is fundamentally flawed, because a subjective experience underlies each cognitive function or ability and these experiences are left unexplained by modern consciousness research. He states:

"It is undeniable that some organisms are subjects of experience. But the question of how it is that these systems are subjects of experience is perplexing. Why is it that when our cognitive systems engage in visual and auditory information-processing, we have visual or auditory experience: the quality of deep blue, the sensation of middle C? How can we explain why there is something it is like to entertain a mental image, or to experience an emotion? It is widely agreed that experience arises from a physical basis, but we have no good explanation of why and how it so arises. Why should physical processing give rise to a rich inner life at all? It seems objectively unreasonable that it should, and yet it does.

*If any problem qualifies as **the** problem of consciousness, it is this one."*

Many potential solutions (or frameworks for solutions) to the hard problem of consciousness have been proposed, but none have gained popular acceptance^[39, 40]. A common criticism of the proposed solutions is that they still focus on solving "easy problems of consciousness", which correlate conscious experiences with functional capabilities of the brain, and then they make the 'unfounded' claim that consciousness emerges from the sum total of these functional capabilities. However, critiques of Chalmers and his supporters claim that their beliefs about the nature of subjective experience are only compatible with mind-body dualism^[41, 42].

1.2.2 Easy Problems of Consciousness

Generally speaking, while awake, humans perceive the world around them, remember the things that happen to them and display behaviors that demonstrate a subjective experience of reality. While it is truly difficult to conceptualize how to explain the neurological mechanisms

underlying subjective experience, it is possible to access information on when subjective experiences are occurring, both through personal reporting and through the monitoring of neurological function. “When has consciousness changed?” is an answerable question, even if it’s hard to pin down exactly what conscious experience is like for any singular individual.

There are demonstrated and relatively well understood differences between being awake and being sleep^[43]. During slow wave sleep, individuals are unconscious and generally immobile. They do not form declarative memories and the thresholds for sensory perception are dramatically increased. There are well characterized differences between cortical activity recorded while awake and during slow wave sleep. In addition, there are physiological characteristics associated with sleep that do not directly access conscious experience but do correlate well with the levels of arousal and fluctuations in consciousness. Pupil size is correlated with increasing drowsiness and different stages of sleep. Glucose metabolism is decreased in deep sleep. Sleep is also associated with decreases in heart rate, respiratory rate, core body temperature and muscle activation.

These types of measurements are important for two reasons: 1) they indicate brain regions and signaling pathways that may be involved in the organization of consciousness, & 2) they provide tools for answering the “easy problems of consciousness”, which don’t necessitate a complete understanding of another’s subjective experience. Figure 1.1 includes a general framework for experiments on “easy problems of consciousness”^[44].

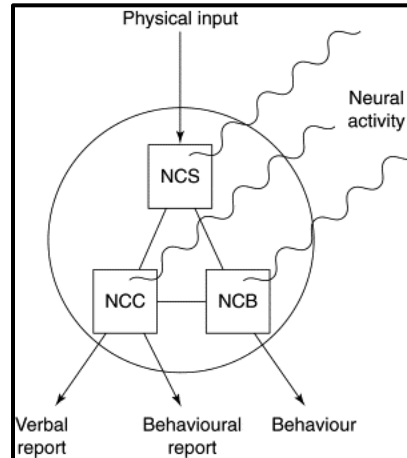


Figure 1.1 – Framework for organization of the neural activity underlying conscious behaviors.

Neural processing underlying consciousness can be classified as pertaining to the neural correlates of sensory stimuli (NCS), neural correlates of behavior (NCB), and the neural correlates of consciousness (NCC). These neural activities do not need to be segregated in different brain regions. Quantification of the stimulus inputs into the brain and observations of behavior can be understood without the need to account for subjective reporting. Verbal and behavioral reporting are best understood in the context of research on humans, where subjective experience can be self-reported. Adapted from Frith et al. 1999, The neural correlates of conscious experience: an experimental framework^[44] with permissions through RightsLink.

1.2.3 Animal Consciousness

While not itself an argument against the existence of animal consciousness, Thomas Nagel’s 1974 paper, “What is it like to be a bat?”, highlights the difficulty in assessing consciousness in animals^[37]. Nagel’s argument can be summarized as follows:

“An organism has conscious mental states if and only if there is something that it is like to be that organism – something that it is like for the organism to be itself.”

Considering this understanding of animal consciousness, a true objective measure of conscious experience in a bat is inaccessible to humans, since we cannot conceptualize what it is like for a bat to be itself.

As a result, arguments in favor of animal consciousness have generally avoided attempts to “prove” subjective experience occurs in animals and focused instead on likely similarities in the neural correlates of consciousness between humans and animals. Neural correlates of consciousness are a minimum set of neuronal responses underlying conscious experience^[45]. In response to anthropocentric views on consciousness, the Cambridge Declaration on Consciousness was issued in 2012:

“The absence of a neocortex does not appear to preclude an organism from experiencing affective states. Convergent evidence indicates that non-human animals have the neuroanatomical, neurochemical, and neurophysiological substrates of conscious states along with the capacity to exhibit intentional behaviors. Consequently, the weight of evidence indicates that humans are not unique in possessing the neurological substrates that generate consciousness. Non-human animals, including all mammals and birds, and many other creatures, including octopuses, also possess these neurological substrates.”

Classical experiments into the contents of animal consciousness have involved assessments of awareness of self and surroundings, often through sensory processing. The “mirror test” has been used as an assessment of self-awareness in research into animal consciousness^[46, 47]. Studies of imitation behaviors have attempted to demonstrate that animals possess a sense of agency and body image^[48]. The use of language in animals has been cited as evidence for subjective experience in animals^[49]. There is still concern^[49] regarding the validity of these tests for assessment of consciousness in animals, but new analysis tools are being developed to address these critiques objectively^[50, 51].

1.3 Changes in States of Consciousness

It is clear that there is a threshold for cortical arousal required to maintain wakefulness in animals. It has also been broadly shown that cognitive abilities can be impacted by states of arousal, as well as damage to specific areas of the brain. In order for the effects of anesthetics to be thought of as truly “temporary and reversible”, there must be no subsequent long-term impact on brain regions important for arousal or cognition.

1.3.1 When has conscious experience changed?

Distinctions between the “level” of consciousness and the “content” of consciousness have been made by multiple researchers^[44, 52]. Classically, the “level” of consciousness describes the behavioral arousal of an individual and the “content” of consciousness is the individual’s state of awareness or quality of experience. Different states of consciousness can then be displayed graphically, as in Figure 1.2 from Laureys 2005^[52]. States with high behavioral arousal but low awareness include sleepwalking and vegetative states. States with lower behavioral arousal and higher awareness include REM sleep and Locked-in syndrome.

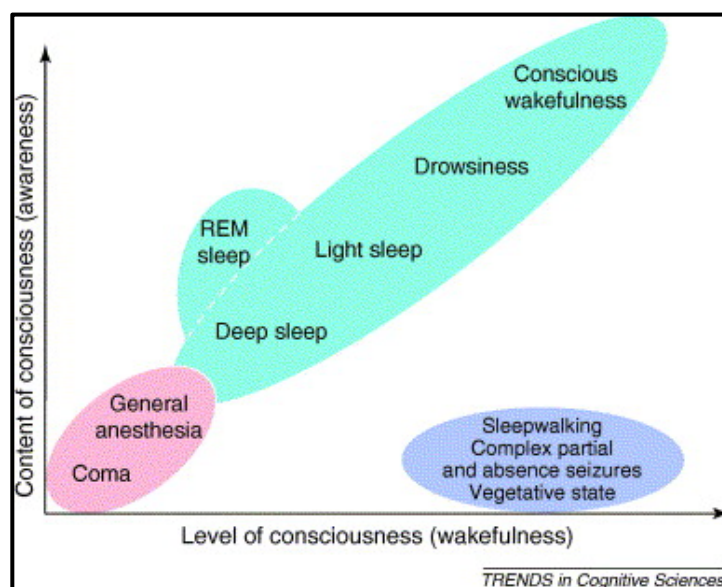


Figure 1.2 – Graph of the hypothetical amounts of arousal (wakefulness) and awareness present in different states of consciousness

Differences in neurophysiology, functional connectivity, and circuit activation have been identified that seem to correlate with different states of consciousness. Related brain states that differ along one axis present potential opportunities to investigate the neural correlates of arousal (coma vs. vegetative state) and awareness (REM vs. NREM sleep). Adapted from Laureys 2005, The neural correlate of (un)awareness: lessons from the vegetative state^[52] with permission through RightsLink.

In animal studies it is difficult to assess the content of consciousness, because this is often assessed via verbal report in humans. Instead, consciousness is often assessed only by determining the level of behavioral arousal. The loss of righting reflex (LORR) has historically been used as a behavioral marker of the loss of consciousness due to anesthesia^[53, 54]. Rats that are awake and aware of their surroundings will resist being placed in a supine position and right themselves immediately. The LORR and subsequent return of righting reflex (RORR) can therefore be used as markers for the induction and emergence from anesthesia. EEG experiments correlate the LORR of righting reflex with a change from low amplitude, high frequency brain activity (characteristic of awake) to high amplitude, low frequency brain activity (characteristic of anesthesia)^[55]. The reversal of this activity is seen during RORR.

1.4 Effects of General Anesthesia

By definition, all general anesthetics cause loss of consciousness. All anesthetics (and all other causes of unconsciousness) are associated with a decrease in the information content of neural activity. Cortical activity driven by lower brain structures is dominated by high amplitude, low frequency oscillations during general anesthesia. For most anesthetics, this effect is thought to be primarily due to an increase in global inhibition, through agonism of gamma-aminobutyric acid (GABA) receptors. However, general anesthetics happen to also share a fairly low drug

potency. Relatively high concentrations are needed to achieve loss of consciousness and at these concentrations off target effects can be plentiful^[56]. As a result, these drugs cause heterogeneous pharmacological, neurophysiological and behavioral effects. This section considers the similarities and differences in anesthetic drug action at each of these three levels, in the context of clinical use and in the study of consciousness.

1.4.1 Pharmacology

Consideration of the GABA_A receptor (GABA_AR) provides an example of the difficulty in succinctly summarizing the pharmacological effects of anesthetics. A proposed mechanism of general anesthesia via GABA_AR signaling would begin with activation of the receptor, opening an ion channel selective for chloride (Cl⁻). The flow of Cl⁻ into the neuron hyperpolarizes the cell and inhibits action potential firing. Mass activation of GABA_ARs by a general anesthetic therefore decreases the likelihood and content of signaling from cortico-cortical connections, cortico-thalamic connections and ascending arousal pathways.

However, (1) at drug concentrations required for surgical anesthesia, all current clinically used anesthetics will bind more than one receptor type. Additional receptor binding could be likely at glycine receptors, NMDA receptors, nicotinic receptors, and 5-HT receptors depending on the drug used, which obscures interpretations regarding potential effects on GABA_ARs^[56]. (2) Anesthetics can modulate receptors present at the synapse or extra-synaptic receptors. Activation of these receptor populations have different effects on phasic and tonic changes in neuronal activity^[57]. (3) GABA_ARs are pentameric transmembrane receptors consisting of different combinations of α , β , and γ subunits. There are at least eight identified GABA_AR subunit conformations in the brain, each with different expression patterns throughout the brain and affinities for general anesthetics, so GABA_AR activation is not uniform in its effects throughout

the brain^[57, 58]. (4) There are changes in homeostatic processes in the brain during anesthesia, such as oxygen consumption^[59] and glucose utilization^[60], that are dose dependent. These effects could further depress arousal during anesthesia. (5) Anesthetics also have peripheral effects at high concentrations, such as modulations of heart rate or respiration, that could further potentiate the effects on the brain^[61, 62]. The combination of these factors, on top of a foggy understanding of the emergence of consciousness from brain activity, makes a cellular mechanism for general anesthesia difficult to define. They also highlight the need for proper intraoperative monitoring of cardiac, respiratory and neurophysiological activity during surgery by anesthesiologists.

Still, when drugs are considered with a focus on clinical endpoints, namely the loss of consciousness or inhibition of pain stimulus, their characteristics are easier to summarize. MAC is a useful measure for anesthetic administration and allows for predictable titration of anesthesia to prevent movement during surgery^[34, 63]. The chemical structures of commonly used anesthetics are varied, but there are similarities in structural properties that allow for subgrouping of anesthetics (Figures 1.3-4). For instance, the addition of an ether (-O-) group to the chemical structure can increase anesthetic potency and substitution of an alcohol (-OH) group in place of the ether will further increase potency^[56]. This effect is likely due to the increasing potential for these functional groups to act as a hydrogen donor at the drug binding site. There are also well-defined critical points for the structural size of anesthetic drugs. Dodecanol (C₁₂H₂₆O) has the highest potency for an alcohol anesthetic, but tetradecanol (C₁₄H₃₀O) does not produce general anesthesia, likely due to steric hindrance^[56]. Better understanding of drug functional groups and established binding sites have helped in the creation of new anesthetics, often designed with the goal of improving broad clinical endpoints, such as faster drug metabolism to improve anesthetic clearance and emergence from anesthesia^[64].

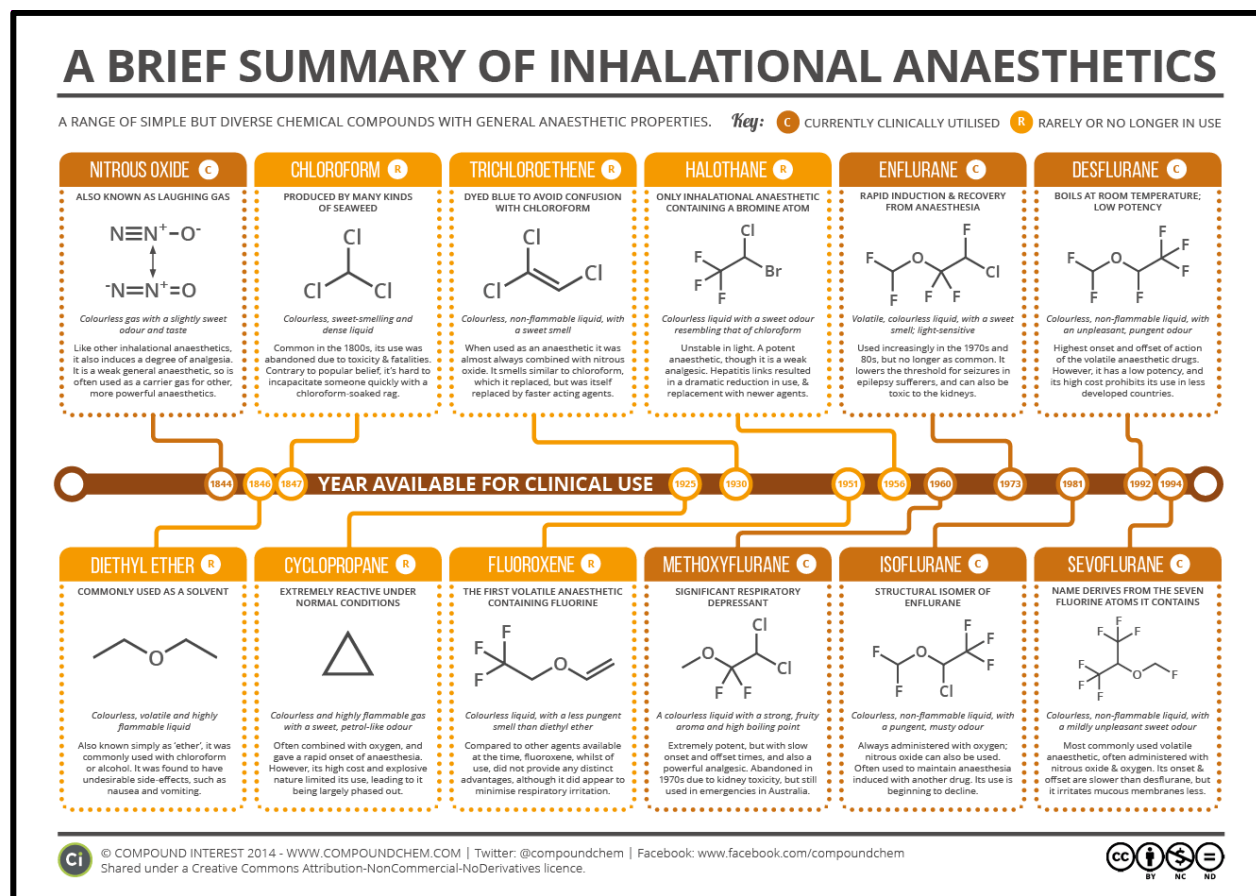


Figure 1.3 – Inhalation anesthetics used in modern Anesthesiology.

Chemical structures and dates of first clinical use are displayed. Adapted with permission from <https://www.compoundchem.com/2014/11/10/anaesthetics-pt1/>, made available through Creative Commons Attribution-NonCommercial-NoDerivatives Internation 4.0 license.

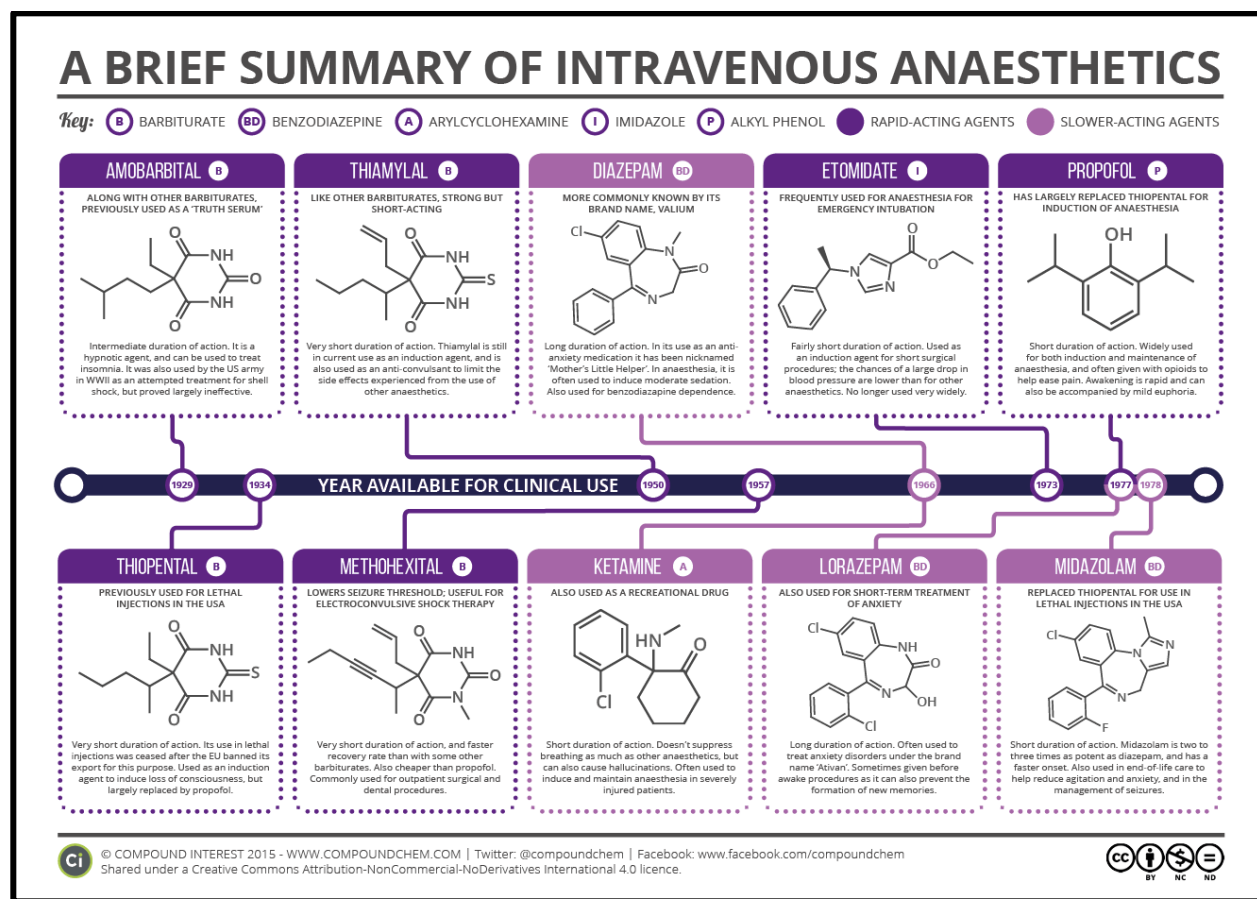


Figure 1.4 – Intravenous anaesthetics used in modern Anesthesiology.

Chemical structures and dates of first use are displayed. Adapted with permission from <https://www.compoundchem.com/2015/09/08/iv-anaesthetics/>, made available through Creative Commons Attribution-NonCommercial-NoDerivatives Internation 4.0 license.

1.4.2 Behavior

Ideally, general anesthesia will achieve amnesia, hypnosis, analgesia, areflexia and immobility during the noxious stimulation of surgery. A combination of these effects suitable for surgery is often not achievable or advisable from administration of a single drug, so polypharmacy is common during surgical anesthesia^[65, 66]. Polypharmacy could be compounded by further administration of anesthetic reversal agents to hasten the return of consciousness following a procedure. While all anesthetics produce varying degrees of immobility, any

unexpected movements by the patient during surgery could have catastrophic consequences, so the immobilizing effects of anesthetic drugs are often supplemented with neuromuscular blockers. Additionally, analgesic effects of anesthetics tend to dissipate shortly after emergence from anesthesia and must be supplemented with additional pain medications. A different collage of effects exists for each drug and the effects of a singular drug may differ based on the concentration delivered.

Taking ketamine as an example, its delivery in high concentrations causes temporary loss of consciousness. It is therefore a general anesthetic. Ketamine is an amnestic, but the psychoactive side effects of ketamine exposure can cause complication during emergence from anesthesia when it is delivered as a sole anesthetic^[67]. However, when it is given in combination with sevoflurane, it actually reduces incidents of emergence agitation in children^[68]. Ketamine causes hypnosis through its action on many different receptor types, including antagonism of NMDA receptors^[69]. The resulting brain activity under ketamine is more akin to that seen under REM sleep than the slow wave sleep-type anesthesia common amongst volatile anesthetics^[70, 71]. Ketamine is a dissociative drug causing euphoric sensations and also potentiates the effects of opioids, making it useful as an analgesic. Ketamine greatly reduces mobility, however catalepsy and movement even at surgical anesthesia concentrations have been reported^[69]. While ketamine has antagonistic effects on muscarinic and dopaminergic receptors, subanesthetic doses have been associated with elevated acetylcholine levels in cortex that appear to hasten anesthetic emergence^[71]. In addition, ketamine anesthesia does not suppress respiratory and cardiac function to the extent seen with other anesthetic drugs^[72].

The combination of these factors makes ketamine a suitable anesthetic for very specific clinical purposes. Worldwide, ketamine, injected intramuscularly or intravenously, is often used

as a sole anesthetic for simple surgeries especially in low and middle income countries that do not have specialized medical institutions due to its limited effects on respiratory and cardiac functions^[72]. For similar reasons, it is the preferred anesthetic for battlefield procedures by the U.S. military^[73]. In these situations, ketamine is quite versatile making short procedures possible without usual anesthesia equipment. In North America and Europe, ketamine is less often used as a sole anesthetic but has seen a resurgence in clinical use for synergy with other anesthetic and analgesic drugs.

1.4.3 Neurophysiology

The EEG represents the summation of electrical inputs onto dendrites of cortical neurons. EEG recordings are non-invasive and thus can be implemented as a monitor of brain activity before, during, and/or after surgery for most patients. Electrodes are affixed to the skin and will record electrical activity from the brain through the skin and skull. During recording, the higher frequency activity of brain will be filtered out of the signal by the skull and the power of the EEG signal recorded will be affected by the number of neurons present in the recording area and the distance between the electrode and the surface of the brain^[1].

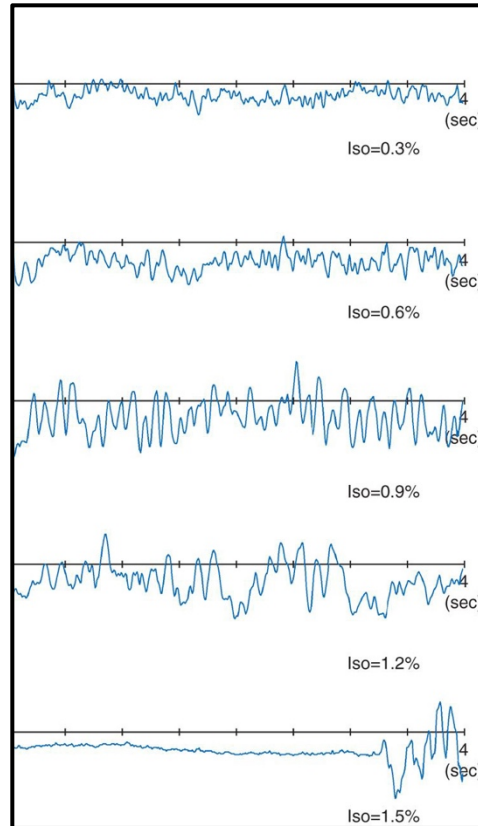


Figure 1.5 - EEG traces demonstrating characteristic EEG voltage changes under increasing concentrations of isoflurane anesthesia.

As isoflurane concentration increases from 0.3% to 1.5%, the EEG trace transitions towards slower, high amplitude voltage changes. The final trace displays a period of burst suppression, where periods of suppression of cortical activity are interrupted by bursts of high amplitude, low frequency activity. Adapted from Hagihara 2015, Changes in the electroencephalogram during anaesthesia and their physiological basis^[74] with permissions through RightsLink.

Raw EEG traces from individual electrodes during wakefulness are generally characterized by low-amplitude, high frequency voltage changes. During anesthesia, the recorded activity transitions towards high amplitude, low frequency voltage changes (Figure 1.5)^[74]. With increasing anesthetic dose, global synchrony decreases while local synchrony increases^[75, 76]. Considering these changes in the context of Shannon's Information Theory^[77], low local synchrony during consciousness represents high informational capacity of the neural

activity at the source location. Higher global synchrony would then represent greater potential for mutual information to be shared between the source and destination region. Anesthesia, then dramatically decreases the amount of information contained within the local neural activity and decreases the fidelity of information transmission between brain regions.

EEG activity can also be described in the frequency domain by computing the spectral power over defined frequency bands (delta: 0.5-4 Hz, theta: 4-8 Hz, alpha: 8-14 Hz, beta: 14-30 Hz, gamma: >30 Hz). For most primarily GABAergic anesthetics, increasing the concentration of the anesthetic increases spectral power in slower frequency bands. Mild to moderate sedation is characterized by increasing power in frequencies less than 14 Hz. With further sedation, alpha power tends to decrease, and the EEG power spectrum is dominated by delta power. Spectral analysis of EEG activity is a guiding principal for “consciousness monitors” that can be used to guide anesthetic drug administration during surgery^[78]. EEG similarities exist among drugs that work through a common mechanism. For instance, the frontal EEG pattern during anesthesia with ketamine is different when compared to propofol and the volatile anesthetics^[78].

At excessively high concentrations of anesthesia, near complete cessation of neuronal electrical activity can be observed in the raw EEG signal. Burst suppression describes periods of isoelectricity (suppressions) followed by bursts of high amplitude voltage changes. Burst suppression has been observed during the administration of high concentrations of enflurane, isoflurane, sevoflurane, desflurane, pentobarbital, methohexital, sodium thiopental, propofol, etomidate and cyclopropane. Burst suppression does not appear to occur even at high concentrations of chloroform, halothane, xenon, nitrous oxide, ketamine or opioids^[79]. There are two proposed mechanisms that have been proposed to explain the appearance of burst suppression. High doses of isoflurane decrease extracellular calcium levels, however during

suppressions the extracellular calcium levels begin to rise^[80]. It is thought that burst suppression is caused by an exhaustion of extracellular calcium during bursting followed by a refractory period where calcium levels begin to restore (suppressions). The neuro-metabolic model shares similar principles of action. High concentrations of anesthesia reduce brain metabolism which decreases ATP production. During bursts, ATP is used to support neural activity, followed by periods of suppression where more ATP is produced^[81]. At the systems level, suppressions have also been explained as a periods of “cortical deafferentation”. Burst patterns are correlated information flow from brainstem nuclei to the thalamus and finally to the cortex, whereas there is little influence from the brainstem and thalamus on cortical activity during suppressions^[82].

1.5 Emergence and Recovery from Anesthesia

The passive emergence from anesthesia is mediated by the metabolism and clearance of anesthetic drugs and an increase in signaling in cortical arousal pathways as anesthetic effects begin to wane. However, there appears to be natural hysteresis in the state transitions between consciousness and unconsciousness caused by anesthesia, suggesting that pharmacological effects alone do not completely account for the threshold for state changes during the induction or emergence from anesthesia. Induction of anesthesia requires a higher concentration of anesthesia than is required for emergence from anesthesia. This resilience to state transitions has been referred to as “neural inertia” and implies that the actions underlying anesthetic induction and emergence are not simply reverse processes^[83].

1.5.1 Anesthetic Reversal

The state of anesthesia can also be reversed by drugs that either (1) compete for binding sites on the protein targets of the anesthetic or (2) activate arousal pathways. Flumazenil is a competitive antagonist for the benzodiazepine-binding site on GABA_ARs and has been used

clinically to treat benzodiazepine overdose^[84]. It has shown promise in the treatment of hypersomnia^[85] and for reversing sedation from volatile anesthetics, although some groups have found no effect of flumazenil on the recovery from anesthesia after surgery^[84]. Flumazenil appears to also function as a competitive antagonist for GABA at the GABA_AR and reduces the increased chloride currents caused by isoflurane binding to GABA_ARs, which may explain its anti-sedative effects^[86].

Stimulation of arousal pathways can reverse the effects of anesthetics, even during continued administration of anesthetic drugs. Atipamezole and Yohimbine have both been used primarily as reversal agents in veterinary anesthesia. Both drugs antagonize the α^2 -adrenergic receptor, which halts the inhibition of norepinephrine release^[84, 87]. Deep brain stimulation and optogenetic stimulation of dopamine neurons in the ventral tegmental area (VTA) induce emergence from anesthesia with isoflurane and propofol^[88, 89]. Thalamic microinjections of nicotine to thalamus has been shown to reverse sevoflurane anesthesia through acetylcholine signaling pathways^[90]. The acetylcholinesterase inhibitor, physostigmine, has also been demonstrated to reverse propofol and sevoflurane anesthesia in humans^[91, 92]. Deactivation of norepinephrine pathways have also been shown to lengthen time to emergence as well^[83].

1.5.2 Canonical Sequence of Emergence and Recovery Behaviors in Rats

The RORR has been used previously in rats to signify the return of consciousness in rats. However, RORR is neither the first behavior observed during the emergence process, nor a sufficient marker of the recovery from general anesthesia. Behavioral markers signaling the end of anesthesia-induced immobility (mastication and limb movement) and the return of normal reflexive and autonomic behaviors (blinking and changes in respiration) have been observed during the process of emergence.

Following emergence from anesthesia, attempts at ambulation are uncoordinated and often unsuccessful. The time to coordinated ambulatory behavior following anesthesia represents the return of baseline motor control. In addition, a modified sticky dot test can be used as a test of sensory perception and coordinated motor movements following anesthesia. Awake rats with intact motor function that have not received anesthesia will routinely remove the sticky dot stimulus within seconds of it being adhered to the rat's forelimb. These behaviors have previously been demonstrated in rats to differentiate recovery times between different anesthetic reversal agents^[87] and emergence times between male and female rats^[93].

1.6 Cognitive Problems Arising after Surgery

The Diagnostic and Statistical Manual of Mental Disorders, Fifth Edition (DSM-5) defines delirium primarily as a disturbance in cognition^[94], which may variably include changes in perception, memory, language, coherent reasoning, and visuospatial processing. There are three motoric subtypes of delirium that can present in patients during recovery from anesthesia: a hyperactive subtype marked by agitation, a hypoactive subtype marked by lethargy, and a mixed subtype featuring aspects of both^[95]. No pharmacologic intervention has been proven to be effective in prevention or treatment of delirium subtypes following surgery, but risk awareness, brain monitoring for titration of anesthetic medications, and post-procedural assessments may decrease the incidence and severity^[1]. This section briefly discusses important perioperative and postoperative cognitive disturbances.

1.6.1 Emergence Agitation

Patients with emergence agitation (EA) experience disorientation and confusion specifically during the emergence from anesthesia, which manifests in hyperactivity and potentially violent behaviors^[96]. EA is most common amongst children, with very young children

(between 2-5 years old) at the highest risk for experiencing EA. Surgery type appears to affect incidence rates of EA in adults, with EA most commonly reported following ear, nose and throat surgeries^[97]. While the exact underlying cause of EA is unknown, there has been a noted increase in the rates of EA amongst children as sevoflurane and desflurane have been adopted for general anesthesia in place of halothane^[96, 98].

Accidental self-harm or harm to hospital staff are primary concerns when dealing with patients with EA. Hyperactivity and confusion during emergence can cause patients to aggravate surgical wounds, self-extubate, remove catheters, or become violent with hospital staff. Restraint and/or supplemental sedation are needed in some cases. However, beyond the immediate risk of injury due to disorientation there are few known long-term consequences associated with EA^[96]. Some children experience behavioral regression in the postoperative period known as postoperative behavioral change (PBC)^[96, 98]. There is a greater frequency of disturbances in nighttime behaviors (such as night terrors, bedwetting and sleeping in parent's bed) amongst children with PBC and PBC is also more common following anesthesia with sevoflurane than with haloflurane.

EA is wholly different from PACU delirium or POD and linkages between EA and increased risk for later neurocognitive disturbances may not exist (Figure 1.6). The nomenclature for EA has historically been inconsistent and made interpretation of previously published data difficult. Previous papers have referred to EA as emergence delirium while using inclusion criteria that would apparently only be suitable for the hyperactive subtype of delirium. The most recent recommendations regarding the standardization of screening processes for postoperative neurocognitive changes have determined that a lucid period following anesthesia should not be used as a distinction between EA and delirium^[99]. This would effectively replace EA as a

separate diagnosis or research designation in the future. Instead what is currently referred to as EA would be replaced with postoperative delirium without lucidity. However, for interpretation of currently published data, presentations of EA are considered continuous with the emergence from anesthesia, whereas diagnosis of delirium occurs after emergence from anesthesia.

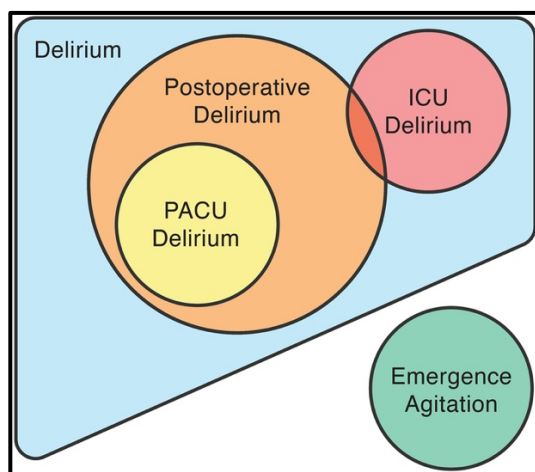


Figure 1.6 – Associations between different delirium subtypes.

PACU delirium is associated with future diagnosis of POD and can be considered subtype of POD. The primary determinant of ICU delirium is diagnosis within the ICU. Depending on patient factors, POD can synonymous with ICU delirium if patients are admitted to the ICU. Emergence agitation is considered separate from delirium. Adapted from Safavynia et al. 2018, An update on postoperative delirium: Clinical features, neuropathogenesis, and perioperative management^[100] with permissions through RightsLink.

1.6.2 PACU Delirium

PACU delirium describes a positive delirium diagnosis following surgery on the day of the operation. The risk for PACU delirium has been associated with administration of perioperative opioids, length of operation, patient age, and high-risk surgery^[101]. Little is known about the association between PACU delirium and longer-term health effects. PACU delirium

can be assessed throughout a patient's stay in the PACU and for the majority of patients, delirium resolves between PACU admittance and discharge^[102]. However, diagnosis of PACU delirium at the time of discharge is associated with increased rates of POD^[101, 103-106]. The hyperactive subtype of PACU delirium increases the risk for accidental self-harm in patients or harm to hospital staff. PACU delirium has also been associated with longer hospital length of stay (LOS) in multiple studies^[103, 104], although one study found increased LOS in patients displaying only the hypoactive subtype^[104].

There are a variety of screening tools currently being used between institutions for PACU delirium assessment, which has led to complications in the evaluation of results gathered between clinical cohorts. Publications have previously used the Nursing Delirium Screening Scale, Confusion Assessment Method for the Intensive Care Unit, Intensive Care Delirium Screening Checklist, Delirium Detection Score, Richmond Agitation-Sedation Scale, Riker Sedation Scale, and the DSM-IV for PACU delirium diagnosis^[101]. These scales differ in their consideration of delayed arousal, confusion and/or cognitive impairment in the detection of delirium. The Richmond Agitation-Sedation Scale and Riker Sedation Scale may only be adequate for detection of the hyperactive or mixed subtypes of delirium as these tools score patients on their level of arousal and agitation^[101]. Additional diagnosis strategies utilizing qEEG analysis during anesthesia maintenance and emergence (covered further in subsection 1.7.4)^[107], pupillometry^[108], and tools for more complete categorization of postoperative arousal and cognitive performance^[109] have proven useful for detection of PACU delirium.

1.6.3 Postoperative Delirium

Postoperative delirium is delirium diagnosed in the days to weeks following an operation, with the varied inclusion criteria typically beginning at postoperative day 1 and extending from

postoperative day 5 to as late as day 30. Compared with PACU delirium, there is more robust information available about POD risk factors and presentation as well as the long-term health problems associated with POD. The majority of POD diagnoses present with either the hypoactive or mixed subtypes of delirium. As a result, rates of POD are likely underreported as confusion and cognitive impairments in patients with hypoactive delirium can easily be missed without proper screening procedures. POD incidence rates can vary widely depending on the patient cohorts studied, from 5-70%. Patient age, preexisting cognitive impairments and surgery type are all associated with POD, with cardiac and emergency surgeries inferring especially high patient risk. POD is also associated with increased hospital length of stay, accelerated cognitive decline, and even patient mortality.

Delirium itself has a complicated and poorly understood pathogenesis, with a number of proposed underlying factors including neurotransmitter imbalance, neuroinflammation endothelial dysfunction, and impaired aerobic metabolism. As a result, there are currently no pharmacological agents that are effective for the treatment of POD. The best current course of treatment involves identification of risk factors for POD/PACU-D prior to surgery to reduce the likelihood of a missed diagnosis during recovery^[100]. Brief cognitive assessments, such as the Mini-Cog, can be employed to quickly gauge whether a patient is going into surgery with a pre-existing cognitive impairment. Guiding perioperative anesthesia maintenance with EEG can reduce patient risk for POD, as well as avoiding the use of longer-acting intraoperative opioids. When delirium is present postoperatively, there are recommended steps that can be taken in the PACU to help reduce recovery time including early mobilization, addressing sensory impairments, and avoiding sleep disturbances.

Functional imaging and EEG recordings suggest that delirium occurs when cortical integration of complex information (CICI) is impaired. Postoperative delirium has been associated with slowing of the EEG trace (corresponding with less cortical information), with increased δ and θ power which sometimes does not resolve even after eye-opening^[110]. Functional imaging studies have shown reductions in directed connectivity during hypoactive delirium^[110] and increased functional connectivity between brain areas in the default mode (DFN) and task positive networks (TPN)^[111]. This is important because the posterior cingulate cortex (from DFN) and dorsolateral prefrontal cortex (from TPN) are typically anticorrelated in awake individuals. The strength of anticorrelation is associated with consistency of performance on behavioral tasks^[112] and disorders of attention^[113].

1.6.4 Postoperative Cognitive Dysfunction

POCD is a research designation that describes a change in cognition between a pre-surgery assessment and follow-up assessment from 1 month to potentially many years following surgery. Patient age is the most consistent risk factor for POCD^[114]. Longitudinal studies on the outcomes of patients with POCD have identified POCD as a risk factor for loss of independence and increased mortality^[115]. While other risk factors have been identified on a study-by-study basis, differences in screening criteria and inclusion criteria (between baseline and follow-up assessment) makes the interpretation of conflicting findings difficult. In response to these difficulties a change in nomenclature has been suggested from POCD to mild or major neurocognitive disorder (NCD)^[99]. NCD criteria are outlined in the DSM-5 which is likely to standardize future screening methods.

Studies on the effects of general anesthesia in animals support the idea that exposure to anesthetic drugs alone can cause persistent cognitive problems associated with increased

neuroinflammation^[116-119]. Human studies, including the first and second International Study on Postoperative Dysfunction (ISPOCD)^[120, 121], found patient age to be the only reliable risk factor for POCD at 3 months. The ISPOCD2 group found similar rates of POCD in patients receiving general and regional anesthetic for major non-cardiac surgery. These findings seem to support the hypothesis that the pathology of POCD is related to the stress of surgery rather than response to general anesthetics, however there are a couple caveats to this finding: 1) it is worth noting that the regional anesthetic group did receive light sedation with propofol & 2) another cohort study on middle aged patients from the ISPOCD2 group found increased POCD with additional administration of regional anesthesia^[122].

There has been doubt expressed about the validity of approaches to studying POCD and the potential for the cognitive decline associated with POCD to be better explained by normal decline due to aging^[123]. These concerns should be addressed by the recent recommendations from the Nomenclature Consensus Working Group^[99]. Standardization of the cognitive testing used for POCD assessment and alignment of POCD diagnosis with the DSM-5 description of mild and major neurocognitive disorders should offer more robust and comparable results between research groups in the near future.

1.6.5 Anesthesia Awareness With Recall

Anesthesia Awareness With Recall (AWR) occurs when a patient is not sufficiently anesthetized and recalls events from surgery. AWR is rare in patients undergoing surgery and many reported incidents of AWR are not reported to cause distress^[124]. However, some patients experience depression or PTSD following AWR and in some cases patients have perceived pain during surgery as a result of AWR^[125]. Potential clinical scenarios leading to insufficient anesthesia include: 1) Equipment malfunction or anesthesiologist error, 2) Inability to detect

patient awareness due to the use of muscle relaxants & 3) Patient factors predisposing individuals to increased resilience to anesthetic drugs^[124].

While AWR is not associated with a postoperative state of confusion, it is worth mentioning because it is a significant cause of preoperative anxiety^[126], despite the low incidence rate of AWR. Preoperative anxiety is not linked with rates of POD^[127] or POCD^[128], but it is a significant predictor of emergence agitation^[129]. Additionally, preoperative anxiety may affect baseline cognitive testing which must be performed prior to surgery in the assessment of POCD^[130]. The timeframe of neurological complications during and after surgery are represented in Figure 1.7 below.

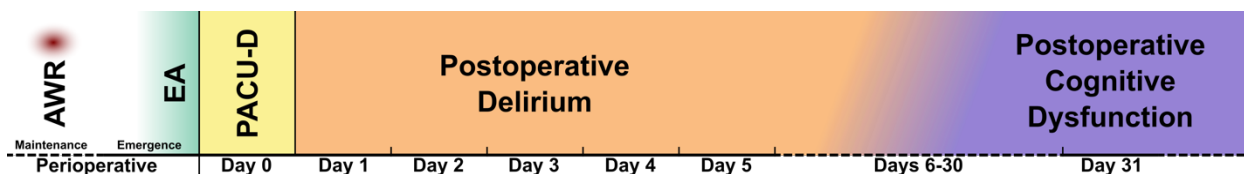


Figure 1.7 – Timeframe for the presentation of perioperative and postoperative cognitive changes.

Anesthetic awareness (AWR) occurs due to insufficient delivery of anesthesia during surgery. AWR is rare, but when it does occur the period of awareness is often transient. Emergence agitation (EA) describes a hyperactive emergence from anesthesia. The etiology, risk factors and associated health problems ascribed to EA differ from other postoperative cognitive changes. Postanesthesia care unit delirium (PACU-D) is a delirium diagnosis during recovery on the day of surgery. Postoperative delirium (POD) is a delirium diagnosis in the days to weeks following surgery. Persistent declines in cognitive performance from a pre-surgery baseline that last months to years postoperatively are referred to as Postoperative Cognitive Dysfunction (POCD).

1.7 General Anesthesia and Postoperative Cognitive Impairments

1.7.1 General Anesthetics and Neurotoxicity

Current research suggests that general anesthetics are neurotoxic, with two major caveats: (1) These effects are most prominent in critical age ranges, namely during early childhood and advanced aging & (2) much of the available data comes from rodents and these results have not yet been replicated in humans.

Anesthetic neurotoxicity is a major concern in pediatric anesthesia. Ketamine, isoflurane and a commonly used anesthetic cocktail (midazolam, nitrous oxide & isoflurane) cause increased apoptosis and impaired neuronal stem cell proliferation and differentiation in developing rats^[131-133]. Results have been varied when the long-term behavioral effects of early life exposure to anesthesia have been studied in preclinical models. Most studies report the presence of neurotoxic processes associated with acute behavioral change, but these differences resolve after days or weeks of recovery. However, persistent behavioral differences following early life anesthesia exposure have been reported. Duration of exposure, differences in anesthetics and selection of rodent strains with more genetic variability have all been hypothesized to explain these inconsistent results^[134, 135]. Replication of cellular impairments has not been possible in human studies, but some cohort studies have shown evidence of learning and memory deficits throughout development following pediatric surgery^[136, 137]. However, the results of these studies do not specifically implicate general anesthesia in the development of cognitive deficits. Other surgical factors and health status prior pediatric surgery may be equally likely to explain later decreases in learning and memory performance.

In aged populations, concern regarding neurotoxicity has focused on the potential for anesthetic drugs to stimulate production of proteins related to AD pathology. Increased amyloid-

β aggregation has been observed following 2-hours of isoflurane exposure^[138]. This same experiment also noted an increase in activation of caspase 3, which could indicate increased apoptotic signaling. Similar results have been shown following isoflurane exposure in naive human H4 neuroglioma cells as well as those overexpressing APP^[139]. Disruptions in Ca^{2+} homeostasis following isoflurane exposure have been demonstrated in cell culture and could be a potential mechanism for isoflurane induced neuron death^[140]. In aged humans, neuronal death following anesthetic exposure may be of greater concern, due to age-related decreases in neuron numbers and a slowing of neurogenesis in areas like hippocampus.

1.7.2 General Anesthetics and Neuroinflammation

Inflammation is a natural response at the site of surgery. In healthy patients that are resilient to the stimulus of surgery, the inflammatory response is likely acute, mostly peripheral and a non-factor in cognitive recovery from surgery. However, neuroinflammation following surgery with anesthesia has been associated with increased risk for POD, POCD and increased neuronal damage in AD. The hypothesized mechanisms for neurological and cognitive insults due to neuroinflammation converge on a similar sequence of events^[114, 141, 142]:

- 1) Acute peripheral inflammation is caused by the noxious surgical stimuli
- 2) There is an increase in pro-inflammatory cytokines in response to inflammation near the surgery site
- 3) Pro-inflammatory cytokines disrupt the blood brain barrier (BBB) increasing permeability
- 4) Microglia are activated in response to cytokines released by bone marrow derived monocytes (BMDM) which cross the more permeable BBB

- 5) Activated microglia can disrupt neurotransmitter systems through cytokine release and damage neurons through release of reactive oxygen species or stimulation of glutamate neurotoxicity
- 6) Activated microglia also activate more microglia and recruit more BMDMs via release of cytokines

This mechanism can further be potentiated by a few additional factors. Risk of POD, POCD and AD increases with age. Age is also associated with increased BBB permeability making the transition from peripheral inflammatory signaling to neuroinflammation more likely. In addition, chronic increases in neuroinflammation are likely in patients with AD. While there has not been much direct association demonstrated between anesthetic agents and neuroinflammation, anesthetic dose can have profound effects on BBB permeability^[143, 144]. Research on this effect has thus far been confined to volatile anesthetics, but BBB permeability increases throughout cortex and thalamus at isoflurane concentrations associated with high burst suppression ratios. The decreased sensitivity to anesthetics seen during normal aging may make anesthetic-induced permeability of BBB an even greater concern.

1.7.3 General Anesthetics and Neurophysiology

Guidance of anesthesia using raw EEG or index values based on qEEG information has been effective for reducing AWR, rates of POD, and the amount of anesthesia delivered during surgery^[145-153]. Some studies have also demonstrated effectiveness at reducing risk of POCD when BIS monitors are used to guide surgical anesthesia, but results are less consistent. Quantitative EEG analysis during maintenance and emergence from anesthesia can be used to identify risk for postoperative pain^[154] or the development of PACU delirium^[107]. Spectral features of the EEG can be used to classify different “patterns” of EEG, similar to the EEG

classifications of sleep stages^[154] (Figure 1.8). During anesthesia, EEG voltage recordings are dominated by higher amplitude, lower frequency changes than seen during wakefulness. General patterns in anesthesia can be separated using relative power in delta (0.5-4 Hz) and alpha (8-14 Hz) frequency bands. Increases in alpha frequency during unconsciousness are also seen in sleep spindles present in Stage 2 NREM sleep. Spindle production is associated with greater sleep stability during Stage 2 & 3 NREM sleep and increased threshold from arousal from sleep^[155].

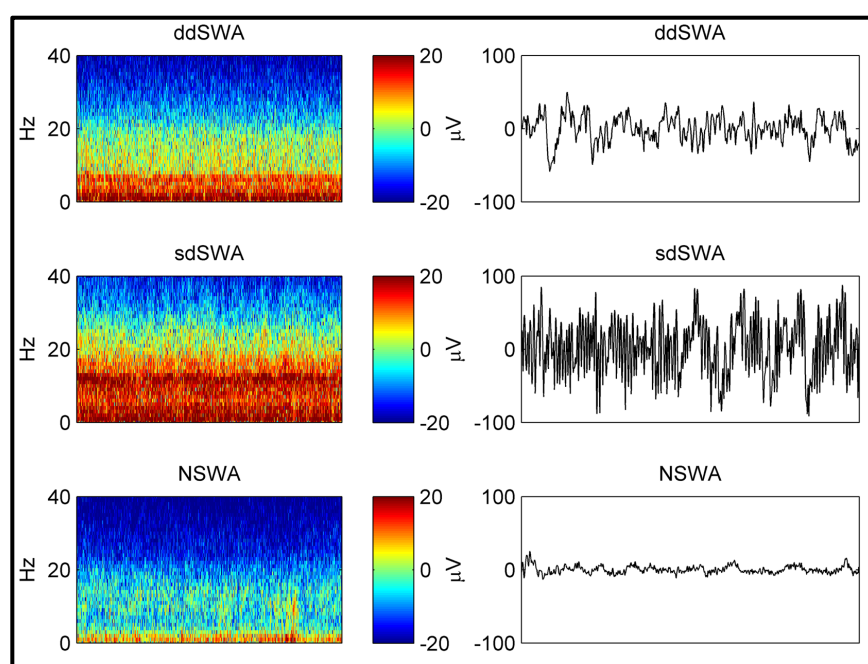


Figure 1.8 – Patterns of EEG during end maintenance of sevoflurane anesthesia as determined by features from the EEG power spectrum.

Panels in the left column display spectrograms depicting the relative EEG power across slow-wave frequency bands. The right column depicts 10 seconds of the raw EEG time series corresponding with each anesthesia EEG pattern. Delta dominant slow wave anesthesia (ddSWA) occurs when the relative delta power (0.5-4 Hz) is higher than alpha-spindle power (8-14 Hz). Spindle dominant slow wave anesthesia (sdSWA) occurs when relative alpha power is higher than delta power. Non-slow wave anesthesia is seen rarely and occurs when power is low in both the delta and alpha frequency bands. Adapted from Chander et al. 2014, Electroencephalographic Variation during End Maintenance and Emergence from Surgical Anesthesia^[154], made available under a Creative Commons CC0 public domain dedication.

Anesthesia emergences that mimic the natural waking from sleep (NREM to REM to wake) are associated with lower incidence rates for postoperative pain. In these patients, emergence from anesthesia features EEG transitions from patterns with high power in slow wave frequency bands (both delta dominated patterns or spindle dominated patterns), to non-slow wave anesthesia and finally to wake. Emergence with transitions straight from slow wave anesthesia to waking were associated with the most postoperative pain, and mimic arousal patterns from sleep that are associated with parasomnias^[156, 157]. When similar analysis of EEG emergence trajectories was applied to a large cohort of surgical patients, emergence trajectories lacking spindle dominant patterns were associated with increased risk for PACU delirium (Figure 1.9). This same analysis found episodes of burst suppression during maintenance of anesthesia to be an independent risk factor for PACU delirium and unassociated with emergence trajectories.

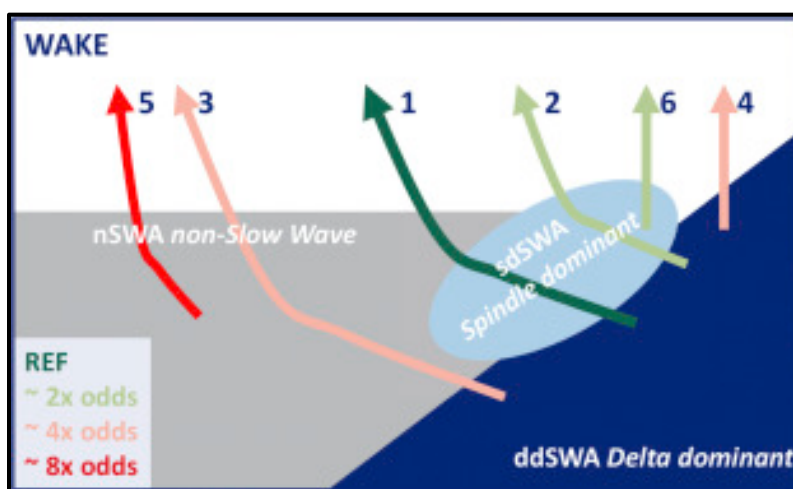


Figure 1.9 – Different emergence trajectories from surgical anesthesia are associated with increased risk for PACU delirium.

Emergence trajectory 1 was associated with the lowest risk for PACU delirium. This trajectory included a transition from delta dominant (ddSWA) to spindle dominant slow

wave anesthesia (sdSWA) followed by non-slow wave anesthesia (nSWA) before reaching wakefulness. Trajectories 2 and 6 featuring sdSWA before waking feature the next lowest odds ratio for PACU delirium. Trajectories 3 and 4 feature ddSWA but not sdSWA and are at higher risk for PACU delirium. The highest odds ratio for PACU delirium was seen in trajectory 5, nSWA to wake. Adapted from Hesse et al. 2019, Association of electroencephalogram trajectories during emergence from anaesthesia with delirium in the postanaesthesia care unit: an early sign of postoperative complications^[107] with permissions through RightsLink.

The appearance of burst suppression during anesthesia is not necessarily associated with decreased cognitive performance in young, healthy participants^[158]. However, the appearance of burst suppression during surgery has been associated with increased rates of POD in large clinical studies^[148, 159] and also associated with increased risk for PACU delirium^[107]. During normal aging, there is an average decrease in the mass of white and grey matter present in the brain which subsequently leads to a decrease in the average EEG power. Normal aging is also associated with a decreased sensitivity to anesthetic drugs, meaning aged patients can exhibit burst suppression at lower anesthetic concentrations. Burst suppression varies in its detection by processed EEG monitors. There is little correlation between BIS monitor values and the burst suppression ratio until suppression ratios are above 40%^[160]. This correlates with BIS readings of 0-30. BIS-guided titration of anesthesia usually recommends surgical anesthesia be administered to maintain patients between values of 40-60. BIS-guidance of anesthesia has shown success improving cognitive outcomes following surgery, however it is worth noting that using BIS alone will likely lead to false negatives in reporting of burst suppression patterns with suppression ratios below 40%. Many devices simultaneously display the raw EEG waveform and may be of benefit beyond the dimensionless index displayed by intraoperative consciousness monitors.

1.9 Gap in Knowledge

A large proportion of the inpatient and outpatient surgeries occur in patients over the age of 65, even though this age group only represents 15% of the US population^[161]. In 2010, approximately 40% of inpatient surgeries and 33% of outpatient surgeries were performed in patients over 65^[162]. These numbers have increased since 2006 (35.3% and 32.2%, respectively) and are expected to continue to increase as average age of the US population increases.

As the average US surgery patient gets older, it will become more and more important to understand the impact that diseases associated with aging will have on surgical outcomes. Two diseases in particular, Alzheimer's Disease (AD) and Type 2 Diabetes Mellitus (T2D), are both of particular importance when considering the risk of perioperative neurocognitive disorders. Disease risk increases with age for both AD and T2D, and as a result the number of surgery patients with AD and T2D will increase in the future. Both diseases have also previously been demonstrated to increase the risk for diagnosis of perioperative neurocognitive disorders. Given the lack of clinical studies on the effects of surgery and general anesthesia on patients with AD and T2D specifically, it is important that alternative approaches are used to investigate why these conditions increase the risk for postoperative cognitive problems. Recent studies, such as those published by Hesse et al. 2019, have demonstrated clear associations between altered emergence and recovery from anesthesia with the later appearance of postoperative delirium^[107]. With this in mind, the present work was undertaken to characterize the emergence and recovery from anesthesia in rodent models of AD and T2D.

1.10 Thesis Outline

Chapter 1 has introduced much of the history of anesthesia, as well as the study and practical considerations of the use of general anesthetics in surgery. While all research in the use of anesthetics seeks to better understand and guide their use in humans, it can often be technically challenging or impossible to use humans as a model for research. Preclinical models can be an important tool for validating and testing hypotheses on the mechanisms underlying the effects of anesthetic drugs. **Chapter 2** will focus on AD-like disease progression in the TgF344-AD rat model. This model has great potential value in helping to understanding how neurodegenerative processes can affect the brain's response to anesthetic drugs. **Chapter 3** details the results of our experiments on the emergence and recovery from general anesthetics in TgF344-AD rats. **Chapter 4** will investigate exercise as a potential strategy for improving recovery from anesthesia in a rodent model with a potential for impaired recovery, the Goto-Kakizaki model of type 2 diabetes. **Chapter 5** discusses the findings of these experiments within the context of what is currently known about the field and suggests potential avenues for future investigation. Extended methods for data analysis are included in the Appendix in **Chapter 6**.

Chapter 2 - Angiotensin Receptor Blockers as a Mediator of AD-like Cognitive Dysfunction **in the TgF344-AD Rat Model**

Adapted From: Candesartan treatment preserves learning and working memory performance in the TgF344-AD rat. Christopher G. Sinon, Jing Ma, Xiancong Zhang, Peter-Jon C. Williams, Paul S. Garcia, Roy L. Sutliff, Ihab M. Hajjar. In Prep.

2.1 Abstract

With increasing ability to identify the prodromal and early stages of Alzheimer's disease (AD) in humans, there are new opportunities to develop treatment strategies that will slow or halt the presentation of clinical AD. AD, cardiovascular disease and vascular dementia share many common risk factors and there is evidence of widespread vascular dysfunction as part of AD. AD progression was monitored via behavioral assays (spontaneous alternation test, novel object recognition, water radial arm maze) and through the quantification of neuropathology in 12 and 18 month rat brains. At 12 months, TgF344-AD rats display brain pathology consistent with the early phase of AD. There is a significant increase in both amyloid- β and GFAP consistent with age-dependent progression of disease. At 12 months, there were no observed behavioral differences between wild type and TgF344-AD rats. There was a significant increase in amyloid- β accumulation between 12 and 18 months in the TgF344-AD rat, regardless of drug treatment. At 18 months, TgF344-AD rats displayed impairments in learning and an increase in perseverative working memory errors on the water radial arm maze. Our results demonstrate the progression of neuropathology and cognitive disturbances in the early disease phase in the TgF344-AD rat.

2.2 Introduction

Alzheimer's disease (AD), the most common cause of dementia, has an extended prodromal phase lasting decades before clinical phase of the disease^[163]. There is currently no known cure for AD and the available treatment options offer only symptomatic relief without altering the progression of the disease^[164, 165]. Recent advances using MRI, PET scan, and biochemical analysis of cerebrospinal fluid^[166, 167] to identify biomarkers for the initial stages of AD in humans have made it possible to focus on treatment strategies designed to slow or ideally halt the disease in the early progression. This chapter contains the results of experiments treating a transgenic rat model of AD with angiotensin receptor blockers (ARBs). Vascular dysfunction has been identified as an early event^[168], possibly the first event^[169], in the progression of AD pathology. ARBs are currently prescribed as a treatment for other conditions with symptoms of vascular dysfunction, such as cardiovascular disease, and we investigated the potential for ARBs to improve disease symptoms in AD-like rats.

2.2.1 The Amyloid Cascade Hypothesis of Alzheimer's Disease

The amyloid cascade hypothesis proposes that the cleavage of amyloid precursor protein into amyloid- β , followed by the subsequent aggregation of amyloid- β into destructive extracellular plaques, is the primary cause of AD disease progression^[170, 171]. Amyloid- β is produced following cleavage of the transmembrane protein amyloid precursor protein (APP) by beta-secretase and gamma-secretase^[172]. It is unclear exactly what role APP or amyloid- β play in a normally functioning neuron, but an imbalance between the production and clearance of amyloid- β can lead to pathologic accumulation that likely play a causative role in AD^[173]. In the 1992 Hardy & Higgins presentation of the amyloid cascade hypothesis^[171], amyloid- β 's presence in the brain increases the vulnerability of neurons to excitotoxic damage^[174-176] and increases

intraneuronal calcium concentrations, which could be a causative event for formation of neurofibrillary tangles from tau protein^[177, 178]. This model explains the pathological hallmarks of AD (amyloid plaques, neurofibrillary tangles, and neuronal cell death).

Much of the evidence supporting this method of disease progression, as well as those reviewed in other foundational papers for the amyloid cascade hypothesis^[179, 180], rely on genetic data gathered from patients and models of familial AD. Familial AD is a rare form of AD linked to mutations in three genes related to the synthesis of amyloid- β ^[181]. In healthy young adults the rate of amyloid- β clearance (8.3%/hr) measured in CSF appears to outpace amyloid- β production (7.6%/hr)^[182], but a separate study enrolling a small number of participants over age 60 found decreased clearance of amyloid- β in participants with AD, while amyloid- β production rates were similar between participating controls and those with AD^[173]. While research on the progression of familial AD has been extremely beneficial for our overall understanding of the disease, there is still much debate about the pathogenesis for the sporadic form of AD^[183].

2.2.2 The Vascular Hypothesis of Alzheimer's Disease

Longitudinal studies have identified many risk factors for the development of the sporadic form of AD. Among these, cardiovascular risk factors are common, including hypertension and obesity^[184, 185]. Greater than half of all patients with AD also show deposition of amyloid- β into the walls of blood vessels in the central nervous system, a condition known as cerebral amyloid angiopathy. Some estimates state that these conditions are comorbid in 90% of AD patients^[186]. Small vessel disease is also a risk factor for AD, and disease risk increases along with increasing severity of atherosclerosis and arteriolosclerosis^[187]. Furthermore, genetic risk factors have been identified that increase the likelihood of AD. Among these APOE4 and TREM2 confer some of the highest risk for AD^[188-190]. The exact role of these genes in sporadic

AD is unclear, but expression of both genes has been shown in decrease clearance of amyloid- β . Taken together, these examples hint towards a common pathway for amyloid- β accumulation in the brain via degradation of pathways for clearance.

The “vascular hypothesis” of AD is an alternative model for disease progression, suggesting that the development of vascular dysfunction may be an important accelerant of disease progression in AD, and potentially a cause of amyloid- β aggregation^[191, 192]. The model as proposed by De la Torre in 1994 focuses on the consistent finding that cerebral capillaries in AD display amyloid deposits and thickening of the basement membrane (amyloid angiopathy)^[193]. These two disturbances can reduce cerebral blood flow and impair the delivery of oxygen and glucose to neurons. One of the primary routes of clearance of amyloid- β from the brain is cellular transport across the blood brain barrier^[194]. However if there is a breakdown in the vasculature of the brain, such as damage to the blood brain barrier, cardiovascular disease, or deposition of amyloid into the blood vessels, this can cause poor clearance of amyloid- β and result in aggregation of amyloid plaques^[165].

2.2.3 The Renin Angiotensin System as a Therapeutic Target in Early Alzheimer’s Disease

The renin angiotensin system (RAS) regulates vascular resistance^[195]. When blood pressure decreases, renin is released by the kidney. Renin cleaves circulating angiotensinogen into angiotensin I, which is then subsequently converted into angiotensin II. Binding of angiotensin II to angiotensin II receptor subtype 1 (AT1) causes vasoconstriction and when AT1 receptors are chronically activated endothelial dysfunction and oxidative stress can occur^[196]. Angiotensin II also increases amyloid- β production by stimulating the processing of APP and increasing γ -secretase activity^[197]. However, blocking angiotensin II’s ability to bind to AT1 receptors with angiotensin receptor blockers stops these disease promoting effects in

cardiovascular conditions. Therapeutic strategies directed towards RAS may address many of the disease pathways proposed by the vascular hypothesis of AD.

2.2.4 Candesartan, An Angiotensin Receptor Blocker (ARB)

In 2002, Hardy and Selkoe published an update to the amyloid cascade hypothesis in *Science*. In it, they describe six potential therapeutic targets for the treatment of Alzheimer's disease based on updated models for disease pathology^[198]. Two are of potential interest for these experiments:

- (1) The enhancement of clearance of amyloid- β from the cerebral cortex.
- (2) Treatment of the inflammatory response to the presence of amyloid- β in the cerebral cortex

Candesartan offers the potential of a drug treatment for both targets. Candesartan is an angiotensin receptor blocker acting on AT1, blocking vasoconstriction mediated by angiotensin II and causing vasodilation and reduction in blood pressure^[13]. Candesartan can cross the blood brain barrier^[199] and also has potent anti-inflammatory effects, which have been demonstrated both peripherally^[200] and in the mediation of inflammatory responses in the brain^[199, 201, 202]. The FDA has approved Candesartan for use in humans, in the treatment of hypertension and heart failure^[203]. Analysis from available AD patient cohorts suggest that patients using ARBs specifically, as opposed to other hypertensive drugs, experienced slower progression of the disease, as measured by both cognitive symptoms and amount of amyloid deposition^[204, 205]. These results suggest that candesartan may be a promising treatment option in the early progression of AD.

2.2.5 *The TgF344-AD Rat Model*

The TgF344-AD rat presents a unique preclinical model for the study of the early stages of AD. The model expresses two genes linked to familial Alzheimer's disease, mutant human APP_{sw} and PS1 Δ E9, and progressive neurodegeneration that recapitulates human AD-like disease hallmarks^[206]. These rats display amyloid plaques, hyperphosphorylated tau, neurofibrillary tangles, neuroinflammation, neuronal loss and behavioral deficits with a stereotyped progression across the lifetime of the rat. Amyloid begins to accumulate in the TgF344AD rat by 6 months and consistently increases through age 15 months. At this age, cognitive symptoms and tauopathies are both present^[206, 207].

2.2.6 *Summary*

This chapter contains the results from our characterization of cognitive performance and pathology in the TgF344-AD aged to 12 months. At this developmental period, there are significant increases in amyloid deposition in the brain, but cognitive symptoms of AD have not been fully detailed. These results will provide a baseline with which to compare the effects of anesthesia in a rodent model of the early stage of AD. Chapter 3 will investigate the effects of anesthesia on TgF344-AD rats aged to 12 months. Also included in this chapter are the results of 6 months of daily candesartan administration on cognitive performance, pathology and vascular function in TgF344-AD rats aged to 18 months. Candesartan is hypothesized to increase the clearance of amyloid- β by sustaining proper vascular function during disease progression. AD is associated with vascular changes due to amyloidosis of the vessels in the brain and due to an association with overall poor vascular health. These results provide some insight into cerebrovascular function in the TgF344-AD rat model.

2.3 Experimental Design and Hypotheses

The goal of the present study was to utilize the TgF344-AD rat to study the effects of vascular dysfunction in the early phase of AD-like neurodegeneration. Cognitive testing consisting of the continuous spontaneous alternation test and novel object recognition test were performed in the week before rats turned 12 months of age. The continuous spontaneous alternation test is used as an assessment of spatial working memory and locomotor activity^[208]. This test involves the rat freely exploring a Y-maze for 8 minutes while the investigator tracks the pattern of arm entries. Rodent models of AD have previously been shown to show a decrease in alternation behaviors^[209] and the loss of spontaneous alternation in rodents has also been linked with hippocampal damage^[210]. Novel Object Recognition is a test of recognition memory^[211]. With short intertrial intervals between training sessions and testing sessions, recognition of the novel object is thought to rely on functioning of the hippocampus and perirhinal cortex^[212].

We administered the angiotensin receptor blocker, Candesartan, an angiotensin II type 1 receptor antagonist, to regulate activation of the RAS in TgF344-AD rats during a critical early period in progression of the rodent form of AD. The timeline of behavioral experiments and drug administration is presented in Figure 2.1. Water Radial Arm Maze was performed at 17.5 months for a total of 12 days to assess learning and spatial working memory. Blood pressure measurements were taken from all rats receiving vehicle and candesartan at the age of 18 months. All rats were then sacrificed with brains collected for quantification of AD-like pathology.

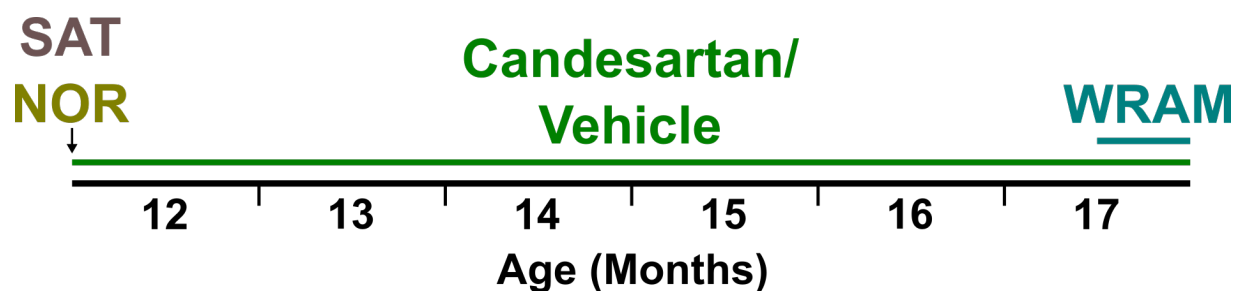


Figure 2.1 – Timeline of behavioral experiments.

SAT and NOR were performed in the days before the start of candesartan (or vehicle) treatment. Drug (or vehicle) treatment continued daily until the rats were aged 18 months. Rats in all experimental groups were tested on the WRAM for 12 total days starting when the rats were aged 17.5 months.

We hypothesized that treatment with an ARB (candesartan) during the early progression of AD would alleviate AD-disease pathology and rescue behavioral deficits in the transgenic rats. We expected to see a decrease in levels of amyloid- β and a marker of astrocyte activation (glial fibrillary acidic protein or GFAP) throughout the brain and specifically within hippocampus in TgF344-AD rats after ARB treatment. We also expected to see improvement in learning and working memory performance for the TgF344-AD rats receiving candesartan on the WRAM at 18-months.

2.4 Methods

2.4.1 Animals

All experiments were conducted at the Atlanta VA Health Care System Animal Facility using rats bred from an established colony of TgF344-AD rats. Transgenic rats and wild type littermates were used for data collection. The rats were housed in 12-hour light cycles with ad libitum access to rodent chow and water. All studies were approved by the Atlanta VA Institutional Animal Care and Use Committee.

2.4.2 Continuous Spontaneous Alternation Behavior Test

The Continuous Spontaneous Alternation Test was performed within a Y-maze. Rodents introduced to a Y-maze display a tendency to alternate arm entries during maze exploration. This tendency towards alternation is thought to result from a preference towards investigation of new environments, and the SAT takes advantage of this behavior as an assessment of spatial working memory^[213]. Rats were allowed to freely explore the Y-maze (San Diego Instruments, San Diego, CA, USA) with all three arms open for 8 minutes. Testing was performed between 12:00-3:00PM during the light phase. If at any time the rat remained stationary for >60 seconds during the session, movement was motivated by briefly grasping and releasing the rat from the base of the tail. The number of arm entries and the path of arm exploration were determined by a blinded observer.

A successful alternation was scored when the rat completed three consecutive arm entries via turns in the same direction. Alternation percentage was determined using the following equation^[214]:

Equation 1:

$$\text{Alternation percentage} = \frac{\# \text{ of Alternations}}{\text{Total \# of Arm Entries} - 2} * 100$$

2.4.3 Novel Object Recognition Test

Following completion of the Y-maze, rats were tested for attention and working memory performance using the novel object recognition test. Testing was performed between 9:00AM-12PM during the light phase. On the first day, rats were allowed to freely explore a high-walled open field arena for 15 minutes to acclimate to the testing environment. On the second day, rats were given another 15 minutes to acclimate to the testing environment. Following a 30-minute break, rats began the training phase of the novel object recognition test. Two identical non-odorous plastic toys (A1 & A2) were affixed with one on each end of the testing environment.

Rats were placed into the center of the environment and given seven minutes to explore the testing environment during the training phase. Rats were then returned to their transfer cage for a 5-minute inter-trial interval. The choice phase was completed using a third identical plastic toy (A3) and new non-identical plastic toy (B). Each phase was recorded by an overhead video camera and the behavioral data was autoscored using Ethovision XT11.5 software (Noldus Information Technology, Wageningen, The Netherlands). For each rat, the time spent on each side of the environment and the time spent exploring each object, measured as the amount of time each rat's nose entered a 2.5-cm radius of the object, was recorded for each session. The novel object observation time (TN) and the familiar object observation time (TF) were recorded. The discrimination index for the testing phase was calculated by $(TN-TF)/(TN+TF)$. Animals were excluded if they did not cross the midpoint of the arena during any of the phases. Animals were also excluded if they spent more than 80% of total object observation time with either object during the training phase.

2.4.4 ARB Treatment

From 12 to 18 months of age, all rats on study were treated daily with either the angiotensin receptor II blocker, candesartan, or vehicle (saline). ARB treatment experimental groups were presented with 5 mg/kg of candesartan in the morning between 10:00AM-12:00PM. Peanut oil proved to be an effective method of daily oral administration for the ARB treatment. All rats on study consistently consumed all of the peanut oil they were offered, regardless of whether it contained candesartan or vehicle. Rats treated with this ARB for one week had no pressor response to an Angiotensin II infusion (data not shown).

2.4.5 Water Radial Arm Maze

The Water Radial Arm Maze (WRAM) consists of eight evenly spaced arms radiating out from a central area. Our protocol for use of the WRAM was adapted from [215]. The maze was filled with opaque water to hide the presence of four escape platforms at the ends of specific maze arms. Unique room cues were placed on the walls around the maze.

At ~17.5 months of age, rats were trained to complete the WRAM for 12 consecutive days. Each training session consisted of four trials which were completed when the rat found an escape platform. Before the first session, each rat was randomly assigned escape platform placements that could be navigated using the cues surrounding the maze and which stayed consistent for all 12 sessions.

Upon finding an escape platform, the rat was allowed to remain on the escape platform for 15 seconds and then placed in a cage under a heat lamp for a 30-second intertrial interval. The discovered platform was removed from the maze after each trial. On any trial, if the rat failed to escape the maze within 120-seconds, they were guided to the nearest platform to complete the trial. Therefore, each rat interacted with all four escape platforms during each training session. For each trial, the latency to find an escape platform and the pattern of arm entries during maze exploration was manually scored by an experimenter blinded to each rat's experimental group assignment. Testing was performed between 10:00AM-2:00PM during the dark phase.

2.4.6 Blood Pressure Readings

Blood pressure measurements were obtained from the femoral artery at 12 months and 18 months of age in the presence and absence of candesartan treatment. Briefly, rats were anesthetized with isoflurane while maintaining a 37 degrees C body temperature on a

thermostatic heating table. The hindlimb region was shaved and disinfected, an incision was made and the vessel was isolated using blunt dissection, avoiding damaging nerve fibers. The isolated artery was tied distally, and a second suture was looped around the vessel proximal to where the cannula will be inserted. A trocar needle was used to puncture the vessel and a high-fidelity catheter (Transonic Systems) was inserted into the vessel. Blood pressure was monitored for 15-20 minutes.

2.4.7 Tissue Collection

Rats were deeply anesthetized using isoflurane for tissue collection. Cardiac perfusion was performed using ice cold phosphate buffered saline. Rat brains were rapidly extracted and bisected into hemispheres. The hemisphere used for immunochemistry was fixed in 4% paraformaldehyde and then transferred to a phosphate buffered saline storage solution containing 0.01% sodium azide. The hemisphere used for proteomics analysis was flash frozen in liquid nitrogen and stored at -80°C.

2.4.8 Tissue Sectioning and Immunohistochemistry

Brain tissue sections were embedded in paraffin and sliced at 8 microns. Sections were deparaffinized and immunohistochemically labeled with antibodies to amyloid- β (4G8) and astrocyte activity (GFAP) on a ThermoFisher autostainer. Amyloid- β sections were pretreated with formic acid, blocked with normal serum, and incubated with primary antibody at 1:10,000, then exposed to biotinylated secondary antibody followed by avidin-biotin complex (Vector ABC Elite kit) and developed with diaminobenzidine (DAB). GFAP sections incubated with primary antibody (anti-GFAP, Dako, Santa Clara, USA) at 1:5000, then exposed to primary antibody enhancer followed by HRP polymer (ThermoScientific UltraVision LP Detection System) and developed with diaminobenzidine (DAB).

2.4.9 Quantification of Immunohistochemistry

High resolution digital scans of stained brain slices were analyzed using Qupath software^[216]. Positive pixel count analysis was performed on slices stained with 4g8 for amyloid- β and GFAP for astrocyte activity. Positive pixel percentage, a measure of the ratio of positively stained pixels to total number of image pixels, was recorded to quantify markers for AD-like pathology in rat brain tissue. Expanded methods for image analysis are detailed in Appendix 1.

2.4.10 Statistical Analysis

Statistical testing was performed using Prism 7.0 (GraphPad Software, San Diego, CA, USA) and IBM SPSS Statistics V26 (IBM Corporation, Armonk, NY, USA). A sample size of 10 rats per group was justified based off of preliminary data collected in the 3xTgAD mouse model. Preliminary data in this model showed a 29% decline in amyloid- β accumulation. Power analysis in G*Power 3.1.9.4 with $\alpha=0.05$, $\beta=0.80$ and an anticipated effect size of 0.8 was adequate to detect a minimal effect of candesartan of 11%. All datasets were tested for normality using the Shapiro-Wilk test. Tests for normality perform poorly with sample sizes comparable to those used in these experiments, so we compared the Shapiro-Wilk test results against visual inspection of the data distributions in the selection of non-parametric vs. parametric tests. Neuropathology data were analyzed with Student's t-test with Welch's correction or Two-way ANOVA with Sidak's test for multiple comparisons. One-way ANOVA was used to analyze changes in neuropathology between 12 and 18 months of age. Student's t-test for independent samples was used for analysis of data from the continuous spontaneous alternation test. For the NOR, the 95% confidence interval was computed for each group. We determined that each group recognized the novel object if the 95% confidence interval did not cross the line at $DI=0.0$

(signifying performance at the level of chance). MAP data was analyzed by One-way ANOVA. WRAM data was analyzed using Two-way ANOVA with Sidak's test for multiple comparisons. Planned contrasts to analyze drug effects on learning and memory performance were analyzed using Sidak's test for multiple comparisons.

2.5 Results

2.5.1 Amyloid- β and GFAP are increased in the hippocampus of 12-month old TgF344-AD rats

Coronal slices taken from approximately -2.5mm posterior from bregma were used to quantify amyloid- β and GFAP staining at the level of the dorsal hippocampus (Figure 2.2A-D). At 12-months old, there were significant increases in amyloid- β throughout the brain slices that were collected to quantify AD-like pathology. Image analysis revealed that there were significantly more pixels that were positive for amyloid- β staining in the hemisphere slices taken from TgF344-AD rats than from WT rats (Student's t-test with Welch's correction, $p < 0.001$, Figure 2.2E). Additionally, there was an increase in GFAP staining across the brain slices collected from TgF344-AD rats when compared with WT rats (Student's t-test with Welch's correction, $p < 0.013$, Figure 2.2I). Similar results were found when quantification was focused on the region of dorsal hippocampus specifically. Both amyloid- β ($p < 0.001$, Figure 2.2G) and GFAP ($p = 0.004$, Figure 2.2K) staining was increased in the dorsal hippocampus of TgF344-AD rats.

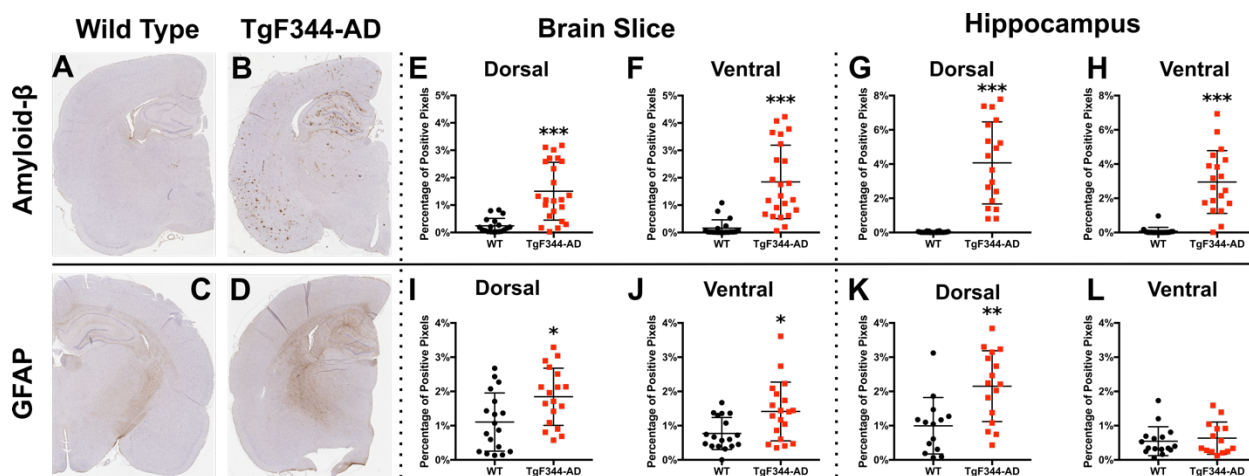


Figure 2.2 – Changes in neuropathology at 12-months for TgF344-AD rats.

At 12-months there are significant differences in amyloid- β and GFAP compared with WT rats. Significance level is denoted as *** for $p < 0.001$, ** for $p < 0.01$, and * for $p < 0.05$. A-D) Examples of stained brain slices used for quantification of amyloid- β and GFAP. DAB staining for amyloid- β and GFAP appears brown on the slides. E-H) TgF344-AD rats display increased accumulation of amyloid- β throughout the entire slice and localized specifically to hippocampus at 12 months (Student's t-test with Welch's correction, $p < 0.001$ for all). I-J) There was a general increase in GFAP throughout the hippocampal formation of TgF344-AD rats at 12 rats. K) However, only the dorsal hippocampus displayed an increase in GFAP over the WT (Student's t-test with Welch's correction, $p = 0.004$). There was no difference seen between strains in the amount of GFAP present in ventral hippocampus.

Quantification of amyloid- β and GFAP was also completed in coronal slices made at the level of ventral hippocampus, approximately -5.0mm posterior from bregma. Amyloid- β was found to be significantly increased in TgF344-AD rats across the slice ($p < 0.001$, Figure 2.2F) and within ventral hippocampus specifically ($p < 0.001$, Figure 2.2H). However, while GFAP was increased for TgF344-AD rats across the slice ($p = 0.012$, Figure 2.2J), there was no differences in staining for GFAP within the ventral hippocampus of WT and TgF344-AD rats ($p = 0.798$, Figure 2.2L).

2.5.2 No differences in Continuous Spontaneous Alternation Test performance or Novel Object Recognition at 12-months in TgF344-AD or WT rats

There were no observed differences in spatial working memory between 12 month old WT or TgF344-AD rats on the continuous spontaneous alternation test. Spontaneous alternation percentage within the Y-maze did not differ between strains (Student's t-test, $p=0.908$, ns, Figure 2.3A). There was also no difference seen in the number of arm entries observed during maze exploration (Student's t-test, $p=0.681$, ns, Figure 2.3B).

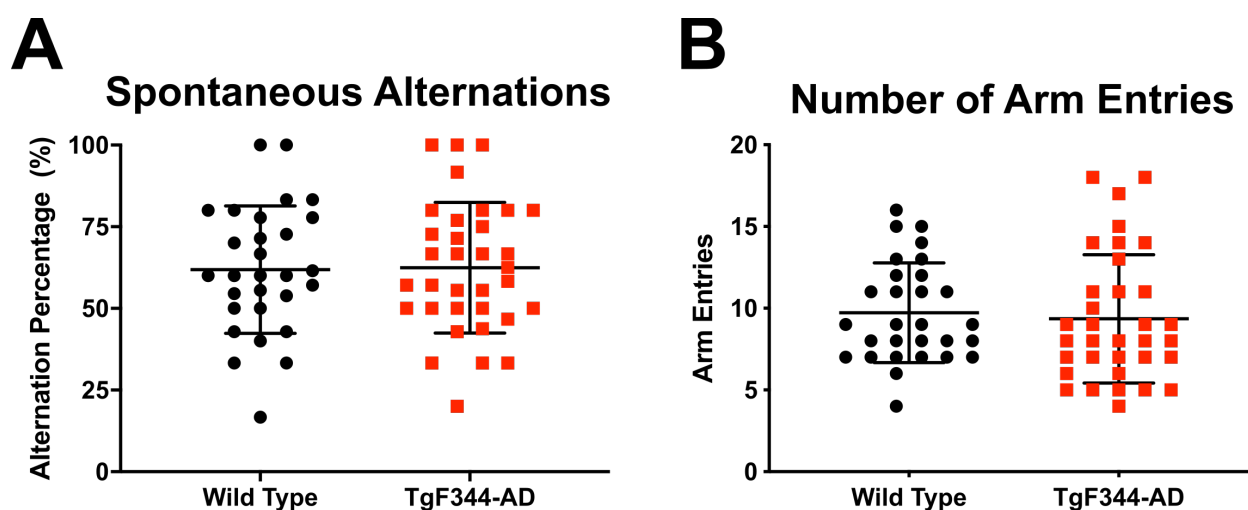


Figure 2.3 – No difference in spontaneous alternation test performance between TgF344-AD rats and WT littermates at age 12 months.

A) There was no difference in alternation behavior observed between TgF344-AD ($n = 34$) and WT ($n = 29$) rats (Student's t-test, $p=0.908$). B) There was no difference in the number of arm entries made during maze exploration between TgF344-AD ($n = 34$) and WT ($n = 29$) rats (Student's t-test, $p=0.681$).

Both WT and TgF344-AD rats were able to recognize the novel object during testing sessions performed at 12-months of age. Results are presented as the calculated group mean for

the discrimination index, with error bars representing the 95% confidence interval of the mean. A discrimination index equal to 0 represents performance at chance for recognition of the novel object. Both WT (DI range = 0.119-0.650) and TgF344-AD (DI range = 0.057-0.693) rats were able to discriminate the novel from the familiar object during the testing phase (Figure 2.4).

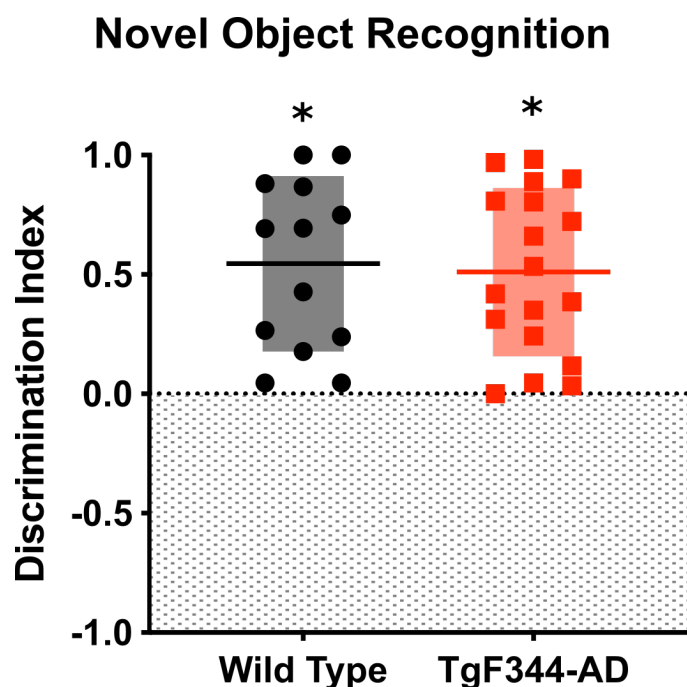


Figure 2.4 – No difference in Novel Object Recognition test performance between TgF344-AD and WT littermates at age 12 months.

Both TgF344-AD (N=13) and WT rats (N=18) can discriminate the novel object from a familiar object during the testing phase of the novel object recognition test. Results are shown as a mean with shaded regions representing the 95% confidence interval. The 95% confidence interval for the discrimination index of both WT (DI range = 0.119-0.650) and TgF344-AD (DI range = 0.057-0.693) rats are do not cross DI=0.0. Asterisk (*) denotes significant difference from performance at the level of chance [DI=0.0]. Therefore, both groups demonstrated preference for the novel object.

2.5.3 Candesartan decreases mean arterial pressure for both WT and TgF344-AD rats

Following six months of daily treatment with candesartan or vehicle, there was a main effect of drug treatment on median arterial pressure (Figure 2.5). Rats receiving regular doses of an ARB displayed a decrease in the recorded mean arterial pressure when compared with the rats receiving vehicle. The effect of candesartan to decrease mean arterial pressure was no different between WT and TgF344-AD rats.

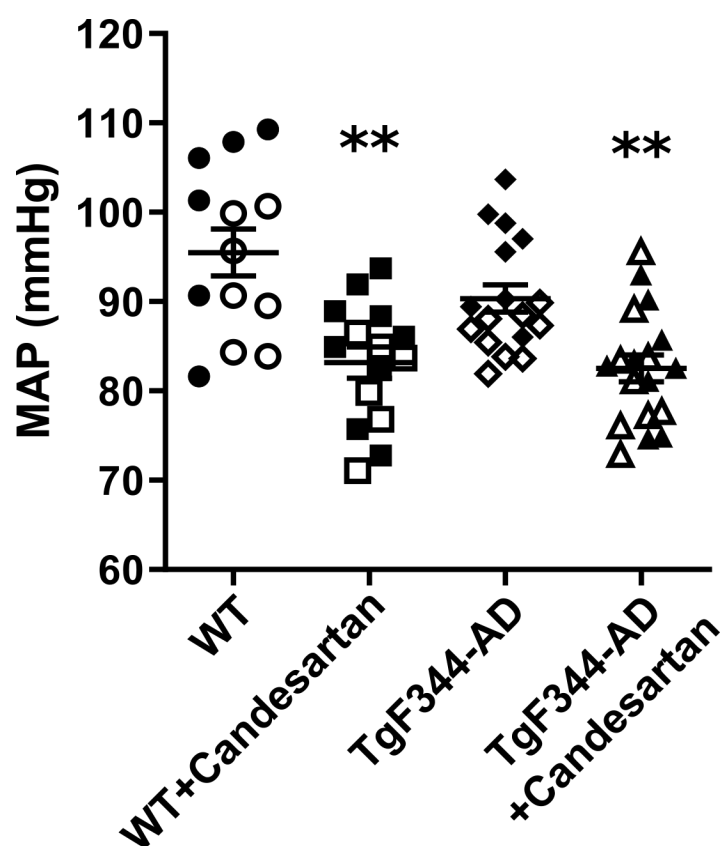


Figure 2.5 – Candesartan decreases mean arterial pressure for both WT and TgF344-AD rats.

Following six months of daily treatment with candesartan or vehicle, there was a main effect of drug treatment on mean arterial pressure. Candesartan effects on mean arterial pressure were not different between WT and TgF344-AD rats. There was a significant difference between treated and untreated groups for each strain ($p < 0.01$, **)

as measured by one-way ANOVA. Open symbols indicate female rats and closed symbols indicate male rats. N=13-18

2.5.4 Amyloid- β and GFAP are increased in the hippocampus of 18-month old TgF344-AD rats

Coronal sections at the level of dorsal hippocampus were taken from WT and TgF344-AD rats at 18 months, after six months of treatment with either candesartan or vehicle (Figure 2.6A-D). Amyloid- β was significantly increased in the dorsal whole brain sections and within the dorsal hippocampus of TgF344-AD when compared with WT rats (main effects of genotype, [F(1,60)=167.4,p<0.001, Figure 2.6E] and [F(1,46)=140.4,p<0.001, Figure 2.6G], respectively). Drug treatment did not affect amyloid- β or GFAP accumulation for either WT or TgF344-AD rats. Post-hoc analysis found all comparisons between WT and TgF344-AD rats to be significant (p<0.001, for all), regardless of the drug treatment for any group. At 18-months old, there is a negligible signal for amyloid- β in slices from the WT rats and a significant presence of staining for amyloid- β in slices from the TgF344-AD rats. The same relationship is observed in stains for amyloid- β in coronal slices taken at the level of ventral hippocampus (Figure 2.6F,H).

There were no observed differences in GFAP between WT and TgF344-AD rats across the full brain slice at the level of the dorsal or ventral hippocampus (Figure 2.6I-J). For TgF344-AD rats, there was an increase in GFAP found within the region of dorsal hippocampus (main effect of genotype, F(1,42)=4.862,p=0.033, Figure 2.6K). However, there were no observed differences in GFAP quantification within ventral hippocampus (Figure 2.6L).

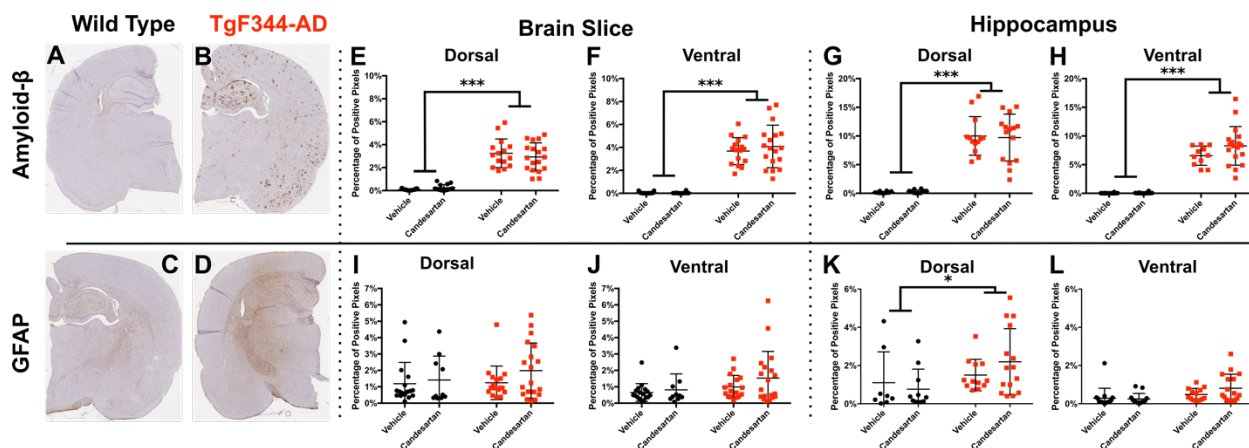


Figure 2.6 – Treatment with candesartan did not affect the accumulation of amyloid- β and GFAP in 18-month old TgF344-AD rats.

A-D) Examples of stained brain slices used for quantification of amyloid- β and GFAP at 18 months. Significance level is denoted as *** for $p < 0.001$ and * for $p < 0.05$. All example images are from rats that received vehicle between 12 & 18 months. E-H) Two-way ANOVA revealed a main effect of genotype for all comparisons of amyloid- β accumulation in WT and TgF344-AD rats at 18 months. Post-hoc tests revealed significant differences between all WT and TgF344-AD experimental groups (not pictured). I-J) There were no significant differences between WT and TgF344-AD in total GFAP at either sectioning location. K-L) There was a significant main effect of genotype on the amount of GFAP staining in the dorsal hippocampus of 18-month old rats. Similar to the results at 12 months, there is a significant increase in GFAP in the dorsal hippocampus of TgF344-AD rats relative to WT rats, but there was no observed differences in GFAP within the ventral hippocampus of TgF344-AD and WT rats.

Brain slices from rats sacrificed at 12 months and 18 months were analyzed to determine whether there were changes in the relative amounts of amyloid- β and GFAP present in the brain at different timepoints of the disease in TgF344-AD rats. There were significant differences in amyloid- β staining observed between 12-month TgF344-AD rats, 18-month TgF344-AD rats receiving vehicle, and 18-month TgF344-AD rats receiving candesartan as determined by a Kruskal-Wallis test ($p < 0.001$). Multiple comparisons revealed there was more diffuse amyloid- β staining in both 18-month experiment groups when compared with the 12-month rats. There

were no observed differences in stain quantification between the two 18-month groups that could be explained by treatment with candesartan. Similar results were observed at the level of dorsal and ventral hippocampus (Figure 2.7A-B). The percentage of pixels positively stained for GFAP did not change in the whole slice during disease progression (Figure 2.7C-D).

TgF344-AD Rats

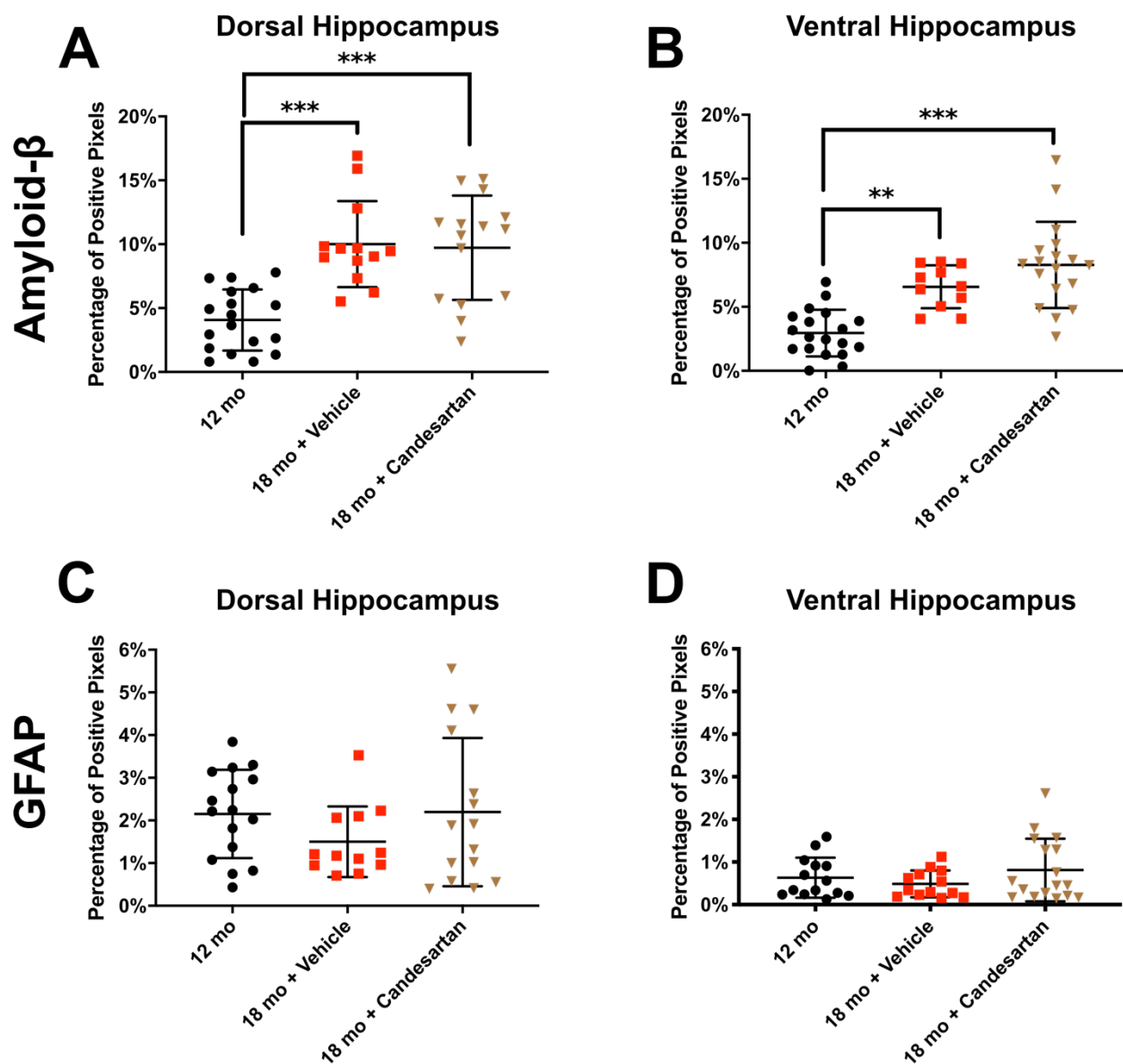


Figure 2.7 – Comparison of 12 & 18 month TgF344-AD rat amyloid- β and GFAP quantification.

A) At 18 months there is a significant increase in amyloid- β in the dorsal hippocampus of TgF344-AD rats compared with levels seen at 12 months (Kruskal Wallis test, $p < .001$). Multiple comparisons confirmed that this increase is seen in both rats receiving vehicle and those receiving candesartan. B) Amyloid- β is also increased in the ventral hippocampus of TgF344-AD rats when comparing the 12 and 18 month cohorts. C) There were no significant differences in the amount of GFAP seen in the dorsal hippocampus of TgF344-AD between any groups. D) There were also no differences in the amount of GFAP noticed in the ventral hippocampus due to time or drug treatment.

2.5.5 Candesartan preserves task learning on the WRAM for TgF344-AD rats

The WRAM can be used to assess working memory, recall, and learning, since performance on the task will ideally improve from session 1 to session 12. To assess learning on the WRAM in WT and TgF344-AD rats, the cumulative latency to reach the escape platforms and the total combined errors of the initial and final training sessions were compared. Data from sessions 1 & 2 were combined for the “initial” training data. Likewise, data from sessions 11 & 12 were combined for the “final” training data.

Both WT and TgF344-AD rats at 18 months of age learned to complete the maze in less time over the course of 12 training sessions. Escape latency decreased for both strains over the training sessions regardless of whether rats were treated with candesartan or vehicle. For WT rats, there was a significant reduction in the latency to reach all escape platforms after training, as measured by two-way ANOVA with repeated measures (main effect of time, $F(1,28)=122, p < 0.001$, Figure 2.8A). Planned contrasts using Sidak’s multiple comparison test revealed a significant improvement in time to complete the maze on the final sessions for WT rats receiving vehicle (Initial: $M=413s$, $SD=117s$; Final: $M=131s$, $SD=90s$) and candesartan (Initial: $M=480s$, $SD=162s$; Final: $M=115s$, $SD=78s$). There was a similar reduction in latency to

reach all platforms across training sessions for TgF344-AD rats (main effect of time, $F(1,32)=60.81, p<0.001$, Figure 2.8C). Planned contrasts showed that TgF344-AD rats receiving vehicle (Initial: $M=400s$, $SD=148s$; Final: $M=214s$, $SD=112s$) and candesartan (Initial: $M=407s$, $SD=107$; Final: $M=157s$, $SD=92s$) both learned to complete the maze more quickly over the course of training.

WT rats reduced the total number of cumulative working memory, reference memory and perseverative errors between the initial and final sessions in the WRAM (main effect of time, $F(1,28)=30.87, p<0.001$, Figure 2.8B). There was a significant reduction in errors over the course of training for groups receiving vehicle (Initial: $M=19.79$, $SD=7.72$; Final: $M=10.79$, $SD=6.89$) and candesartan (Initial: $M=19.81$, $SD=6.54$; Final: $M=9.25$, $SD=6.30$) as determined by planned contrasts. There was also a significant reduction in total number of errors performed between the initial and final WRAM sessions for TgF344-AD rats (main effect of time, $F(1,32)=8.952, p=.005$, Figure 2.8D). However, planned contrasts revealed that there was a reduction in the total errors performed after training for TgF344-AD rats receiving candesartan (Initial: $M=19.73$, $SD=5.84$; Final: $M=12.47$, $SD=5.96$). TgF344-AD rats receiving vehicle did not learn to reduce the number of errors performed on the WRAM over the course of training (Initial: $M=19.11$, $SD=6.10$; Final: $M=16.95$, $SD=8.12$).

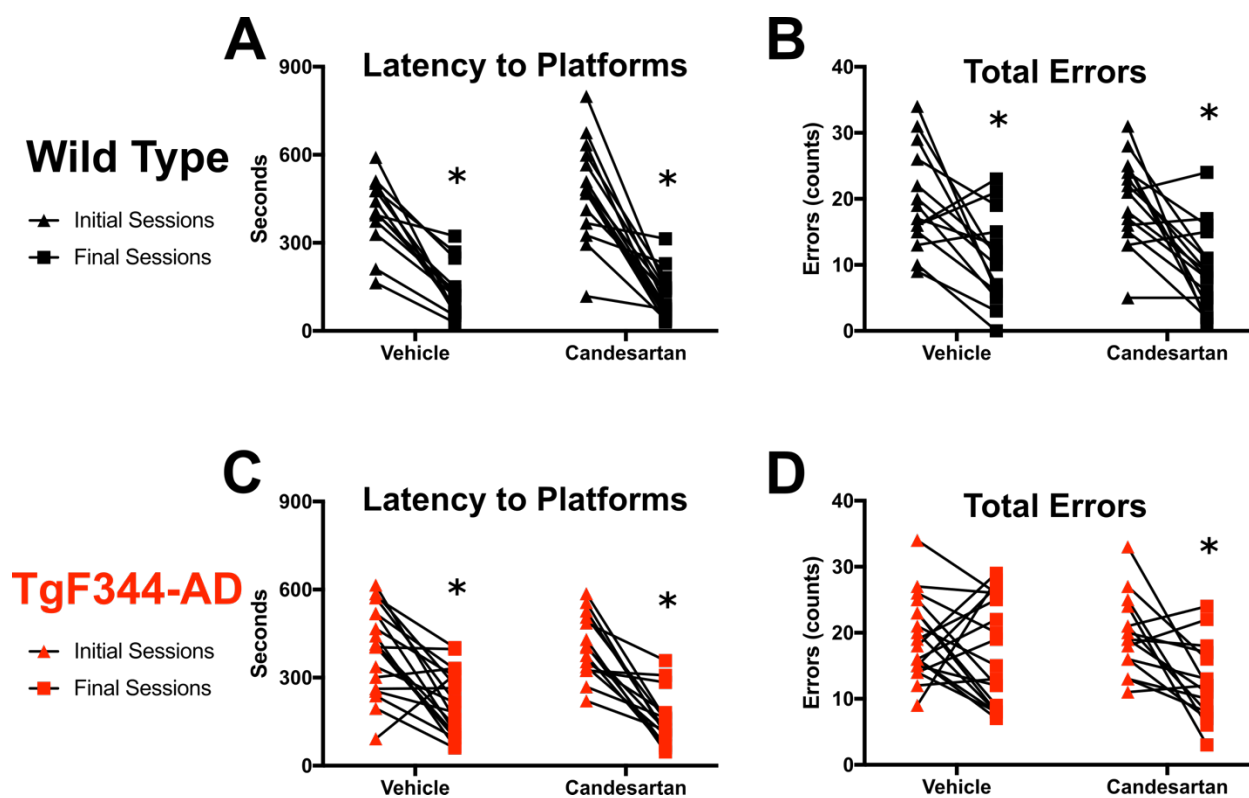


Figure 2.8 – 18-month old TgF344-AD rats treated with learn to complete the WRAM faster with training but only reduce the total errors committed after treatment with candesartan.

A) Repeated measures comparisons revealed that there was a significant decrease in the time WT rats took to complete the WRAM over the course of 12 days of training (two-way ANOVA with repeated measures, $F(1,28)=122, p<0.001$). B) WT rats also learned to complete the WRAM with fewer total errors ($F(1,28)=30.87, p<0.001$). C) TgF344-AD rats also learned to decrease the time needed to complete the WRAM by the final sessions ($F(1,32)=60.81, p<0.001$). D) However, only TgF344-AD rats treated with candesartan learned to decrease their total cumulative errors by the final sessions. TgF344-AD rats that were administered vehicle committed as many total errors on their final sessions as they had in the initial training sessions.

2.5.6 Working and Reference memory impairment in 18-month old TgF344-AD rats is partially rescued by treatment with candesartan

Working and reference memory performance was assessed by comparing each experimental group on their time to complete the maze and the types of errors committed across the final WRAM training sessions (days 11 & 12). 18 month old TgF344-AD rats took longer to complete the maze when compared with WT rats, as measured by a significant increase in the latency to reach the escape platforms (main effect of genotype, $F(1,60)=6.978, p=0.011$, Figure 2.9A).

TgF344-AD rats committed more reference memory errors than WT rats on the final WRAM training sessions (main effect of genotype, $F(1,60)=8.149, p=0.006$, Figure 2.9B). A reference memory error was scored when a rat made the first entry into a maze arm that never contained an escape platform. The significant increase in reference memory errors for TgF344-AD rats indicates that these rats had an impaired ability to navigate throughout the maze and retain escape platform locations using the wall cues around the maze.

TgF344-AD rats also performed more perseverative working memory errors compared with WT rats on sessions 11 & 12 in the WRAM (main effect of genotype, $F(1,60)=5.411, p=0.023$, Figure 2.9C). There was also a main effect of drug treatment on perseverative working memory errors, with rats receiving candesartan performing fewer errors than those receiving vehicle ($F(1,60)=5.453, p=0.023$). Perseverative working memory errors were scored whenever a rat made repeat entries into the same unrewarded arm within the same trial. Sidak's multiple comparisons test revealed that both of these main effects were being driven by a significant increase in perseverative working memory errors in the TgF344-AD rats

that received vehicle ($M=3.263$) compared with other groups: WT rats receiving vehicle ($M=1.071$) and TgF344-AD rats receiving candesartan (1.067).

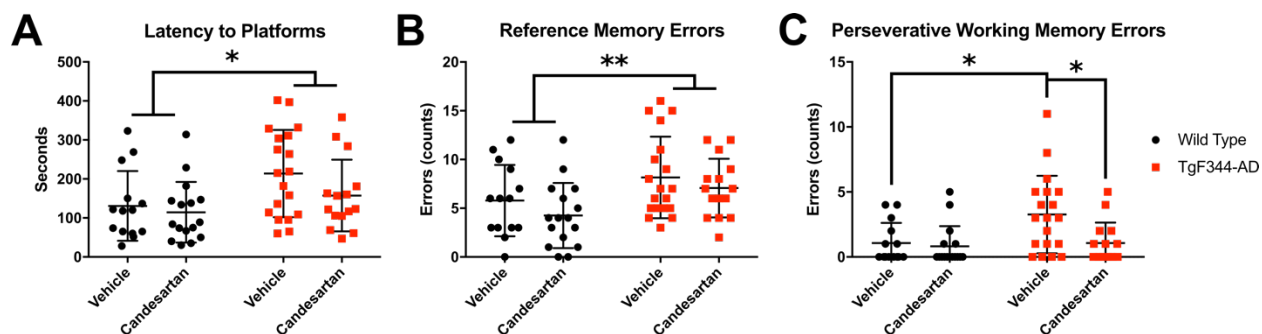


Figure 2.9 – WRAM performance on training days 11 & 12 for TgF344-AD and WT rats treated with Candesartan.

A) TgF344-AD rats are slower to complete the WRAM when compared with WT rats (main effect of genotype, $F(1, 60) = 7.196$, $P=0.0094$). B) TgF344-AD rats make more reference memories during maze completion when compared with WT rats (main effect of genotype, $F(1, 60) = 8.149$, $P=0.0059$). C) Rats receiving Candesartan commit fewer working memory incorrect errors when compared with rats receiving saline (main effects of genotype and drug treatment, [$F(1,60) = 5.411$, $p=0.023$] and [$F(1, 60) = 5.453$, $p=0.023$], respectively). This effect is explained by the reduction in working memory incorrect errors seen in TgF344-AD rats receiving Candesartan when compared with those receiving saline (Sidak's multiple comparisons test, $p=0.0206$).

2.6 Discussion

Our results demonstrate angiotensin receptor blockers administered throughout the early disease phase reduce the degree of cognitive disturbances in the TgF344-AD rat. In our experiment, the TgF344-AD rat reliably displayed an age-dependent disease progression featuring many hallmarks of the typical human transition from prodromal AD through clinical AD. At 12-months, the TgF344-AD rat displayed significant amyloidosis and increases in GFAP levels throughout the brain but appeared cognitively normal on the spontaneous alternation test

and novel object recognition when compared with age-matched wild type littermate controls. These findings are in line with previously published work using this model which identifies ~15 months of age as a time point where TgF344-AD rats begin to display significant cognitive impairments^[206, 207]. Multiple investigators have replicated findings suggesting that this model develops amyloid and tau pathology with a stereotyped progression beginning at 6 months and continuing through frank AD pathology at 16 months^[206, 217, 218]. Our quantification of amyloid- β at 12-months similarly supports this progression. Some reports using this model have demonstrated deficits in reversal learning as early as 6 months and impaired performance in a water maze at 10-11 months when compared to WT rats^[219, 220]. While we did not observe similar evidence of cognitive impairments during our behavioral testing at 12 months, we did observe consistent perseverative errors and evidence of inefficient WRAM platform search strategies in our 18 month old TgF344-AD rats treated with vehicle.

Daily treatment with candesartan from 12 to 18 months was associated with improvements in learning of the WRAM and a decrease in perseverative working memory errors in TgF344-AD rats. At 18 months, both WT and TgF344-AD rats treated with vehicle were able to learn to complete the WRAM more quickly over the 12 sessions. However, the inability of TgF344-AD rats to reduce the total number of errors performed within the maze and the significant increase in perseverative errors relative to other groups suggests that these rats chose to investigate maze arms randomly in search of escape platforms, rather than using maze cues to learn platform locations.

Despite the observed improvements in the WRAM, candesartan did not slow the aggregation of amyloid- β in TgF344-AD rat brains. There are a few potential explanations for

this result. The TgF344-AD rat is transgenic model created using two genes linked to the familial form of AD. The potential for increased production of amyloid- β as a result of the expression of mutant human APP_{SW} and PS1 in the TgF344-AD rat may offset the potential for candesartan to improve amyloid- β clearance indirectly via vascular changes. Candesartan also has anti-inflammatory properties and may potentially slow disease progression through decreases in neuroinflammation. Complex interactions between amyloid- β , neurofibrillary tangles and neuroimmune cells can lead to chronic neuroinflammation which could potentially exacerbate AD progression^[221]. Candesartan has shown some success in modulating neuroimmune cell activity in support of neuroprotective mechanisms^[222]. We did see an expected decrease in mean arterial pressure as a result prolonged treatment with candesartan to coincide with our behavioral results.

Interestingly, levels of GFAP in the brain remained consistent from 12 to 18 months in TgF344-AD rats. In AD, GFAP levels typically increase along with increases in amyloid plaques^[223, 224]. Astrocyte activity can be an important mediator of amyloid deposition, but chronically activated astrocytes in AD brain can become neurotoxic^[223]. At 18 months there was no difference between WT and TgF344-AD rats in the amount of GFAP expression throughout most of the brain. This may be due to a natural upregulation of GFAP in the WT rat with advancing age^[225].

The results of this study demonstrate the potential for angiotensin receptor blockers improve the behavioral symptoms of AD when administered in the early disease phase. Further studies are needed to determine the biological mechanisms underlying the effects of the candesartan on AD disease progression.

Chapter 3 - Delayed Anesthetic Recovery in 12-Month TgF344-AD Rats

Adapted from: Delayed anesthetic recovery occurs prior to disease onset in the TgF344-AD rat. Christopher G. Sinon, Peter-Jon C. Williams, Roy L. Sutliff, Ihab M. Hajjar, Paul S. Garcia. In Prep.

3.1 Abstract

The use of general anesthetics for surgery is predicated on the belief that the effects of these drugs are temporary and reversible. However, increasing concern about cognitive performance immediately following general anesthesia has drawn attention to the potential for common anesthetics to stimulate apoptotic or neurodegenerative processes. Anecdotally, individuals with a prior diagnosis of Alzheimer's disease (AD) emerge and recover slower from general anesthesia. Prior diagnosis of mild cognitive impairment or Alzheimer's-type dementia are independent risk factors for development of postoperative delirium (POD) and other perioperative neurocognitive disorders. Incidents of delirium are also associated with an increased risk for future diagnosis of dementia. We characterized the time to display stereotyped emergence and recovery behaviors following isoflurane administration in a transgenic rat model of AD. Twelve-month old TgF344-AD rats are considered to be in the early disease phase. We assessed differences in anesthetic sensitivity of TgF344-AD rats to sevoflurane anesthesia via EEG analysis for burst suppression. In early AD, TgF344-AD rats display hastened emergence from anesthesia followed by a delay in the appearance of recovery behaviors. TgF344-AD rats demonstrate a resistance to cortical suppression during sevoflurane anesthesia. Brain slices following sevoflurane administration also display increased levels of amyloid- β and GFAP in hippocampus. Hastened emergence and anesthetic resistance suggest a general shift towards cortical arousal in the 12-month TgF344-AD rat. Delayed recovery from isoflurane may be related to anesthesia-associated increases in AD protein accumulation.

3.2 Introduction

The use of general anesthetics for surgery is predicated on the belief that the effects of these drugs are temporary and reversible by the anesthesiologist. However, this should not be taken to mean that the entry and exit from anesthesia are simply a reversal of the same processes. While a “unified theory of general anesthesia” explaining the mechanisms of control of consciousness remains elusive, it is clear that there are separate patterns of synaptic, cellular, and circuit level events occurring during the induction and emergence from general anesthesia^[83].

There are several of known comorbidities that can increase the risk for perioperative complications and postoperative cognitive impairments. Among these are factors that indicate the presence of previous or ongoing neurological insult, including prior history of stroke or a diagnosis of mild cognitive impairment or Alzheimer’s-like dementia^[226, 227]. Additionally, increased age, patient frailty and those with lower levels of educational attainment are at a higher risk for postoperative delirium and perioperative neurocognitive disorders, suggesting there is a role for a patient’s “cognitive reserve” in assessing the likelihood for postoperative impairments^[226, 228].

Based on practical considerations within a hospital environment, there is traditionally more attention paid to the pre- and perioperative care for patients from the anesthesiologist. Despite well-established concerns regarding the potential for postoperative cognitive impairments in patients, the factors influencing these impairments are poorly understood. Few clinical studies have been performed on these topics, owing to a number of factors: 1) the difficulty in compiling data sets on patient outcomes, 2) the variability in anesthetic protocols used amongst patients considered in the review, 3) differences among screening protocols for

cognitive impairments, & 4) the likelihood that postoperative issues are being underreported^[95, 229].

3.2.1 Alzheimer's Disease and Anesthesia

Due to its progressive nature, Alzheimer's disease often presents in elderly patients. In fact, the primary risk factor for AD is age. AD affects nearly 5.7 million people in the United States, with greater than 95% of those affected over the age of 60^[230, 231]. Diagnosis of AD involves cognitive testing and neurological examination of the patient alongside interviewing the family members of the patient to comment on changes in the patient's mood and behavior. Quantifiably, the risk of acquiring an AD diagnosis doubles every 5 years after the age of 65, and 95% of AD cases occur after age 60^[232]. With life expectancy of the general population on the rise, the projected prevalence of AD worldwide is expected to rise to 65 million people by 2030 and 115 million people in 2050^[66, 233, 234]. Geriatric patients undergoing surgery are more likely to have AD or to be at risk for AD development. With this in mind, it is important for anesthesiologists to consider the effects of anesthesia, surgery, and approaches to perioperative care in patients with AD.

We are only beginning to understand how anesthesia affects the development and progression of AD, and currently there are no standards of best practice for the anesthetic management of patients with AD. Researchers have identified commonalities between the pathophysiology of neurodegeneration in AD and the cellular and systematic effects of anesthesia^[235]. Further, several studies have identified that AD pathogenesis may be affected by anesthesia and perioperative care^[236, 237]. The appearance of postoperative cognitive impairments is both more likely in individuals with a prior diagnosis of AD and a risk factor for future development of AD^[235, 238, 239].

3.2.2 Alzheimer's Disease and anesthetic sensitivity

Advanced age increases sensitivity to anesthetic drugs in both humans and rodents^[240-242]. While the genesis of increased anesthetic sensitivity is unknown, it is likely that many elderly surgical patients receive excessive concentrations of general anesthesia for surgery. Intraoperative anesthetic guidance via consciousness monitors significantly decreases the risk of perioperative neurocognitive disorders^[145, 148]. Additionally, the appearance of burst suppression, an EEG pattern characterized by periods of near complete suppression of cortical activity, is associated with increased risk for POD^[243, 244]. These findings suggest that excessive administration of anesthesia should be an area of clinical concern in individuals at risk for increased anesthetic sensitivity. There are currently no best practice standards for anesthetic management of patients with AD, despite increased risk for postoperative cognitive impairments and the potential for increased anesthetic sensitivity both due to age and disease progression.

3.3 Experimental Design and Hypotheses

The following experiments were conducted in the TgF344-AD rat, the same rodent model that was used in the previous chapter. We compared cognitive function and pathology between 12-month WT and TgF344-AD rats. We then observed the emergence and recovery from Isoflurane anesthesia in these rats, using experimental protocol similar to those previously described^[87, 93]. After 2-hours of maintenance of isoflurane anesthesia, we recorded the time to reach a canonical series of emergence and recovery behaviors in each rat. The timeline for behavioral experiments is represented in Figure 3.1A. In a separate group of 12-month old rats, we used EEG to assess the neurophysiological response to increasing doses of anesthesia in both strains, as represented in Figure 3.1B.

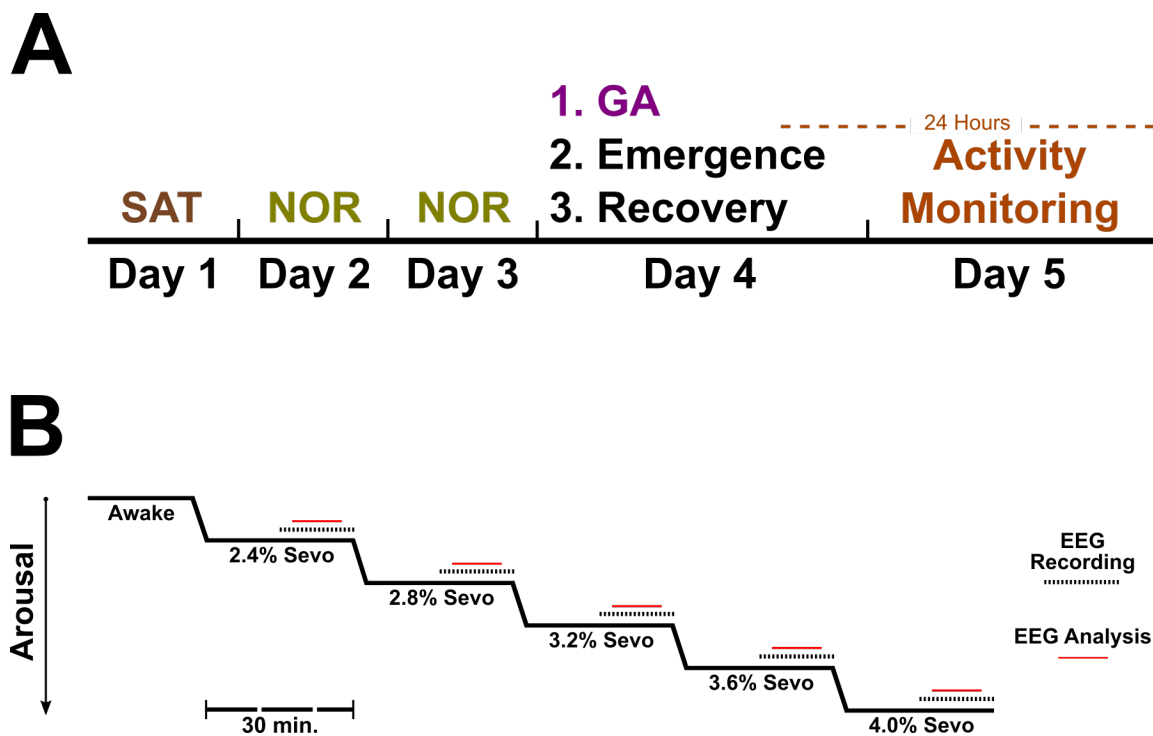


Figure 3.1 – Experimental workflows for behavioral testing and EEG recordings in TgF344-AD rats.

Separate cohorts were used for each series of experiments. A) Timeline of behavioral testing to assess cognitive function in rats aged 12 months. SAT = Spontaneous alternation test, NOR = Novel object recognition test, GA = General anesthesia. B) Timeline for sevoflurane administration and acquisition of EEG recordings. Each rat was maintained at each sevoflurane concentration for a total of 30 minutes. Inspired and expired sevoflurane concentration was monitored at each step. At each concentration, rats were given 15 minutes for equilibration to the current concentration before the start of recording. Extradural EEG was acquired for 15 minutes and the middle 10 minutes of each recording was analyzed for suppression of cortical activity.

We expected there to be no statistical difference in performance on our cognitive tasks at 12-months of age (which would replicate our findings from Chapter 2). We did expect to see an increase in the presence of A β and GFAP between WT and TgF344-AD rats, indicating that an Alzheimer's-like disease pathology had begun in the brains of the TgF344-AD rats at this age. It has previously been established in humans and in rats that aging increases the sensitivity to general anesthetics. It is hypothesized that this response may be due to a gradual loss of

cortical neurons during aging. It is currently unclear whether neurodegenerative diseases also increase sensitivity to anesthetics^[240-242]. We hypothesized that TgF344-AD rats in the early disease state would display a delayed recovery from anesthesia. In addition, we tested whether this effect may be related to increased sensitivity to anesthetics by assessing the amount of EEG suppression to increasing concentrations of sevoflurane.

3.4 Methods

3.4.1 Animals

All experiments were conducted at the Atlanta VA Health Care System Animal Facility. Rats used for data collection were bred from an established colony of TgF344-AD rats. Transgenic rats and wild type littermates were used for data collection. The rats were housed in 12-hour light cycles with ad libitum access to rodent chow and water. All studies were approved by the Atlanta VA Institutional Animal Care and Use Committee.

3.4.2 Continuous Spontaneous Alternation Behavior Test

The Continuous Spontaneous Alternation Test was performed within a Y-maze. Rodents introduced to a Y-maze display a tendency to alternate arm entries during maze exploration. This tendency towards alternation is thought to result from a preference towards investigation of new environments, and the SAT takes advantage of this behavior as an assessment of spatial working memory^[213]. Rats were allowed to freely explore the Y-maze (San Diego Instruments, San Diego, CA, USA) with all three arms open for 8 minutes. Testing was performed between 12:00-3:00PM during the light phase. If at any time the rat remained stationary for >60 seconds during the session, movement was motivated by briefly grasping and releasing the rat from the base of the tail. The number of arm entries and the path of arm exploration were determined by a blinded observer.

A successful alternation was scored when the rat completed three consecutive arm entries via turns in the same direction. Alternation percentage was determined using the following equation^[214]:

Equation 1:

$$\text{Alternation percentage} = \frac{\# \text{ of Alternations}}{\text{Total \# of Arm Entries} - 2} * 100$$

3.4.3 Novel Object Recognition Test

Following completion of the Y-maze, rats were tested for attention and working memory performance using the novel object recognition test. Testing was performed between 9:00AM-12PM during the light phase. On the first day, rats were allowed to freely explore a high-walled open field arena for 15 minutes to acclimate to the testing environment. On the second day, rats were given another 15 minutes to acclimate to the testing environment. Following a 30-minute break, rats began the training phase of the novel object recognition test. Two identical non-odorous plastic toys (A1 & A2) were affixed with one on each end of the testing environment. Rats were placed into the center of the environment and given seven minutes to explore the testing environment during the training phase. Rats were then returned to their transfer cage for a 5-minute inter-trial interval. The choice phase was completed using a third identical plastic toy (A3) and new non-identical plastic toy (B). Each phase was recorded by an overhead video camera and the behavioral data was autoscored using Ethovision XT11.5 software (Noldus Information Technology, Wageningen, The Netherlands). For each rat, the time spent on each side of the environment and the time spent exploring each object, measured as the amount of time each rat's nose entered a 2.5-cm radius of the object, was recorded for each session.

The novel object observation time (TN) and the familiar object observation time (TF) were recorded. The discrimination index for the testing phase was calculated by (TN-

TF)/(TN+TF). Animals were excluded if they did not cross the midpoint of the arena during any of the phases. Animals were also excluded if they spent more than 80% of total object observation time with either object during the training phase.

3.4.4 Isoflurane Anesthesia

Our anesthesia protocol was modified from our previous work ^[86]. A state of general anesthesia was induced in rats using an induction chamber pre-charged with 2% isoflurane in oxygen (O₂). When rats displayed a loss of righting reflex and a visible decrease in respiration rate, they were transferred to a nose cone delivering 2% isoflurane in O₂ at a rate of 1 L/minute. General anesthesia was maintained for 2 hours via nose cone with respiration rate and body temperature recorded for each rat in 5 minute intervals. Body temperature was maintained at 38±0.5°C via heating pad and monitored via rectal thermometer. Isoflurane anesthesia was reduced to a 1.5% dose shortly after the transfer to the nose cone and dose was then titrated to respiration rate (between a 1.5-2% dose) as needed throughout the course of the experiment. Sham general anesthesia in the form of 2 hours of exposure to O₂ at 1 L/minute in an induction chamber was delivered to half of the rats in the study.

3.4.5 Anesthetic Emergence & Recovery

After 1-hour & 50-minutes of general anesthesia, a small piece of adhesive tape (~0.5cm x 3cm) was wrapped around the rat's left forepaw and the temperature probe was removed. At the two-hour mark, the isoflurane concentration was reduced to 0% and a stopwatch was started simultaneously. For these experiments, we chose to distinguish between the period of emergence from isoflurane anesthesia and the period of recovery from the effects of isoflurane anesthesia, similar to methods applied in ^[87, 93]. Anesthetic emergence was defined as the period between cessation of isoflurane delivery (ISO OFF) and the return of righting reflex. The time to each of

the following anesthetic emergence milestones was recorded for each rat receiving isoflurane: limb movement, sudden changes in respiration, blinking, mastication and return of righting reflex. Anesthetic recovery was defined as the period from the return of righting reflex until the first attempt to remove the adhesive tape from the left forepaw. The modified sticky dot test used in these experiments, and as previously reported^[87], requires perception of the adhesive tape and the return of grooming behaviors following the regaining of consciousness.

3.4.6 Activity Monitoring

After receiving anesthesia, at ~4:00pm rats were transferred to a monitoring chamber with beam breaks (Oxymax/CLAMS, Columbus Instruments, Columbus, OH, USA) for 24 hours of continuous locomotor activity scoring. Rats were given ad lib access to food and water during activity scoring and the chambers were fitted with raised grid floors so waste would collect below. Activity scoring for the dark phase began at 6:00pm and the rats were monitored continuously until 6:00pm the following day. To track ambulation in the chamber (rather than grooming or postural adjustments) we included only consecutive beam breaks that were made along one axis in series. Breaking the same beam multiple times in a row would be ignored for data collection.

3.4.7 Wireless EEG Transmitter Implantation

A two-channel, wireless EEG Transmitter (Epoch Sensor, Biopac Systems Inc., Goleta, CA, USA) was implanted using aseptic surgical technique. Rats were anesthetized with isoflurane (3-4% in O₂), the scalp and neck were trimmed with hair clippers, and eye ointment was applied. Metacam (1 mg/kg) was administered pre-surgery by subcutaneous injection. A bolus of warm saline (1 mL/100 g) was also injected subcutaneously. The rat was positioned within a stereotaxic frame with temperature support provided by warm water blanket beneath the

animal. Isoflurane dosage was reduced to 2-2.5% in O₂ for surgical maintenance. Surgical draping was used to cover the rat keeping fur from entering the surgical site. The scalp was cleaned with alternating administrations of betadine and 70% ethanol applied in circular motions outwards center of the scalp.

When the respiration rate was steady at 60-80 breaths per minute with no response to toe pinch, the surgery was begun. A single incision was made along the midline of the skull, rostral to caudal, starting between the eyes and terminating caudal to the ears. The skull was exposed and blood and fascia were cleared. Five burr holes were drilled into the skull exposing the dura mater. Holes were drilled at (1) 1.0 mm posterior to bregma and 3.0 mm lateral to the central suture, (2) 4.0 mm anterior to lambda and 3.0 mm lateral to the central suture, (3) 2.5 mm posterior to lambda along the midline, (4) 2.5 mm posterior to bregma and 4.5 mm lateral of the central suture, and (5) 2.0 mm anterior to lambda and 4.5 mm lateral to the central suture.

The leads for channels 1 and 2 were positioned in burr holes 1 and 2, respectively. The reference lead was positioned in hole 3. Two anchoring screws were positioned in holes 4 & 5. The transmitter was affixed to the skull using dental cement powder and dental acrylic. Once dried, the remainder of the incision was sutured closed with PDO absorbable monofilament suture, thereby leaving the transmitter exposed and unencumbered, and completing the surgery.

Rats received a subcutaneous injection of Buprenorphine SR-LAB (1 mg/kg) following surgery. For the first three days post-surgery, rats were kept on a soft diet of nutritional gel (DietGel Recovery, ClearH₂O, Portland, ME, USA) and received daily subcutaneous injections of Metacam (1 mg/kg). Each rat was given an additional 10 days to recover from surgery before EEG recordings were made.

3.4.8 EEG Recording

EEG recordings were made using the corresponding Epoch Receiver (Biopac Systems Inc, Goleta, CA, USA) and MATLAB software (MathWorks, Natick, MA, USA). Recordings were made under general anesthesia with sevoflurane in O₂ delivered via nose cone at 2 L/min. Anesthesia was induced with 2.4% sevoflurane and the concentration was increased by 0.4% for each subsequent recording. Rats were maintained at each sevoflurane concentration for 30 minutes total. Rats were given 15 minutes to equilibrate to each sevoflurane concentration and EEG recordings were made during the last 15 minutes of maintenance for each concentration step. Inspired and expired sevoflurane concentrations were continuously monitored during the equilibration period to verify that EEG recordings were made at once sevoflurane concentrations had reached a steady state. Supplemental heating was provided by heated water blanket during equilibration and via heated saline bags (38-39°C) during EEG recording. Saline bags were consistently rotated from a hot water bath to prevent hypothermia during sevoflurane anesthesia. Methods and MATLAB code for burst suppression analysis are provided in Appendix 2. EEG was bandpass filtered between 0.1-70Hz and line filtered at 60Hz. Wavelet denoising was performed on each file using the “wdenoise” function in MATLAB with a soft SURE threshold. Cortex recordings were denoised down to level five using the tenth order Daubechies wavelet and hippocampus recordings were denoised down to level five using the fourth order Symlet wavelet. Detailed methods for selection of EEG filtering steps are detailed in Appendix 3.

3.4.9 Tissue Collection

Rats were deeply anesthetized using isoflurane for tissue collection. Cardiac perfusion was performed using ice cold phosphate buffered saline. Rat brains were rapidly extracted and bisected into hemispheres. The hemisphere used for immunochemistry was fixed in 4%

paraformaldehyde and then transferred to a phosphate buffered saline storage solution containing 0.01% sodium azide. Brains from EEG implanted rats were harvested 24 hours after sevoflurane administration.

3.4.10 Tissue Sectioning and Immunohistochemistry

Brain tissue sections were embedded in paraffin and sliced at 8 microns. Sections were deparaffinized and immunohistochemically labeled with antibodies to amyloid- β (4G8) and astrocyte activity (GFAP) on a ThermoFisher autostainer. Amyloid- β sections were pretreated with formic acid, blocked with normal serum, and incubated with primary antibody at 1:10,000, then exposed to biotinylated secondary antibody followed by avidin-biotin complex (Vector ABC Elite kit) and developed with diaminobenzidine (DAB). GFAP sections incubated with primary antibody (anti-GFAP, Dako, Santa Clara, USA) at 1:5000, then exposed to primary antibody enhancer followed by HRP polymer (ThermoScientific UltraVision LP Detection System) and developed with diaminobenzidine (DAB).

3.4.11 Quantification of Immunohistochemistry

High resolution digital scans of stained brain slices were analyzed using Qupath software^[216]. Positive pixel count analysis was performed on slices stained with 4g8 for amyloid- β and GFAP for astrocyte activity. Positive pixel percentage, a measure of the ratio of positively stained pixels to total number of image pixels, was recorded to quantify markers for AD-like pathology in rat brain tissue. Expanded methods for image analysis are detailed in Appendix 1.

3.4.12 Statistical Analysis

Statistical testing was performed using Prism 7.0 (GraphPad Software, San Diego, CA, USA) and IBM SPSS Statistics V26 (IBM Corporation, Armonk, NY, USA). A sample size of

12 rats per group was justified using a power analysis in G*Power 3.1.9.4 with $\alpha=0.05$, $\beta=0.80$ and an anticipated very large effect size of 1.2 due to the effects of the inserted transgenes. All datasets were tested for normality using the Shapiro-Wilk test. Tests for normality perform poorly with sample sizes comparable to those used in these experiments, so we compared the Shapiro-Wilk test results against visual inspection of the data distributions in the selection of non-parametric vs. parametric tests. Cognitive test data and emergence & recovery data were analyzed using Student's t-test for independent samples, Two-way ANOVA with Sidak's test for multiple comparisons, or comparison of the 95% confidence interval with performance at the level of chance. Despite the low sample size collected for the EEG data, we chose to analyze this data using parametric tests for two reasons. Where there were significant differences the data were clearly separated such that analysis with non-parametric tests using rank-sum or signed-rank comparisons could not fully characterize the data distributions. Results of parametric tests are informative for approximating the expected effect size for future experimentation. Two-way ANOVA with repeated measures and Sidak's test for multiple comparisons was used to analyze differences in burst suppression ratios. Welch's t-test was used to analyze the changes in neuropathology between TgF344-AD rats with and without exposure to sevoflurane during EEG recording.

3.5 Results

3.5.1 Cognitive Testing

We used similar cognitive testing assays to those used in Chapter 2, with the addition of post-anesthesia monitoring of locomotor activity for 24 hours in a novel home cage. Patients with AD also experience stereotyped non-cognitive impairments, in addition to impairments in memory and cognitive function. A series of motor dysfunctions including rigidity, postural

changes, changing gait and bradykinesia are common with the disease and likely to worsen along with AD progression. Additionally, due to the effects of anesthetic drugs on brain regions important for circadian function, there is speculation that exposure to anesthetics could impair sleep/wake cycles and overall activity levels^[86]. To assess this, we housed the rats in separate, novel home cage in the 24-hours following administration of isoflurane anesthesia. Locomotor activity was tracked by quantifying the number of consecutive beam breaks along the length of the cage, to eliminate the influence of grooming or postural adjustments on the assessment of activity.

There were no differences between WT rats and TgF344-AD rats on spatial working memory or activity level as measured by the continuous spontaneous alternation test (Figure 3.2A-B). The percentage of arm entries that completed a full maze alternation were the same between groups (Student's t-test, $p=0.914$, ns). Both strains also completed the same average number of arm entries (Student's t-test, $p=0.807$, ns).

There were also no differences in recognition memory between groups as measured by the novel object recognition test (Figure 3.2C). For each group, we used the discrimination index (DI) to quantify the time spent with the novel and familiar objects. $DI = 1$ represents 100% of exploration time spent on the novel object, and a $DI = 0$ represents an equal amount of time spent with the novel and familiar objects. For each group, we determined the mean DI and the error bars represent the 95% confidence interval. For both WT rats and TgF344-AD rats, the entire range of the 95% confidence interval is greater than $DI=0$, indicating a consistent recognition of the novel object for both groups.

WT and TgF344-AD rats had similar activity levels in the 24-hours following exposure to anesthesia. Both strains were more active during the dark phase than they were in the light

phase (Figure 3.2D). Two-way ANOVA revealed a main effect of time on locomotor activity ($F(1,24)=75.68, p<0.001, ***$). However, there were no differences between the strains on their performance during either time period.

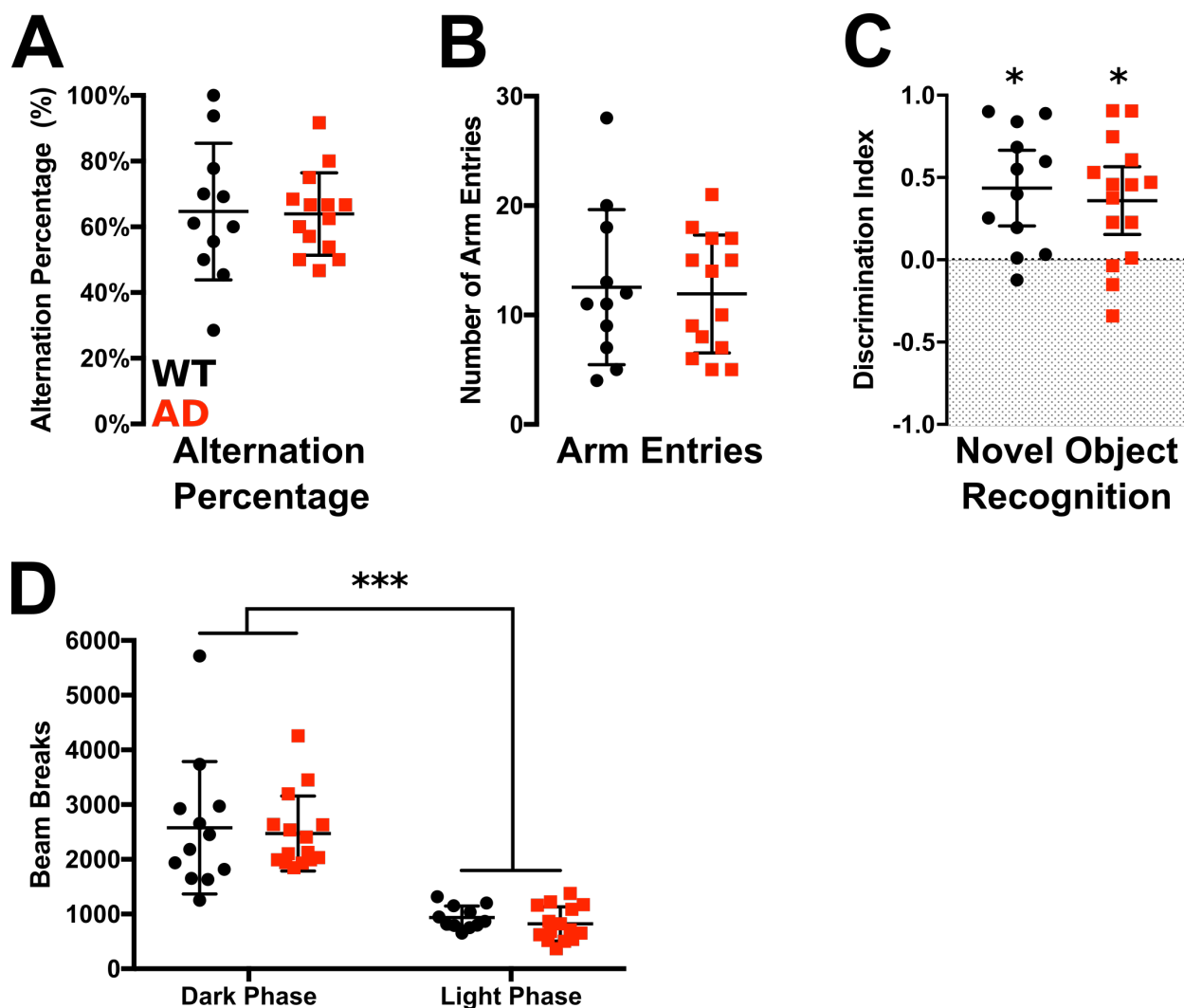


Figure 3.2 – There were no observed differences in test performance on the SAT or NOR at 12 months between WT and TgF344-AD rats.

Similar activity patterns were seen during 24-hours of monitoring following anesthesia. There was no difference in alternation percentage (A, $p=0.914$) or arm entries (B, $p=0.807$) within a Y-maze for WT and TgF344-AD rats. C) Both WT and TgF344-AD groups spent more time investigating the novel object in the NOR testing phase. Error bars represent 95% confidence intervals for each group. D) Both strains displayed similar

activity in the dark and light phases after anesthesia exposure (Two-way ANOVA, significant main effect of light cycle, $F(1,24)=75.68$, $p<.001$).

3.5.2 Emergence and Recovery from Isoflurane

Rats will resist being placed in a supine position and will reflexively reorient themselves to an upright stance. Traditionally, experiments on the effects of anesthesia use the loss of righting reflex and return of right reflex (RORR) to signify the timepoint of anesthetic induction and emergence, respectively. For these experiments, we differentiated between the emergence from anesthesia (RORR) and the continuation of the recovery from anesthesia by noting the time to return of ambulation and time to complete a modified version of the sticky dot test.

TgF344-AD rats displayed a hastened time to emergence compared with WT rats. There was a significant main effect of rat strain on the time elapsed between the first emergence behavior (Sighing) and the final emergence behavior (RORR) [Two-way ANOVA, $F(1,88)=5.625$, $p=0.012$]. However, multiple comparisons revealed no significant differences between WT and TgF344-AD rats on the time between the cessation of isoflurane delivery and any individual emergence behaviors. Additionally, two-way ANOVA revealed a main effect of behavior across the emergence process [$F(3,88)=4.6$, $p=0.005$], demonstrating that all rats displayed the observed emergence behaviors in the canonical order reported in previous publications^[87, 93].

TgF344-AD rats displayed a delayed recovery from anesthesia compared with WT rats. There was a significant interaction affect between the time to reach the observed recovery behaviors and recovery time for each rat strain as measured by Two-way ANOVA [$F(1,66)=11.65$, $p=.001$]. There was a significant difference in the time to reach each recovery behavior [$F(2,66)=94.07$, $p<.001$]. Sidak test for multiple comparisons revealed significant

differences between the latency to RORR [Mean WT (M_{WT})= 211.4s & Mean AD (M_{AD})=126.3] and both the latency to ambulation [M_{WT} =638.1s & M_{AD} =855.4s] or attempted removal of the adhesive tape [M_{WT} =1340s & M_{AD} =2195s]. There was significant increase in the latency to investigate the sticky dot for TgF344-AD rats when measured both during the recovery period only [Two-way ANOVA, main effect of rat strain, $F(1,66)=11.65$, $p=0.001$] and from the end of isoflurane delivery [Sidak multiple comparisons test, M_{WT} =1340s, M_{AD} =2195s, $p<.001$]. TgF344-AD rats regained consciousness following general anesthesia (as measured by RORR) earlier than WT littermates, however their time to recovery as measured by sticky dot was significantly lengthened. The sequence of emergence and recovery behaviors and the comparisons of the latency for WT and TgF344-AD rats to reach each behavior are represented in Figure 3.3.

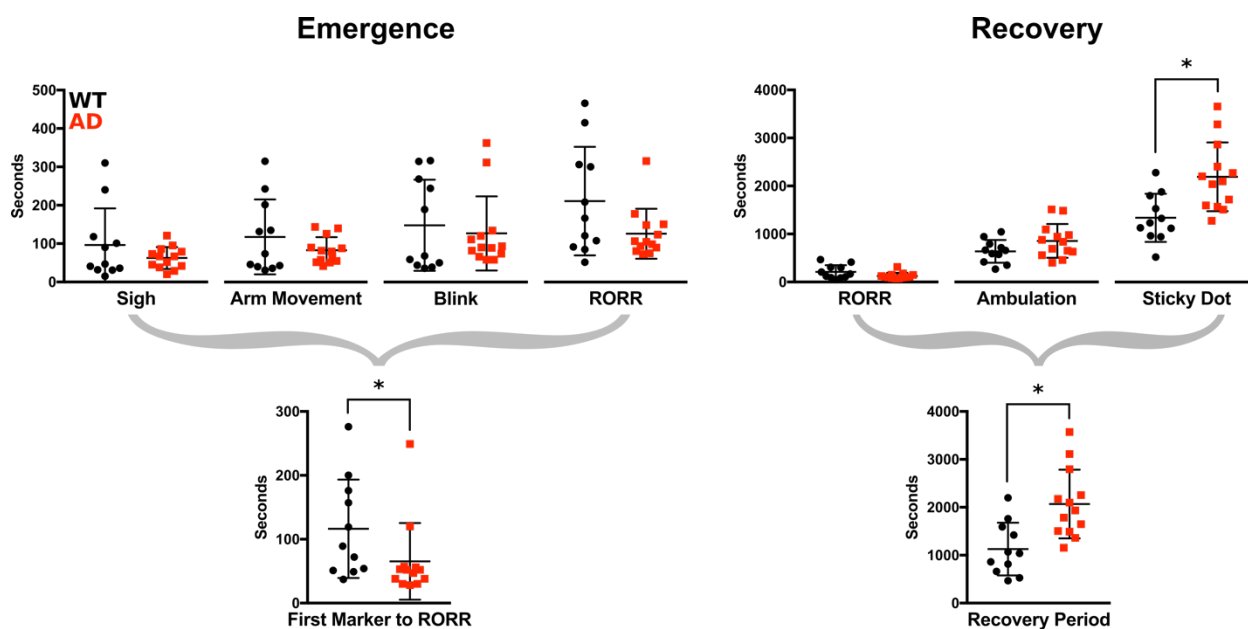


Figure 3.3 – Isoflurane emergence period is hastened and recovery is delayed in TgF344-AD rats.

Graphs on the top row plot the durations between ISO OFF and each emergence or recovery behavior. Graphs on the bottom row plot the duration for the emergence period

(First behavior to RORR) and the recovery period (RORR to Sticky Dot) separately. There was a shorter overall emergence period duration for TgF344-AD rats ($F(1,88)=5.625$, $p=0.012$), but no individual emergence behavior was significantly different between strains. The time to recover from anesthesia was lengthened in the TgF344-AD rats when measured from the end of emergence ($F(1,66)=11.65$, $p=0.001$) and from ISO OFF ($p<0.001$, Sidak's). Black circles = WT, Red squares = TgF344-AD. Emergence and recovery periods were analyzed using separate two-way ANOVA.

3.5.3 *Burst Suppression*

Illustration of burst suppression analysis and examples of burst suppression EEG are demonstrated in Figure 3.4 and discussed further in Appendix 2. Suppression of cortical activity is interspersed with bursts of high-amplitude, low-frequency voltage changes in cortical EEG. Bursts and suppressions were identified via a voltage threshold implemented on the absolute value of voltage from the filtered rat EEGs. The EEG signal was simplified to a binary time series (0=cortical bursts, 1=cortical suppression), EEG was subdivided into 15 second analysis epochs, and the ratio of suppression time to epoch time was computed for the entire recording. EEG electrodes were positioned (1) above the anterior portion of primary somatosensory cortex and (2) above the mediolateral portion of visual cortex 2 and hippocampus. Analysis from these EEG electrodes are referred to as (1) cortex and (2) hippocampus.

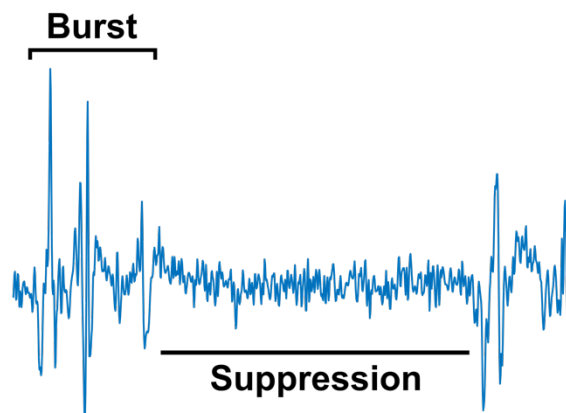
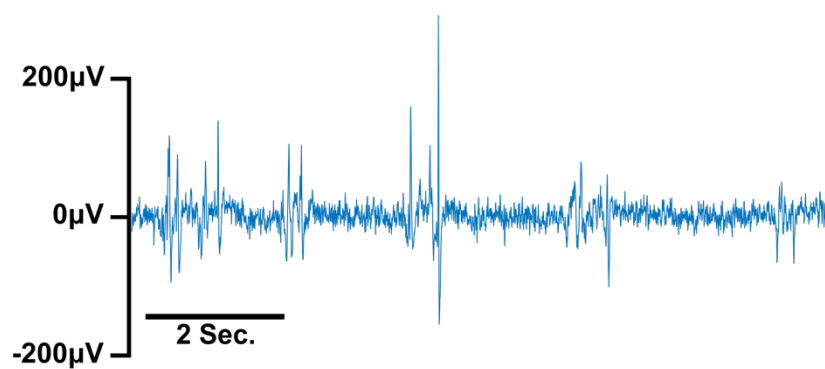
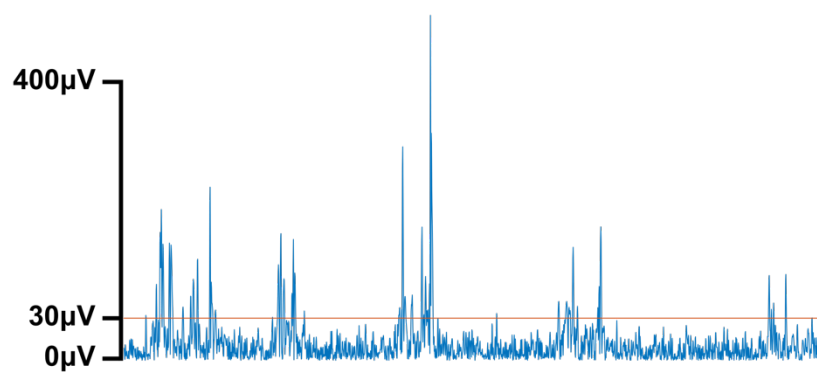
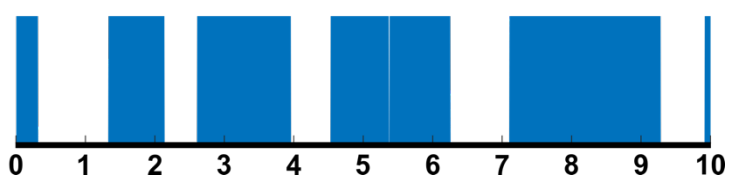
A**B****Cortical EEG****Filtered EEG****Binary Time Series**

Figure 3.4 – Example EEG recordings of cortical burst suppression.

A) Four seconds of EEG demonstrating a period of suppressed cortical activity between two bursts. The suppression in this segment lasts 2.2 seconds. The calculated BSR for this example is 0.55. B) Ten seconds of EEG recorded from a rat feature burst suppression during administration of 3.6% sevoflurane. The top voltage trace displays the unfiltered EEG recording. The middle trace displays recording after filtering (absolute value of voltage). The voltage threshold for bursts is set at 30 μ V. The bottom graph displays the corresponding binary time series labelling burst and suppressions. Suppressions are plotted in blue and bursts are plotted in white.

TgF344-AD rats did not demonstrate an increased sensitivity to sevoflurane anesthesia when compared with WT rats. Continuous BSRs (15s epochs, 14 second overlap between epochs) were computed for each rat over 10 minutes of EEG recording at each sevoflurane concentration (Analysis and supplemental figures in Appendix 2). There was little variation in the continuous burst suppression ratios. As a result, statistical comparison was completed using a mean BSR for each EEG recording, computed from non-overlapping 15s analysis epochs. Recordings from cortex demonstrated resilience to burst suppression during sevoflurane anesthesia for TgF344-AD rats. There was a significant interaction effect between sevoflurane concentration and rat strain. There were significant increases in BSR for TgF344-AD rats from 2.8% sevoflurane to concentrations of 3.2% ($p=0.034$), 3.6% ($p=0.001$), and 4.0% ($p<0.001$) as measured by Sidak multiple comparisons test. BSR from WT rats at 2.8% sevoflurane did not differ from BSRs at higher concentrations. There were no significant differences between BSRs in WT and TgF344-AD rats on recordings from the hippocampus electrode.

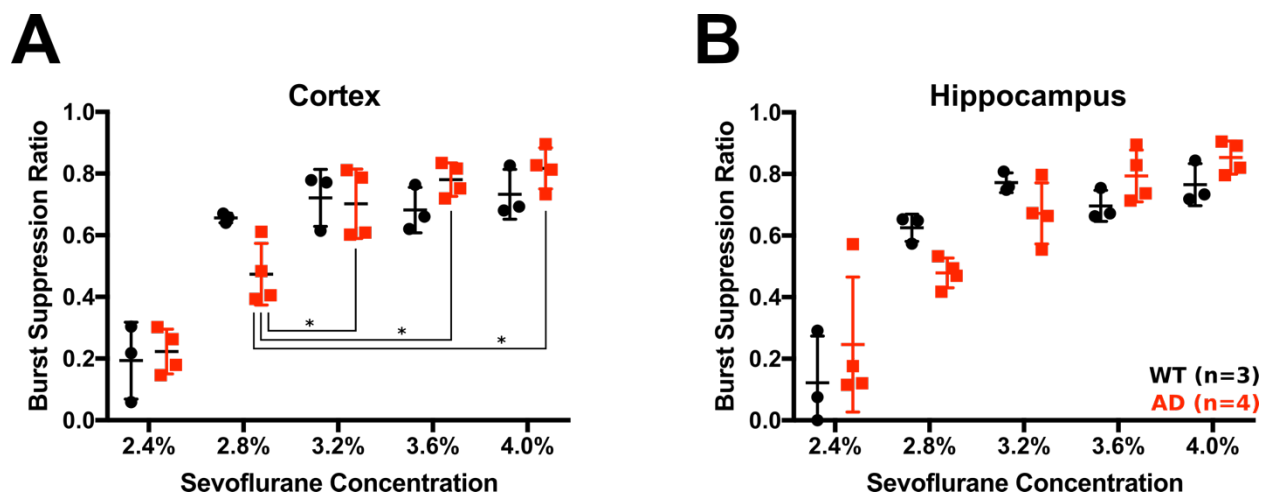


Figure 3.5 – TgF344-AD rats do not display increased sensitivity to sevoflurane.

A) There is a significant interaction between sevoflurane concentration and rat strain on burst suppression ratio [$F(4,25)=3.086$, $p=0.034$]. Multiple comparisons revealed significant differences between the BSR for TgF344-AD rats at 2.8% sevoflurane and those computed at 3.2% ($p=0.034$), 3.6% ($p=0.001$), and 4.0% concentrations ($p<0.001$). These comparisons were not significant for WT rats. Results suggest that TgF344-AD are resilient to cortical suppressions during administration sevoflurane. B) WT and TgF344-AD rats demonstrated no differences in burst suppression ratio on hippocampal electrode EEG recordings at any sevoflurane concentration.

3.5.4 Increased amyloid- β and GFAP in TgF344-AD rats after burst suppression

Amyloid- β and GFAP levels increased in dorsal hippocampus following exposure to sevoflurane anesthesia in TgF344-AD rats during EEG recordings (Figure 3.6). We used Welch's t-test, which makes no assumptions regarding group variances, to compare 3,3'-Diaminobenzidine (DAB) staining for both proteins between EEG implanted rats and age matched TgF344-AD rats (cohort used in Chapter 2). There was a significant increase in amyloid- β within dorsal hippocampus of TgF344-AD rats following burst suppression experiments ($p=0.001$, $M_{Con}=4.068$, $M_{BS}=6.949$). GFAP levels were also increased in dorsal hippocampus of TgF344-AD rats after sevoflurane anesthesia with burst suppression ($p=0.029$,

$M_{Con}= 2.153$, $M_{BS}=7.497$). WT brain slices ($n=2$) displayed no deposition of amyloid- β in dorsal hippocampus following sevoflurane anesthesia (0% positive pixel analysis, qualitative analysis).

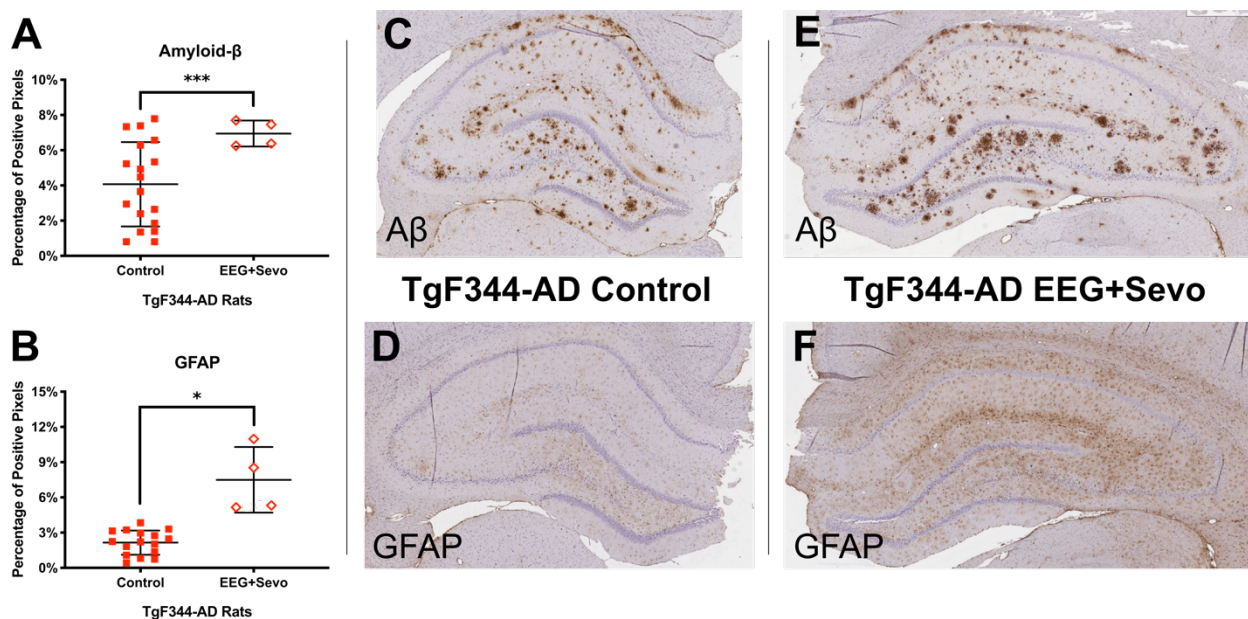


Figure 3.6 – Amyloid- β and GFAP levels are increased following sevoflurane administration in TgF344-AD rats.

Amyloid- β (A, Welch's t-test, $p=0.001$) and GFAP (B, Welch's t-test, $p=0.029$) levels are increased in the dorsal hippocampus of TgF344-AD rats after general anesthesia with sevoflurane. Examples of DAB stained brain slices used for quantification of amyloid- β and GFAP in TgF344-AD rats are displayed. Immunohistochemistry results from TgF344-AD rats aged to 12 months (C & D, cohort from Chapter 2) were compared with TgF344-AD rats receiving sevoflurane general anesthesia (E & F).

3.6 Discussion

These experiments demonstrate delayed recovery from anesthesia for TgF344-AD rats in the early disease phase. At the age of 12 months, these rats have begun to accumulate amyloid and demonstrate increased glial activity (results from Chapter 2) but do not yet display cognitive decline. TgF344-AD rats displayed a hastened emergence from isoflurane followed by an increased recovery duration. These results are not well explained by strain differences in

anesthetic sensitivity. The amount of burst suppression observed was mostly similar between WT and TgF344-AD rats, with the exception of a decrease in sensitivity to the 2.8% concentration of sevoflurane in TgF344-AD rats. Our results demonstrate an increase in both amyloid- β and GFAP in TgF344-AD rats following sevoflurane administration with burst suppression.

We did find evidence of resilience to cortical suppression by sevoflurane anesthesia in the TgF344-AD rat. These results complement previous experiments by Bianchi et al. on the induction of anesthesia by volatile anesthetics in Tg3xAD mice^[245]. In that study, Tg3xAD mice required exposure to higher concentrations of halothane, isoflurane and sevoflurane to achieve loss of righting reflex. Human AD is associated with altered sleep/wake behavior, with more fragmented sleep patterns and lower proportions of slow wave and REM sleep^[246]. In our previous work with the TgF344-AD rat, increased sleep/wake transitions and shorter bouts of REM and NREM sleep were recorded at 17 months old (Kruezer et al., in review). At 17-months, isoflurane exposure further exacerbated sleep/wake disturbances, with these rats displaying increased wakefulness during active periods and increased sleep fragmentation (Kruezer et al., in prep). These results together suggest a generalized increase in signaling from arousal pathways in AD that may compete with the hypnotic effects of general anesthetics.

Increased gamma band EEG activity has been described in AD, which is consistent with a greater overall influence of lower brain structures important for sensory perception and arousal on cortical processing^[247, 248]. It remains unclear whether increases in “bottom-up” gamma activity could result from increased brainstem signaling resulting from AD progression or due to a decrease in top-down processing resulting from cortical cell death^[249]. Additionally, our previous EEG recordings in TgF344-AD rats have demonstrated a narrowing of the dynamic

range of cortical activity between wake and sleep states during frank AD (Kreuzer et al., in prep). At 12-months, in early AD, emergence from isoflurane anesthesia was hastened in TgF344-AD rats and anesthetic recovery was significantly lengthened. These results are consistent with an increase in the influence of cortical arousal pathways in TgF344-AD rats during emergence from anesthesia. However, a faster emergence from anesthesia did not improve recovery from anesthesia.

It is not clear whether increased levels of amyloid- β are caused by sevoflurane administration or previous EEG surgery. Inhalation anesthetics have been previously demonstrated to increase amyloid- β oligomerization and cytotoxicity in cell culture^[250]. Prolonged isoflurane exposure is associated with increased caspase activity and extracellular amyloid accumulation in human neuroglioma cells^[251] and in adult WT mice^[138]. The effects of sevoflurane on amyloid- β have been studied previously in rodents. Sevoflurane is thought to activate apoptotic pathways which subsequently increase the production of amyloid- β ^[252]. The presence of amyloid- β further potentiates caspase-3 activation by sevoflurane creating a feedback loop resulting in even more amyloid- β production^[253]. The increase in amyloid- β and neuroinflammatory response following exposure to volatile anesthetics interfering in cortical processing is a potential mechanism for delayed recovery from anesthesia in TgF344-AD rats.

There are few studies available on interactions between sevoflurane and GFAP. Use of sevoflurane increased GFAP levels in rats given infusions of A β ₁₋₄₀ solution in hippocampus^[254] and in diabetic rats^[255], however sevoflurane is thought to be neuroprotective when administered following stroke and has been demonstrated to decrease post-ischemia GFAP levels. While transient increases in GFAP have been reported following surgery, protein levels appear to return

to baseline within 48 hours^[256]. Given the 14-day recovery period following EEG surgery, it is likely that increased GFAP levels are in response to sevoflurane anesthesia.

TgF344-AD rats display a delayed recovery for isoflurane anesthesia. Delayed recovery is preceded by a hastened emergence from anesthesia, leading to a significant increase in the total recovery time when compared to WT control rats. Delayed recovery is not likely to result from increased anesthetic sensitivity in TgF344-AD rats. In fact, the opposite is true, TgF344-AD rats display a resilience to the effects of volatile anesthetics that is consistent with a previous report in a mouse model of AD. Following prolonged administration of high concentrations of sevoflurane, we detected increased levels of amyloid- β and GFAP in dorsal hippocampus. Hastened emergence from anesthesia may best be explained by an increase in the influence of arousal pathways on cortical activity, which is supported by results from our previous experiments in TgF344-AD rats at a later disease stage. Delayed recovery may best be explained by an increase in AD protein levels during general anesthesia that may impact post-anesthesia cognitive function.

Chapter 4 - Prehabilitative Exercise Hastens Anesthetic Recovery in Diabetic and non-Diabetic Rats

Adapted From: Prehabilitative Exercise Hastens Anesthetic Recovery in Diabetic and non-Diabetic Rats. Christopher G Sinon, Amy Ottensmeyer, Austin N. Slone, Dan C. Li, Rachael S. Allen, Machel T. Pardue, Paul S García. *Anesthesia & Analgesia* - In Review. 2019.

4.1 Abstract

Type 2 diabetes mellitus, the most prevalent metabolic disease worldwide, increases the risk for experiencing cognitive impairments. It has been previously reported that diabetic patients experience impaired cognitive function following cardiac surgery, especially on speed-related tasks. In an animal model of type 1 diabetes, exposure to isoflurane anesthesia without surgery is sufficient to cause memory problems. Exercise is often prescribed as a treatment for diabetic patients and regular physical activity is hypothesized to decrease the risk of postoperative cognitive impairments. This study examined the effects of diabetes, with and without prehabilitation exercise, on recovery from isoflurane anesthesia in a type 2 diabetic rat model. Wistar control (n=32) and Goto-Kakizaki (GK) type 2 diabetic (n=32) rats between 3-4 months old underwent treadmill exercise for 30 min/day for ten days or remained inactive. Pre-anesthesia spontaneous alternation behavior was recorded with a Y-maze to determine cognitive performance on a spatial memory task. Rats then received either a 2-hour exposure to 1.5-2% isoflurane in oxygen at 1L/minute or oxygen only. After 2 hours, the time to reach anesthetic emergence and post-anesthesia recovery behaviors, including the use of a modified sticky dot removal test, was manually recorded for each rat. PSD-95 protein levels were quantified from hippocampus using western blot. Diabetic rats show a decrease in spontaneous alternation behavior ($p=0.044$) and in maze exploration ($p<0.001$). Active and inactive rats displayed no difference in their emergence times from isoflurane general anesthesia, but exercise hastened the total anesthesia recovery time

($p=0.008$) and the time between emergence and the final post-anesthesia recovery behavior ($p=0.006$) for both Wistar and GK rats. Following 10 days of exercise, both Wistar and GK rats show increased levels of PSD-95 in the hippocampus, an important regulator of synaptic strength. Exercise training prior to general anesthesia resulted in hastened recovery from isoflurane regardless of the presence of diabetes, potentially due to increased synaptic proteins in the hippocampus. These results suggest that prehabilitation with moderate intensity exercise, even on a short timescale, could be beneficial for anesthesia recovery, regardless of metabolic disease status.

4.2 Introduction

4.2.1 Diabetes and Surgery

As surgical practice continues to improve worldwide, patient risk factors, as opposed to surgical risk factors, show a stronger association with postoperative complications and mortality^[257, 258]. Diabetes Mellitus (DM) is a major public health problem, with approximately 9.4% of the U.S. population affected^[259, 260]. The number of patients with type 2 DM has doubled within the last two decades and the rising prevalence of the disease necessitates a better understanding of the risks faced by patients with DM during surgery. DM is a metabolic disorder that negatively affects brain and cognitive function^[261]. Patients with DM are more likely to experience cognitive impairment due to both cerebrovascular and neurodegenerative mechanisms^[262]. Diabetic patients undergoing surgery are at a greater risk for perioperative and postoperative neurological complications, such as stroke^[263] and diminished cognitive function^[264]. Patient history of diabetes has been independently associated with increased risks for both postoperative delirium (POD)^[265] and postoperative cognitive dysfunction (POCD)^[228]. Risk for POCD increases in diabetic patients with poorer glycemic control and higher hemoglobin A1c level^[228].

4.2.2 General Anesthesia and Cognitive Dysfunction

General anesthesia has been associated with higher rates of postoperative cognitive dysfunction than local or regional anesthesia^[266]. Animal models have shown that a single anesthetic exposure leads to an increase in apoptotic signaling and changes in synaptic morphology^[267], arguing that anesthesia itself may be responsible for observed cognitive deficits. The process of emergence from anesthesia involves distinct regulation of neurological activity and neurotransmitter release^[83]. This process is not simply a reversal of the induction of anesthesia,

and therefore changes in neurological function may differentially affect the processes of anesthetic induction, emergence and recovery. In diabetic models, rats with hallmarks of metabolic syndrome displayed cognitive deficits after surgery and a streptozotocin-induced rat model of type 1 DM displayed cognitive deficits after anesthesia challenge^[268, 269]. The cognitive effect of an anesthesia challenge on a model of type 2 diabetes, the most common form of DM^[270], has not been studied.

4.2.3 The Effects of Exercise on Cognitive Reserve

Cognitive reserve is a research construct that attempts to explain the variability in cognitive function seen in individuals at high risk for cognitive decline, especially in relation to AD and normal aging^[271]. The concept of cognitive reserve has received attention in attempts to define “at risk” populations for postoperative cognitive impairments, as low educational attainment and premorbid ability as well as frailty are independent risk factors for POCD^[272]. Cognitive reserve is also modifiable and there are a number of known translational approaches for increasing cognitive reserve^[273]. Increasing physical activity is known to improve cognitive reserve and reduce risk for dementia^[274]. Boraxbekk et al. found that humans with an active daily lifestyle had increased average volumes of cortical grey matter compared with sedentary participants^[275]. In active individuals, EEG activity is better correlated within well-defined functional connectivity networks, such as the Default Mode Network and Task Positive Network. Sedentary patients over the age of 65 are at higher risk for postoperative cognitive impairments following surgery than similarly aged, physically active patients^[272]. In addition, exercise is known to be beneficial in both managing blood glucose levels in patients with type 2 DM and for improving neurological health and function^[230, 276, 277]. As a result, exercise represents a promising prehabilitative intervention that may reduce postoperative cognitive complications for patients with type 2 DM.

4.3 Experimental Design and Hypotheses

The goal of this work was to investigate the influence of moderate exercise on both anesthetic emergence as well as post-anesthesia recovery behaviors in a type 2 diabetic rodent model, the Goto-Kakizaki (GK) rat, and in non-diabetic Wistar control rats. The GK rats are a spontaneously occurring hyperglycemic, non-obese model of type 2 diabetes^[278, 279]. All experiments were performed on rats between 3-4 months of age. The experimental timeline and breakdown of experimental groups for all rats are presented in Figure 4.1A-B.

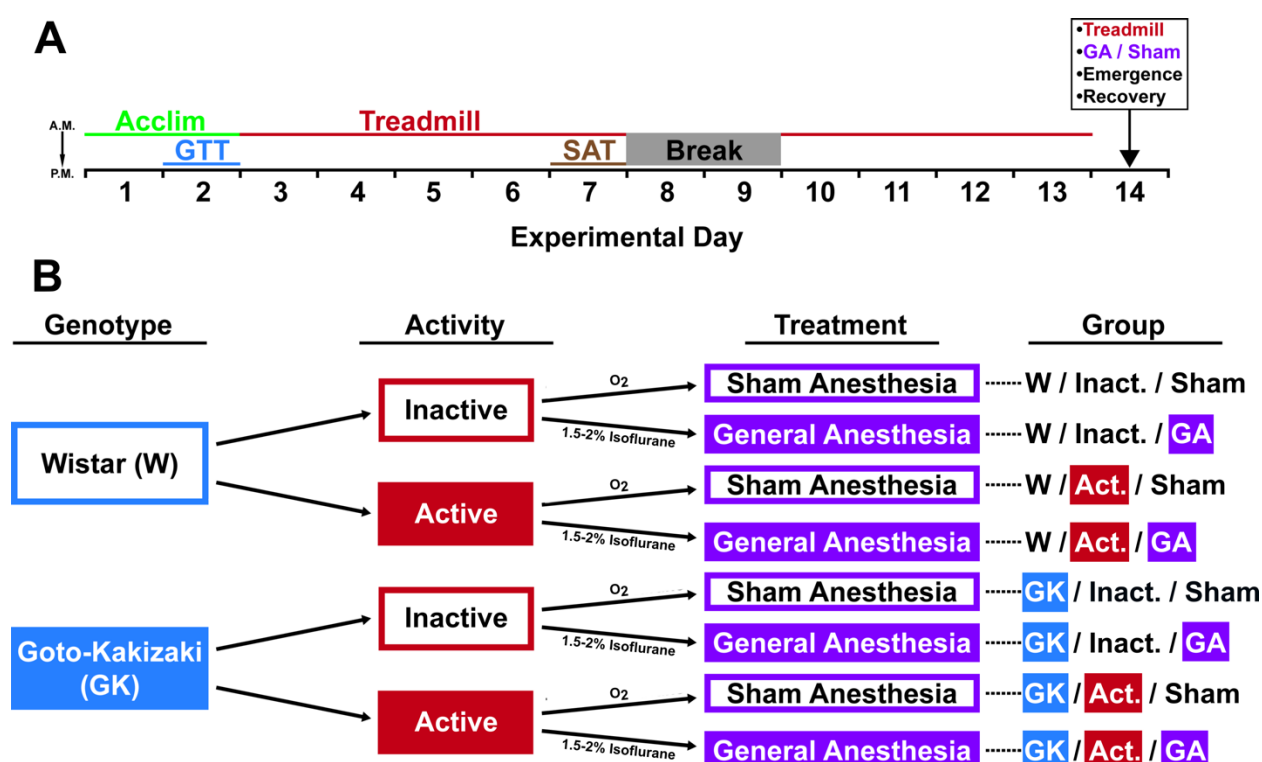


Figure 4.1 – Illustration of experimental timeline and design.

A) Full experimental timeline for each rat in the study. Acclim = Treadmill Acclimation, GTT = Glucose Tolerance Test, SAT = Continuous Spontaneous Alternation Behavior Test, GA = General Anesthesia, Sham = Sham Anesthesia. B) Experimental groups in 2 x 2 x 2 study design.

We hypothesized that GK rats receiving isoflurane would show delayed anesthetic emergence and recovery, while GK rats undergoing exercise training would display no differences on these tests when compared with Wistar control rats.

4.4 Methods

4.4.1 Animals

All experiments were conducted at the Atlanta VA Health Care System Animal Facility. Wistar (n=34) and GK (n=37) rats were used for data collection. Over the course of this study, 7 rats (2 Wistar & 5 GK) were removed for failure to complete treadmill running resulting in a total of 8 rats per experimental group. Wistar and GK breeders were ordered from Charles River Laboratories and then a breeding colony of each strain was maintained. All experiments were performed on rats between 3-4 months of age. The rats were housed in 12-hour light cycles with ad libitum access to rodent chow and water.

4.4.2 Glucose Tolerance Test (GTT)

GK rats demonstrate impaired response to glucose challenge^[280]. To verify the presence of type 2 diabetes symptoms in our GK rats, the glucose tolerance test was performed. Rats were food deprived for 6 hours. Blood glucose levels were monitored by test strip (FreeStyle Lite, Abbott Diabetes Care Inc., UK). An intraperitoneal injection of glucose (2 mg per kilogram body weight in sterile water) was administered and blood glucose levels were recorded at 15, 30, 60 and 120 minutes post-injection.

4.4.3 Treadmill Exercise

Active rats completed an exercise routine consisting of forced treadmill running for 10 days (Exer 3/6 Animal Treadmill, Columbus Instruments, Columbus, OH, USA), as previously reported^[281]. All exercise sessions were performed on Monday-Friday between 9-11 am. Rats

were trained to run on treadmills in 30-minute sessions starting with a treadmill belt speed of 10 meters per minute. Exercise intensity was gradually increased over the first 5 days to a treadmill belt speed of 15 meters per minute. If 10 shocks were received during any single training session, the session was aborted. Failure to train to under 10 shocks received per session within the first 5 days of training resulted in removal of that rat from the study. Following 2 days of rest, the five days of treadmill exercise were completed with belt speeds of 15 meters per minute. Inactive rats were placed on a stationary treadmill to control for environment. Over the course of this study, 7 rats (2 Wistar & 5 GK) were removed for failure to complete treadmill running.

4.4.4 Continuous Spontaneous Alternation Behavior Test

The Continuous Spontaneous Alternation Test was performed within a Y-maze. Rodents introduced to a Y-maze display a tendency to alternate arm entries during maze exploration. This tendency towards alternation is thought to result from a preference towards investigation of new environments, and the SAT takes advantage of this behavior as an assessment of spatial working memory^[213]. Rats were allowed to freely explore the Y-maze (San Diego Instruments, San Diego, CA, USA) with all three arms open for 8 minutes. If at any time the rat remained stationary for >60 seconds during the session, movement was motivated by briefly grasping and releasing the rat from the base of the tail. The number of arm entries and the path of arm exploration were determined by a blinded observer.

A successful alternation was scored when the rat completed three consecutive arm entries via turns in the same direction. Alternation percentage was determined using the following equation^[214]:

Equation 1:

$$\text{Alternation percentage} = \frac{\# \text{ of Alternations}}{\text{Total \# of Arm Entries} - 2} * 100$$

4.4.5 Isoflurane Anesthesia

Our anesthesia protocol was modified from our previous work [86]. A state of general anesthesia was induced in rats using an induction chamber pre-charged with 2% isoflurane in oxygen (O₂). When rats displayed a loss of righting reflex and a visible decrease in respiration rate, they were transferred to a nose cone delivering 2% isoflurane in O₂ at a rate of 1 L/minute. General anesthesia was maintained for 2 hours via nose cone with respiration rate and body temperature recorded for each rat in 5 minute intervals. Body temperature was maintained at 38±0.5°C via heating pad and monitored via rectal thermometer. Isoflurane anesthesia was reduced to a 1.5% dose shortly after the transfer to the nose cone and dose was then titrated to respiration rate (between a 1.5-2% dose) as needed throughout the course of the experiment. Sham general anesthesia in the form of 2 hours of exposure to O₂ at 1 L/minute in an induction chamber was delivered to half of the rats in the study.

4.4.6 Anesthetic Emergence & Recovery

After 1-hour & 50-minutes of general anesthesia, a small piece of adhesive tape (~0.5cm x 3cm) was wrapped around the rat's left forepaw and the temperature probe was removed. At the two-hour mark, the isoflurane concentration was reduced to 0% and a stopwatch was started simultaneously. For these experiments, we chose to distinguish between the period of emergence from isoflurane anesthesia and the period of recovery from the effects of isoflurane anesthesia, similar to methods applied in [87, 93]. Anesthetic emergence was defined as the period between cessation of isoflurane delivery (ISO OFF) and the return of righting reflex. The time to each of the following anesthetic emergence milestones was recorded for each rat receiving isoflurane: limb movement, sudden changes in respiration, blinking, mastication and return of righting reflex. Anesthetic recovery was defined as the period from the return of righting reflex until the first

attempt to remove the adhesive tape from the left forepaw. The modified sticky dot test used in these experiments, and as previously reported^[87], requires perception of the adhesive tape and the return of grooming behaviors following the regaining of consciousness.

4.4.7 Western Blot

Hippocampal tissue collected from rats receiving isoflurane anesthesia (Wistar, n=13 [7 active, 6 inactive]; GK, n=14 [6 active, 8 inactive]) was analyzed for levels of post-synaptic density protein 95 (PSD-95). PSD-95 is a scaffolding protein that acts as an important regulator of synaptic strength^[282]. Tissue was homogenized in lysis buffer [137 mM NaCl, 20 mM tris-HCl (pH=8), 1% igepeal, 10% glycerol, 1:100 Phosphatase Inhibitor Cocktails 1 and 2 (Sigma-Aldrich) and 1:1000 Protease Inhibitor Cocktail (Sigma-Aldrich, St. Louis, MO, USA)] and protein concentrations were determined by a Pierce BCA Protein Assay kit (Thermo Fisher Scientific, Waltham, MA, USA). 20 µg of each sample was separated by SDS-page on a 7.5% gradient, stain-free Tris-glycine gel (Bio-Rad Laboratories, Inc., Hercules, CA, USA), and total protein images were obtained prior to transfer. Next, samples were transferred to a PVDF membrane (Bio-Rad) and blocked with 5% non-fat dry milk for 1 hour. The membrane was incubated overnight at 4 °C in primary antibodies, including ERK42/44 [1:500; Cell Signaling (Product #9102)] and PSD-95 [1:5000; Cell Signaling (Product #3450)]. Following 1 hour of incubation in secondary antibodies [goat anti-rabbit peroxidase labeled IgG (Vector Laboratories, Burlingame, CA, USA)], immunoreactivity was assessed using a chemiluminescence substrate (Thermo Fisher Scientific). Both total protein and immunoreactivity was quantified using the ChemiDoc MP Imaging System (Bio-Rad).

4.4.8 Statistical Analysis

Statistical testing was performed using Prism 7.0 software (GraphPad Software, San Diego, CA, USA). All values are reported as mean \pm SD. Glucose levels were compared using Welch's t-test, while glucose tolerance tests were analyzed using two-way repeated measures analysis of variance (ANOVA) followed by post hoc tests using Sidak's correction for multiple comparisons. Unpaired Student's t-test was used to compare behavioral data from the continuous SAT. Two-way ANOVA with Sidak's post hoc comparisons was also used for comparing emergence and recovery data as well as PSD-95 levels.

4.5 Results

4.5.1 Glucose Tolerance Test

Fasted blood glucose levels in Goto-Kakizaki rats were significantly different from controls (79.56 ± 11.78 , $n=32$ for Wistar, 122.3 ± 36.76 , $n=32$ for GK, $p<0.001$, Welch's t-test) (Table 1). This finding is similar to previous results demonstrating elevated levels of blood glucose during fasting in GK rats^[278-280]. Following intraperitoneal injection of glucose, blood glucose levels were consistently higher for GK rats when compared with controls. There was a two-fold increase in blood glucose concentration between groups at 15 and 30 minutes post-injection and three-fold increases at both 60 and 120 minutes post-injection (Interaction effect $F(3, 186)=16.44$, $p<0.0001$) (Table 4.1).

Table 4.1. Blood glucose levels as measured by test strip for GTT

Time Point	Blood Glucose (mg/dL)	
	Wistar (n = 32)	GK (n = 32)
Baseline	79.56 +/- 11.78	122.3 +/- 36.76***

15 min	142.1 +/- 35.84	250.5 +/- 75.01***
30 min	149.6 +/- 32.03	313.6 +/- 60.93***
60 min	103.9 +/- 18.6	314.2 +/- 74.04***
120 min	82.47 +/- 11.6	242.8 +/- 79.77***

4.5.2 Y-maze Continuous Spontaneous Alternation Behavior Test Performance

The continuous spontaneous alternation test was performed in a Y-maze for all rats 7 days prior to anesthesia exposure. There were no statistical differences in test performance as a result of prior treadmill training for either strain, so all strain data was grouped together for comparison. GK rats displayed decreased spatial working memory when compared with Wistar controls ($p=0.044$) (Figure 4.2A). Spontaneous alternation percentage was higher for Wistar rats (73.06 ± 9.46 , $n=32$) than GK rats (67.63 ± 12.5 , $n=32$) as measured using an unpaired Student's t-test. There was also a notable decrease in exploratory behavior between strains during the continuous spontaneous alternation test. GK rats completed significantly fewer arm entries than Wistar rats during maze exploration (23.78 ± 6.833 , $n=32$ for Wistar, 12.88 ± 3.687 , $n=32$ for GK, $p<0.001$) (Figure 4.2B). Overall, GK rats display a decrease in spatial working memory in addition to a decrease in maze exploration, similar to a previous report^[283].

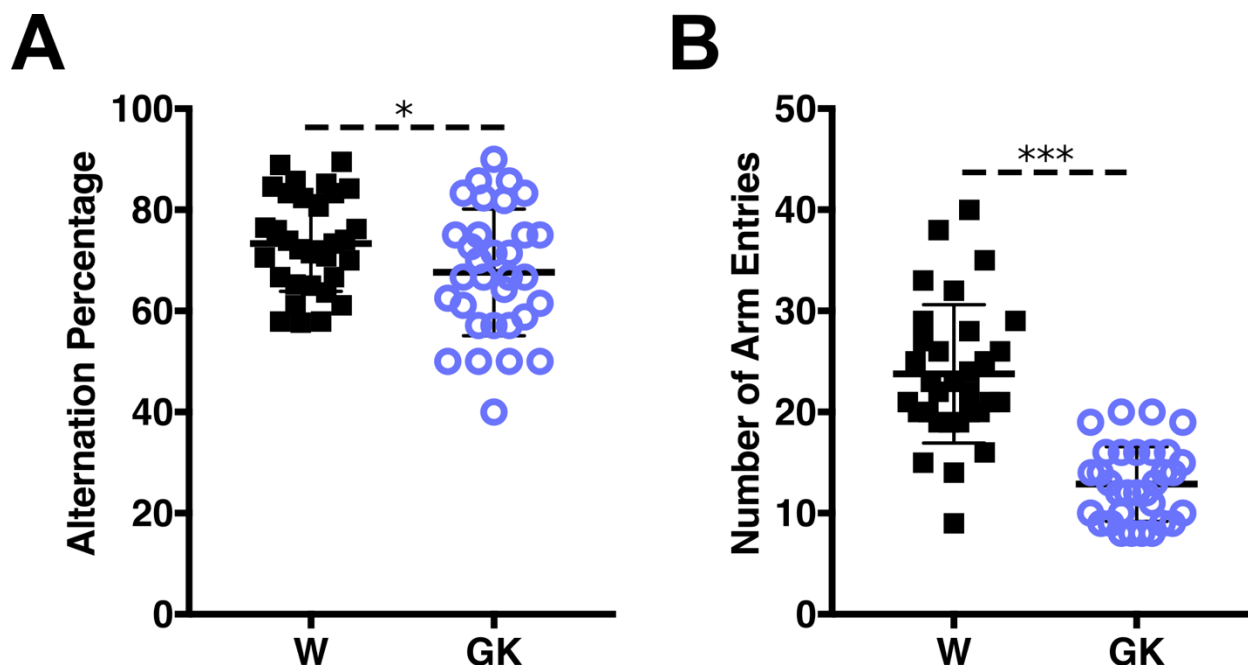


Figure 4.2 – GK rats perform worse than Wistars on a test of spatial working memory.

A) Wistar (W, n=32) rats were more likely than GK rats (n=32) to alternate between maze arms during Y-maze exploration (Student's t-test, $p=0.044$). B) GK rats perform significantly fewer arm entries during maze exploration when compared with Wistar rats (Student's t-test, $p<0.001$). Results are represented as group mean with standard deviation.

4.5.3 Anesthetic Emergence and Recovery

There were no significant main effects of genotype or activity in sticky dot test performance from rats receiving sham anesthesia (data not shown). There was no difference between any groups in time to emergence from isoflurane as determined by two-way ANOVA (Figure 4.3A). Active rats showed a significant reduction in time to notice the sticky dot following isoflurane anesthesia (two-way ANOVA, $(F(1,28)=8.197, p=0.008, \text{Figure } 4.3B)$). The recovery period was defined for each rat as the difference in time from return of righting reflex to the first sticky dot removal attempt. Active rats recovered more quickly following return of righting reflex than those that remained inactive (two-way ANOVA, $(F(1,28)=8.585, p=0.006)$).

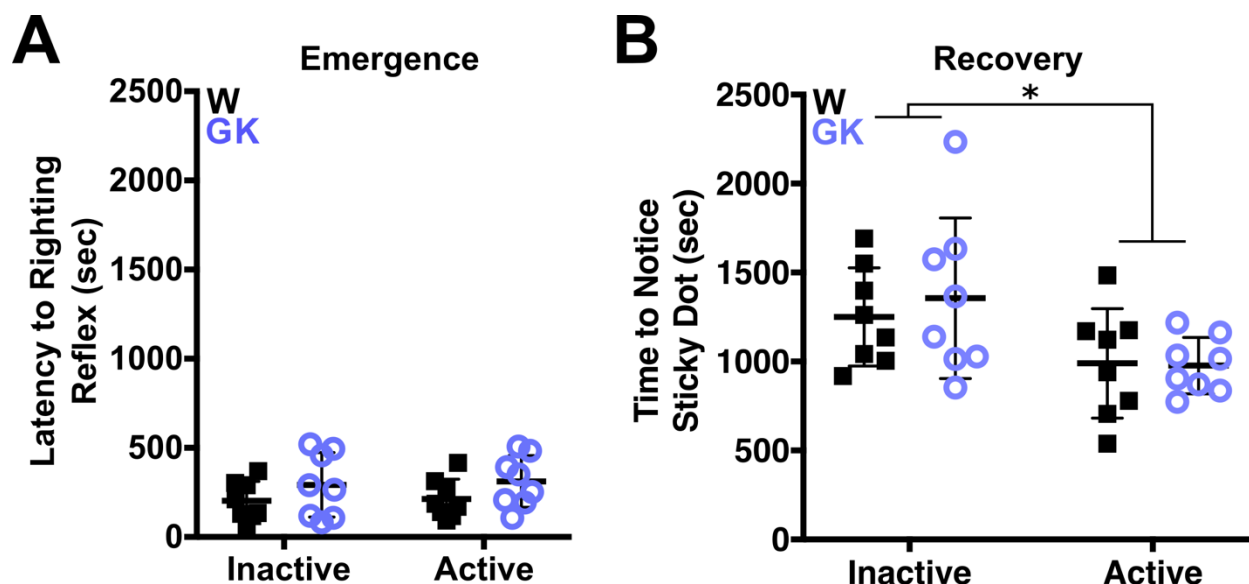


Figure 4.3 – Exercise hastens recovery from general anesthesia in both Wistar and GK rats but has no effect on anesthetic emergence.

A) For rats receiving general anesthesia, there was no effect of genotype or exercise on the time to emergence from isoflurane anesthesia, defined as the time from ISO OFF to return of the righting reflex. B) Exercise decreased the time to notice the sticky dot for both Wistar and GK rats ($F(1,28)=8.197$, $p=0.008$).

4.5.4 PSD-95 Levels in Hippocampus

Synaptic protein levels in the hippocampus showed a significant interaction between diabetes and exercise (Two-way ANOVA ($F(1,23)=34.47$, $p<0.001$). Western blots are pictured in Figure 4A. Treadmill exercise increased hippocampal PSD-95 levels for both Wistar ($p<0.001$) and GK rats ($p=0.016$). Wistar rats displayed a larger increase in PSD-95 levels as a result of exercise than GK rats ($p<0.001$) (Figure 4B).

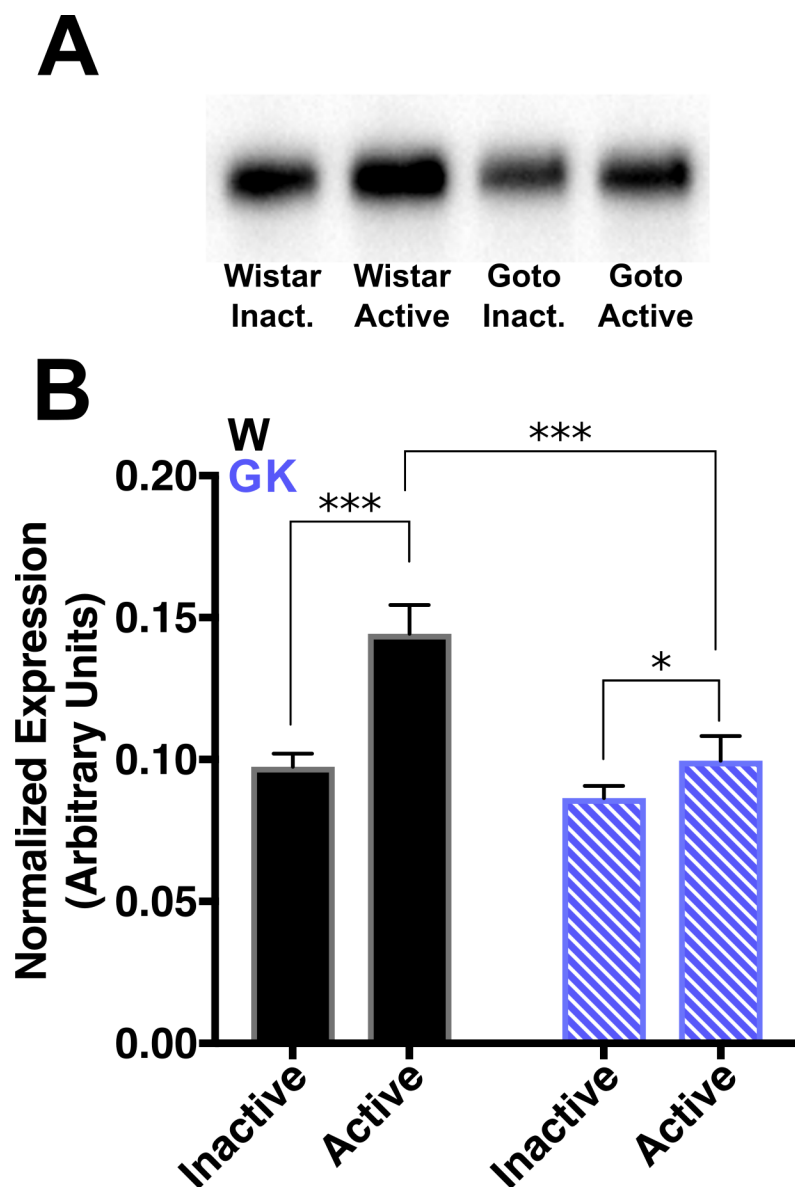


Figure 4.4 - Wistar and GK rats both demonstrate increased PSD-95 levels in hippocampus after 10-days of treadmill exercise.

A) Western blots for PSD-95 from hippocampal tissue are shown. B) Exercise increases hippocampal PSD-95 levels (Interaction effect, $F(1,23)=34.47$, $p<0.001$). Hippocampal PSD-95 levels increased in both Wistar ($p<0.001$) and GK rats ($p=0.016$), but Wistar rats demonstrate a greater overall increase in PSD-95 from pre-exercise levels ($p<0.001$).

4.6 Discussion

Our results highlight the positive effect of exercise on recovery from anesthesia. In both the diabetic GK and control Wistar rats, 10 days of moderate exercise hastened recovery after isoflurane anesthesia.

The GK rats in the present study displayed higher fasted blood glucose levels and impaired glucose metabolism compared with Wistar rats. GK rats also demonstrated decreased spatial working memory performance and overall activity levels at 3 months of age. Delayed emergence from general anesthesia can be a cause of serious concern in the immediate and intermediate postoperative period^[284]. When anesthetic factors are ruled out, the delayed emergence may be caused by metabolic disorders or perioperative complications such as cerebral hypoxia or hemorrhage. Despite impaired glucose metabolism, differences in activity levels and a mild decrease in spatial working memory, emergence from anesthesia was unaffected in GK rats. Similarly, we saw no difference in anesthetic recovery time, as measured using the modified sticky dot test, between Wistar and GK rats.

Both strains were able to adapt to a moderate daily exercise routine consisting of forced treadmill running. Prehabilitative exercise training decreased the time to recovery from general anesthesia for both diabetic and control rats. While our initial hypothesis was that exercise may hasten recovery in diabetic rats, it was surprising that exercise also hastened recovery time in adult control rats. Young adult humans, without additional medical diagnoses like DM or neurodegenerative disease, are not often thought of as at risk for postoperative cognitive problems that might be mediated through prescription of exercise^[285, 286]. While comparing relative ages in humans and rats is fraught with difficulty, the 3-4 month age range for rats included in our experiments would place them developmentally between sexual maturity at 6 weeks and the end

of skeletal growth at 7-8 months^[287]. Future studies on the influence of exercise on anesthetic recovery in rodents may benefit from a focus on physiological changes resulting from exercise that may correlated with hastened anesthetic recovery that can be seen in healthy adult rats.

Cognitive complications in the acute recovery period from surgery are correlated with lengthened hospital stays and an increased likelihood of readmissions in the subsequent 30 days^[107]. Early postoperative mobilization and exercise appears to be an effective step towards reduction of cognitive impairments^[285, 288, 289], and preoperative exercise remains a promising intervention for improving patient fitness for surgery^[230]. In humans, exercise interventions have been shown to increase performance on learning and memory tasks. These benefits have been hypothesized to result from an increase in factors promoting neurogenesis and synaptogenesis following exercise, including upregulation of neurotrophins such as brain derived neurotrophic factor (BDNF)^[281] and increased proteins regulating synapse growth and stability such as PSD-95^[277]. The binding of BDNF to TrkB receptors has been shown to regulate the transportation of PSD-95 to the synapse and, in addition, the formation of PSD-95-TrkB complexes is important for intact BDNF signaling^[290]. Indeed, studies in rats using similar treadmill designs with low or moderate intensity exercise have demonstrated increases in hippocampal BDNF and PSD-95 levels that correlate with improved performance on memory tasks^[291].

Our results demonstrate increased PSD-95 levels in hippocampus following treadmill exercise, suggesting that our exercise regimen was effective for increasing factors that regulate synapse integrity in rats. We did observe a significant difference in PSD-95 protein levels between active Wistar and GK rats. Insulin signaling in the brain has been shown to an important regulator of synapse growth and stability. For example, activation of insulin receptors has been shown to increase PSD-95 synthesis in hippocampus through the PI3-kinase-Akt-mTOR

pathway^[292]. It is possible that the difference in PSD-95 levels between strains following exercise is due to insulin resistance in the GK rats. The present study did not assess blood glucose or insulin levels following treadmill exercise in the Wistar or GK rats. A previous report using a higher intensity, 8-week treadmill exercise regimen in the GK rat demonstrated no change in glucose concentrations in blood plasma after training, however there was a significant decrease in insulin concentrations. Further study is needed to determine if changes in PSD-95 levels in these strains are dependent on alterations in insulin signaling following exercise.

The results of this study show that exercise is effective for reducing recovery time following isoflurane general anesthesia. Altogether these observations suggest that prehabilitative exercise may help to improve cognitive outcomes in patients receiving general anesthesia.

Chapter 5 - General Discussion

5.1 Introduction

The modern history of anesthesia is inherently linked with the modern history of surgery. As the practice of anesthesiology developed and knowledge within the discipline progressed, surgical procedures became longer and more invasive. Successful open-heart surgery was performed within 100 years of the 1846 public demonstration of ether by William Morton. Successful organ transplants were performed by the 1950s. Surgery has gradually become a safer, more routine and increasingly out-patient procedure. As a result, patient risk factors are often the most significant considerations for operative success and there is an increasing focus on optimizing preoperative and postoperative care to improve surgical outcomes. Most often successful surgeries result in improvements in the health of the patient. These might lead to a more active lifestyle and result in cognitive improvement. However, it is also clearly demonstrated that cognitive disturbances can result from surgery in humans, especially in the vulnerable brains of the very old, very young and the very sick. A better understanding of the risk factors and etiology of these conditions will result in better pre-, peri- and postoperative treatments.

There are currently no accepted animal models for perioperative neurocognitive disorders (PNDs), such as postoperative delirium (POD) and persistent perioperative neurocognitive disorders (PPNDs) which used to be grouped under the vaguely defined (POCD). Previous experiments in animals have shown anesthesia-induced deficits on learning and memory tasks lasting days to weeks, suggesting that POCD could arise from similar anesthesia-induced mechanisms^[116, 118]. A major caveat of these experiments is neither the neurocognitive assessments performed in humans nor the cognitive tests performed in rodents have been standardized between research groups, which makes the interpretation of conflicting clinical and

preclinical results difficult. The potential for future standardization of the clinical screening for mild and major NCD (the proposed nomenclature changes for POCD) will also create more favorable parameters for translatable preclinical experimentation.

Despite these concerns, anesthesia has well-validated and reproducible behavioral effects that are advantageous for the study of anesthetics in preclinical models. In *C. elegans*, immobility is a behavioral proxy for achievement of surgical anesthesia. In fish, anesthesia is sufficient for surgery when there is a loss of equilibrium and muscle tone combined with a lack of response to touch. In amphibians, surgical anesthesia is achieved when righting reflex, gular movements and toe pinch reflexes cease. In mammals like rodents, many laboratories distinguish between sleepiness due to sedation and unconsciousness consistent with general anesthesia with the righting reflex (RR). The loss of righting reflex (LORR) is a commonly used and easily determined behavioral marker for the induction of anesthesia and the return of righting reflex (RORR) is a convenient behavioral marker for the end of anesthesia emergence. For the experiments contained in this thesis, we hypothesized that a reliable behavioral marker for the prolonged recovery from anesthesia could be established through ethological observations beyond RORR.

This thesis contains experiments which tested the use of the sticky dot test in the assessment of anesthetic recovery in rat models of early AD and type-2 diabetes. **Chapter 2** investigated the behavioral and pathological effects of expression of FAD-associated proteins in Fischer 344 rats at 12 and 18 months of age. There were no differences between WT and AD rats on cognitive tests performed at 12 months of age, despite significant increases in whole brain amyloid- β and GFAP. These results are consistent with the early stages of human AD where significant amyloid- β accumulation and chronic neuroinflammation are seen before cognitive

symptoms^[293]. At 18 months, TgF344-AD rats displayed improved learning and working memory performance on the WRAM after 6 months of treatment with the ARB, candesartan.

Chapter 3 demonstrated hastened emergence from anesthesia followed by delayed recovery in TgF344-AD rats in the early stage of AD progression. EEG recordings in rats of the same age did not demonstrate any changes in anesthetic sensitivity in response to sevoflurane at 12 months between TgF344-AD and WT rats. **Chapter 4** contained the results of experiments on anesthetic emergence and recovery in Wistar and Goto-Kakizaki rats following treadmill exercise. Wistar and Goto-Kakizaki rats did not differ in their duration to emergence or recovery from anesthesia, however all rats with prior treadmill exercise recovered more quickly from anesthesia than those that remained inactive.

5.2 Sticky Dot Test

The modified sticky dot test (also known as the adhesive removal test) has traditionally been used in rodents as a test of sensorimotor function in the context of neurodegeneration, stroke and traumatic brain injury^[294]. The sticky dot test also has the benefit of being a very sensitive behavioral test, similar to assessments of LORR and RORR, because the adhesive tape stimulus is a powerful motivator of stereotyped movements. When the stimulus is applied to the forepaw these movements include attempts to pull the tape using the mouth or opposite forelimb and rapid shaking of the taped forelimb.

Use of the sticky dot test during recovery from anesthesia in rodents has been reported in response to two different anesthetic reversal agents, yohimbine and atipamezole^[87]. The contained work demonstrates that the sticky dot test is sensitive to changes in the duration for recovery of sensorimotor function following anesthesia exposure in rodent models of disease. 12-month-old TgF344-AD rats displayed an increased duration to notice the sticky dot stimulus

when measured from both the end of isoflurane administration ($M_{AD}=2195s$) and from the end of emergence ($M_{AD}=1935s$) when compared with WT littermates ($M_{WT}=1340s$ & $M_{WT}=1039s$, respectively). We also reported a generalized main effect of exercise to hasten anesthetic recovery in diabetic and control rats, as measured by a decrease in the time to notice the sticky dot.

Our utilization of the sticky dot test involves the use of tape on one forepaw and we reported only the time to notice the sticky dot test. In contrast, in stroke and lesion studies, rodents often have tape placed on multiple paws and the time to successful removal is also reported. In our experiments, the tape stimulus needed to be very securely affixed to the forepaw in order to remain in position throughout the entire duration of emergence and recovery. Our rats were often unable to remove the adhesive tape on their own during our observation. This approach limits our ability to objectively measure motor coordination during late recovery using this assay.

The adhesive removal test was originally designed as a preclinical analog for the Double Simultaneous Tactile Stimulation exam used in humans to identify unilateral brain damage^[294]. In stroke and lesion studies, rodents will reliably first notice and attempt to remove adhesive tape positioned ipsilateral to damage. Adhesive tape positioned contralaterally is usually detected later, or not at all in the case of significant damage. Our use of the test administers only one stimulus, but it is still sensitive to the time for detection of this stimulus. In lesion and stroke models, delays in contralateral time to notice the sticky dot have been proposed to be related to damage to sensory-motor cortex or due to sensory hemi-neglect. Sensory hemi-neglect is reported to be especially pronounced in response to damage to the right hemisphere in humans and has been demonstrated in response to damage in frontal cortex, posterior parietal cortex,

subcortical areas and white matter^[295-297]. One study in rats receiving middle cerebral artery occlusion (MCAO) found that sensory deficits (latency to contact contralateral sticky dot & latency between contact of ipsilateral and contralateral sticky dot) were correlated with the degree of thalamic atrophy^[294]. In humans, treatment of sensory hemi-neglect focused on dopaminergic and noradrenergic pathways have shown positive results^[298, 299]. These brain regions and pathways are all proposed to be important for the mechanisms for alterations of consciousness induced by anesthetic drugs and the subsequent emergence from anesthesia.

5.3 Emergence from Anesthesia with AD

The concentration of an anesthetic required to induce anesthesia is often greater than the concentration of anesthetic at which an individual will emerge from anesthesia. This phenomenon is referred to as “neural inertia”, the degree of resistance to state changes between wakefulness and unconsciousness^[300]. Our work did not examine dose response for induction and emergence to a single anesthetic. However, in separate TgF344-AD rat cohorts, we demonstrated hastened emergence from isoflurane anesthesia and resistance to burst suppression under sevoflurane anesthesia. These results could be consistent with either a collapsing of neural inertia in AD or a generalized rightward shift in the dose response to anesthesia in AD. We speculate that these results likely result from a collapse of neural inertia. The Kelz lab at UPenn created dose response curves for induction of anesthesia with halothane, isoflurane and sevoflurane in 3xTgAD mice and found a consistent resistance to volatile anesthetics compared with WT mice^[245]. The average EC₅₀ for emergence was unchanged between WT and Tg3xAD mice, suggestive of a collapsing of neural inertia with AD. Neural inertia was not mentioned in their manuscript, which predates the published definition of neural inertia by 5 months (although this definition was also authored by the Kelz lab). Neural inertia has only been quantified in the

context of anesthesia, however considering the conceptual definition an increase in sleep/wake transitions would suggest changes in neural inertia. Increased sleep fragmentation is common in Alzheimer's disease and has been observed in TgF344-AD rats at 17 months (Kreuzer et al., in review).

The mechanisms underlying control of neural inertia are only partially understood in animals. Manipulation of genes associated with sleep homeostasis in *Drosophila Melanogaster* have a tendency to cause a collapsing of neural inertia^[301]. Experimental stimulation of midbrain cholinergic and dopaminergic pathways can induce emergence from anesthesia, suggesting that these pathways can play a role in regulation of state changes between consciousness and unconsciousness. However, slice experiments demonstrate no changes in hysteresis loops due to changes in tissue excitability, which would be expected if neural inertia is a consequence of brain activity rather than pharmacokinetics of the drugs being delivered^[302].

The quantification of neural inertia is a relatively new field of study and potential methods have only recently published in humans. Slow-wave activity measured by EEG appears to display hysteresis from induction to emergence similar to the behavioral effects seen in animal studies, however humans did not display any hysteresis in the concentration of anesthesia necessary for loss and return of behavioral responses^[303]. In this study, an increase in neural inertia was seen in older individuals which also correlated with increased delirium and confusion in the first 15 minutes following emergence. Older individuals tended to get "stuck" in an unconscious state with EEG patterns dominated by slow-wave activity even when drug concentrations reached nearly 0 MAC, before abruptly transitioning to wakefulness. It is worth noting that only patients with clear slow-wave activity during emergence could be included in

this analysis, though most study participants did display slow-wave activity both during induction and emergence.

We examined rats that demonstrated characteristics of early AD. Alterations in excitatory/inhibitory (E/I) balance are common in AD and patients with MCI/AD are at an increased risk for seizure. The accumulation of amyloid appears to directly impair normal GABAergic activity in cortex, resulting in reduction of cortical inhibition and increasing the E/I ratio. In early stages of AD, the spectral power of the EEG increases in the theta range (4 – 8 Hz) while beta (14 – 40 Hz) power decreases. With cell loss in later stages of AD in humans, EEG delta (0.5 – 4 Hz) power increases as alpha power decreases^[304]. The neurological changes underlying these trends in neurophysiological recordings may exacerbate changes in neural inertia. While all alterations in pathways important for sleep homeostasis in *Drosophila* resulted in the collapse of neural inertia, rats possess a more complicated neuroanatomy than flies. The TgF344-AD rat may show promise as a model for future study into the mechanisms underlying neural inertia and changes in hysteresis loops resulting from disease mechanisms. If neural inertia does collapse as a function of disease progression, this could create a scenario where patients who are the most sensitive to cognitive dysfunction after surgery with general anesthetics actually require higher drug concentrations to maintain surgical anesthesia.

5.4 Recovery from Anesthesia with AD

In our experiments, 12-month TgF344-AD rats were significantly delayed in their recovery from isoflurane general anesthesia. At 12 months of age, these rats display evidence of amyloid- β accumulation and increased astrocyte activity despite a lack of cognitive symptoms.

As age advances throughout adulthood, there is a reduction in the concentration of anesthetic drugs required to prevent movement. In other words, sensitivity to anesthetic drugs

increases in advanced age. Older rats with increased sensitivity to anesthetics demonstrated a delayed emergence from isoflurane and propofol compared to young rats. These results suggest that altered pharmacodynamics due to aging underlie the delay in behavioral endpoints observed following anesthesia. Decreasing the strength of arousal pathways or increasing the rate of cortical inhibition have both been hypothesized to underlie changes in anesthetic sensitivity. Normal aging is associated with both thinning of cortical grey matter and degeneration of arousal systems. AD causes widespread neurodegeneration and is known to impact sleep/wake cycle, so AD seemed likely to influence anesthetic sensitivity.

We found that early AD does not increase sensitivity to sevoflurane anesthesia as measured by burst suppression ratios. Further, AD rats appeared to demonstrate resistance to a moderately high dose of sevoflurane compared with WT rats. While isoflurane and sevoflurane are not the same anesthetic, they are both halogenated ether anesthetics with primary action on GABA_ARs and similar off target receptor effects. The anesthetic sensitivity changes demonstrated previously in humans and rats have shown consistent changes in sensitivity across the GABAergic anesthetics. A change in anesthetic sensitivity to isoflurane would not be expected to occur without a complimentary change in anesthetic sensitivity to sevoflurane. The observed delay in recovery in TgF344-AD rats is not likely to be due to changes in pharmacodynamics from the anesthetic.

In regard to cognitive function specifically, the recovery of cognition following surgery with anesthesia appears to occur when there is a return of complexity in cortical information which is successfully integrated between brain regions and unencumbered by perioperative neurological damage. Preclinical evidence suggests that perioperative neurological damage can result from neurotoxic actions of anesthetic drugs. Specifically, volatile anesthetics have been

shown to increase caspase activity and amyloid accumulation. Excessive anesthesia doses appear to also be associated with weakening of the integrity of the BBB^[144], making the brain more vulnerable to damage from peripheral inflammation. We found evidence of increased amyloid- β and GFAP in TgF344-AD rats following exposure to high concentrations of sevoflurane. The anesthesia protocol and drug used for the EEG and emergence/recovery experiments were different, however these results are useful for informing future studies regarding delayed recovery in AD rodent models.

5.5 Emergence and Recovery from Anesthesia with T2DM

Goto-Kakizaki rats are a non-obese, type-2 diabetes model derived by multiple generations of selective breeding of rats with high blood glucose concentrations. These rats did not receive supplemental insulin for management of blood glucose. Given that emergence times were also unchanged between Wistar and GK rats, isoflurane anesthesia alone appeared to be well-tolerated overall by GK rats.

This was surprising considering that diabetic status increases the risk for both POD and POCD. Additionally, patients with “poorly controlled” diabetes are assigned an ASA surgery risk classification of 3. Separate studies identifying surgery risk using ASA status have found that POD and POCD risk increases with ASA classifications above level 2. Diabetes can alter cerebral vasoregulation & glucose metabolism, impair cognitive performance, cause chronic neuroinflammation and lead to grey matter atrophy in the brain. All of these factors are likely to influence individualized risk for postoperative neurocognitive disorders. It is less clear whether diabetes is associated with any common localized impairments in brainstem or midbrain systems important for arousal. Sleep disorders are common in humans with T2DM, however this association is likely not due to impairments in glucose metabolism. T2DM often presents in

individuals with obesity and obesity increases the risk for sleep apnea. Sleep apnea causes sleep fragmentation, reducing sleep quality and duration while also increasing daytime sleepiness. Interestingly, shorter average sleep duration has been identified as a risk factor for later development of T2DM in children^[305]. Interpretation of this data creates a chicken/egg problem, are sleep disorders an early step in pediatric T2DM pathogenesis or are shorter sleep durations caused by early T2DM pathogenesis? In mice, Zhang et al. demonstrated neuron loss in locus coeruleus resulting from metabolic stress brought on by extended wakefulness^[306]. Sleep disturbances are also associated with alterations in energy metabolism and appetite that increase obesity risk^[307], thereby increasing risk for sleep apnea. Future investigations on recovery from anesthesia considering diabetic status may want to consider differentiating between type-1 and type-2 diabetic patients or include obesity/BMI as an interacting factor.

Regarding preclinical models, previous study in GK rats demonstrated significant increases in hypothalamic dopamine and noradrenaline concentrations at 7 weeks^[308] and altered regulation of monoamine transporter gene expression has been seen in streptozotocin-induced diabetic rats^[309]. Our data do not suggest that there are significant changes in function within arousal pathways in GK rats, as evidenced by the similar emergence and recovery durations with WT rats.

5.6 Recovery from Anesthesia after Exercise Training

Two weeks of treadmill exercise prior to anesthesia exposure significantly reduced the time to notice the sticky dot in both diabetic and control rats. Time to emergence from anesthesia was unchanged in Wistar and GK rats following exercise. Exercise consisted of 30 minutes of ambulation on a treadmill with a belt speed of 15 m/min., a setting that forces the adult rat to

maintain a brisk walk to avoid a tail shock. The hastened recovery in both strains was also associated with increased PSD-95 within hippocampus.

This observation is important for two reasons. First, it verifies that our treadmill settings were effective to stimulate expression of factors important in synapse development and stability in hippocampus. There appears to be an inverted-U shaped relationship between exercise stress and the expression of PSD-95. Exercise has been demonstrated to increase factors promoting synapse development like PSD-95 and BDNF. However, high intensity exercise is less efficient at increasing these factors than lower intensity routines. Shih et al. found that high intensity exercise (20 m/min) in rats resulted in no change in cognitive performance or in PSD-95 or BDNF levels in hippocampus from baseline^[291]. However, low intensity exercise (8 m/min) resulted in improved cognitive performance and increased levels of PSD-95 and BDNF. Second, exercise has a number of beneficial health effects, but perhaps the most direct effect on the brain is the stimulation of neuroprotective and synaptogenic processes. PSD-95 is required for the organization of the excitatory postsynaptic density^[310]. Decreases in PSD-95 in hippocampus have been reported following exposure to volatile anesthetics in mice and rats that are associated with post-anesthesia cognitive decline^[311-313]. Cognitive impairments and reductions in PSD-95 associated with exposure to volatile anesthesia have been rescued in AD transgenic mice with cyclophilin D knockout. Cyclophilin D regulates the opening of the mitochondrial permeability transition pore. Dysregulation of mitochondrial permeability can lead to mitochondrial swelling and damage followed by neuron death^[311]. This suggests a potential role for mitochondrial damage underlying anesthesia induced reductions in PSD-95. Interestingly, reductions in PSD-95 in spinal cord have been demonstrated to increase sensitivity to isoflurane anesthesia^[314, 315], likely due to weakening stability of NMDA receptors and decreasing excitatory tone^[316].

However, we did not see changes in time to emergence from anesthesia after exercise, suggesting that exercise did not change anesthesia sensitivity in our rats. Therefore, improved recovery from anesthesia after exercise is likely due to improved neurological function following anesthesia rather than exercise-induced alterations in the pharmacodynamics of anesthetics.

5.7 Relationship between T2DM and AD

T2DM greatly increases susceptibility to AD. Changes in circulating insulin levels and evidence of insulin resistance within the brain have been reported in sporadic Alzheimer's disease. Increased insulin levels may play a role in amyloid- β clearance. The insulin degrading enzyme will degrade both insulin and amyloid- β , but shows preference for insulin when circulating insulin levels are high. Insulin signaling in the brain modulates glycogen synthase kinase 3 (GSK3), which itself has a role in the phosphorylation of tau. Insulin resistance has therefore been hypothesized to be a cause of pathological tau hyperphosphorylation. T2DM itself has been demonstrated to decrease brain volumes and cognitive function.

Late onset diabetes has been proposed by some to be a "type 3 diabetes". Administration of intranasal insulin has shown promise in improving cognitive function in animal studies as well as in both cognitively healthy and MCI/AD patients. These improvements have been correlated with preserved brain volumes after intranasal insulin administration that correlated with improvements in cognitive function. However, there are a number of unanswered questions regarding the relationship between T2DM and AD. First off, the time course of insulin resistance in the brain has not been demonstrated in relation to other pathological developments in AD. It is possible that insulin resistance develops as a result of prior stages in AD progression. T2DM also affects vascular health and could exacerbate AD pathology through mechanisms that align more

closely with the vascular hypothesis of AD. However, the lack of a clear pathogenesis for sporadic AD makes insulin signaling in AD an interesting topic for further investigation.

Despite the established connections in disease pathology, our results do not contribute much to conversations concerning the interactions between T2DM and AD. For one, there is a large gap in the ages of rats used within these studies (GK: 3-4 months, TgF344-AD: 12 months). If disruptions in insulin signaling are involved in sporadic AD then clearly pathology takes many years, decades even, to manifest in disease symptoms in humans. GK rats have been proposed as a promising preclinical model for an T2DM-associated AD-like phenotype, because these rats are non-obese and develop metabolic changes mimic human disease progression with a pre-diabetes-like state preceding T2DM, but we did not assess AD-protein levels in our GK rats. However, one study has characterized alterations in plasma tau in GK rats at 3 months. This study also found a decrease in plasma BDNF at 3 months. Pintana et al. found that at 12.5 months of age, female GK rats have increased whole brain amyloid- β and decreased PSD-95 as measured by Western Blot. Phosphorylated tau was also shown to be increased at this age; however, the effect was similar between Wistar and GK rats. Given the interest in further study of the role of T2DM and AD in postoperative neurocognitive disorders, the GK rat may present a promising preclinical model for future experimentation.

5.8 Summary

Alzheimer's Disease and type-2 diabetes are both important patient considerations for an individual's fitness for surgery and risk of postoperative cognitive changes. Our work demonstrates the ability to identify changes in the behavioral and neurophysiological response to anesthetics in the immediate emergence and recovery from general anesthesia. In an AD rat model, altered emergence and recovery could be seen early in disease progression, before

cognitive changes were apparent. Hastened recovery could also be observed following 10-days of moderate intensity exercise in Wistar rats and the Goto-Kakizaki type-2 diabetes rat model.

In humans, recent evidence supports the idea that EEG features rather than behavioral endpoints may be more promising for evaluating changes in emergence (Figure 5.1). Features of the EEG can help to narrow hypotheses into the underlying causes of patient specific delays in emergence or impaired cortical recoveries from surgery. Emergence trajectories discovered via qEEG analysis are associated with postoperative pain, POD risk and can be used identify changes in neural inertia.

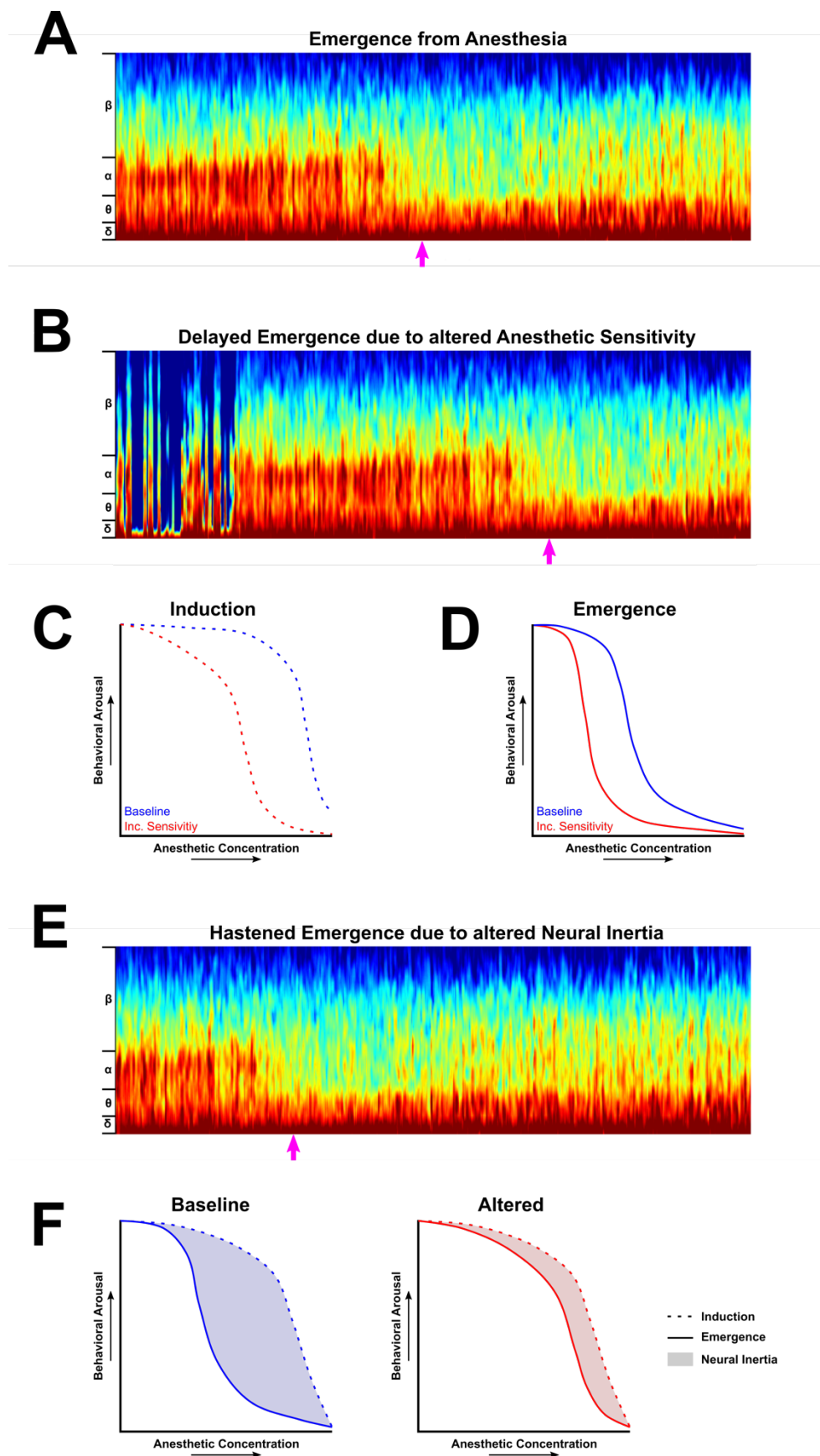


Figure 5.1 – Hypothetical EEG correlates of different postoperative emergence durations.

10-minutes of simulated patient data displaying spindle-dominant slow-wave anesthesia (sdSWA), followed by emergence is displayed in panel A. Simulated recordings begin at the point where administration of the anesthetic is stopped and the pink arrow below displays the expected time of emergence. B) Time to emergence is delayed due to increased sensitivity to anesthetics. Burst suppression is present at the start of the recording, indicating that this patient would have been excessively anesthetized for surgery. Delayed behavioral response is explained by decreased resilience to anesthetic drugs. Hypothetical population-average dose response curves for baseline response and those with increased anesthetic sensitivity during induction and emergence are displayed in panels C & D, respectively. E) EEG recording of hastened time to emergence. Hastening of emergence could be due to collapse of neural inertia if pharmacokinetic explanations are ruled out. Panel F displays population-average dose response curves for baseline response and altered neural inertia. Emergence at lower doses of residual anesthesia decreases the area contained by the hysteresis loops between induction and emergence.

The potential for standardized anesthesia recovery scoring criteria with focus on identifying delirium should lead to more informative clinical studies in the future. However, care will need to be taken to differentiate characteristics of EA from those of PACU delirium and POD, as these conditions are proposed to be grouped within the same future nomenclature. POD is associated with serious long-term health problems or mortality, whereas EA tends to resolve quickly without further issue. A number of factors have been proposed to be underlying impairments in postoperative cognitive recovery. These factors are summarized below in Figure 5.2.

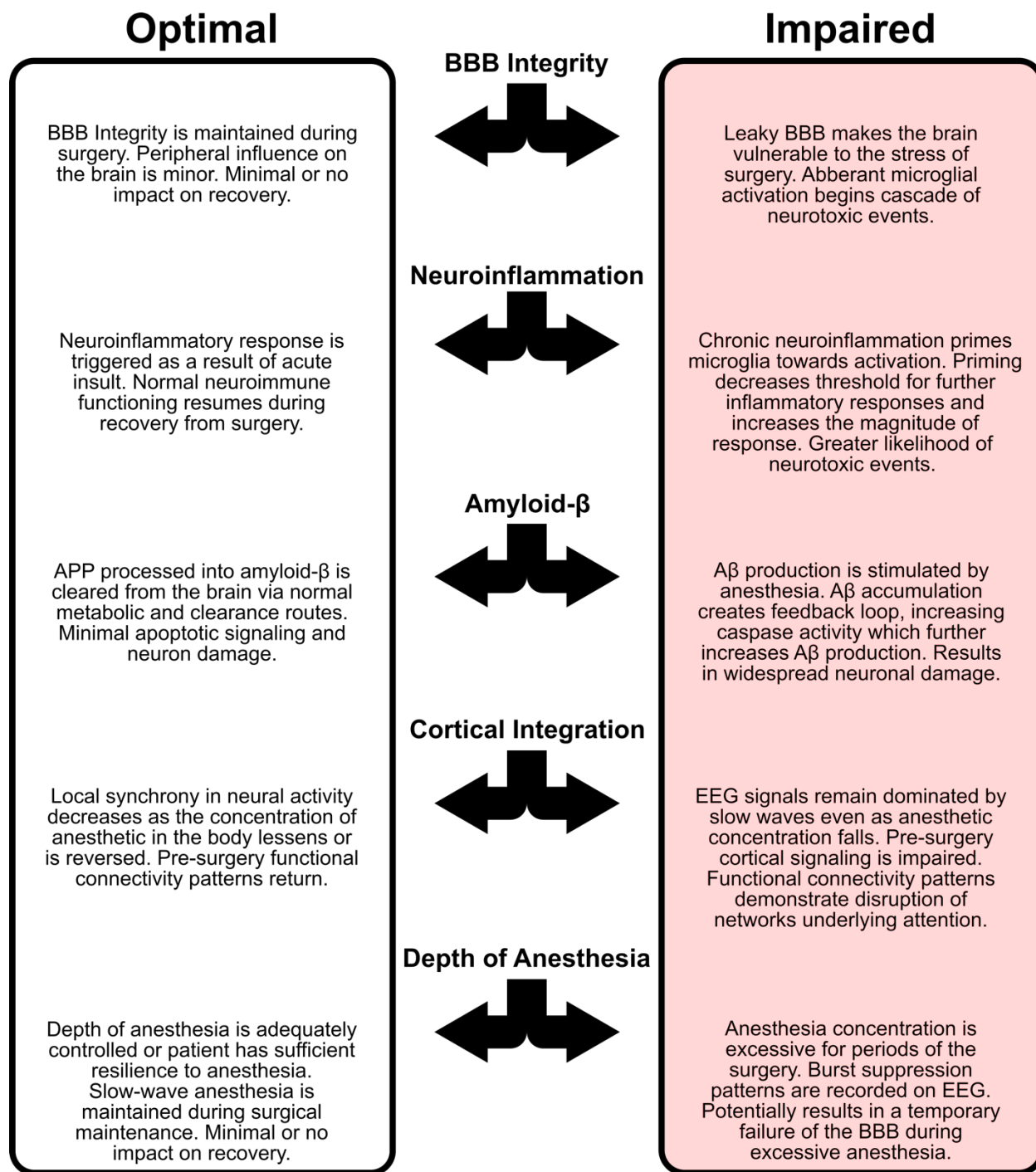


Figure 5.2 – Factors influencing postoperative cognitive recovery.

5.9 Persistent Perioperative Neurocognitive Disorders

A full recovery from surgery occurs when the patient achieves their preoperative physiological state. Clinical postoperative recovery is typically subdivided into three phases. Early recovery is the return of reflexes and motor function, similar to what we have chosen to call ‘emergence’ in our rats. Intermediate recovery occurs when the patient is judged to meet criteria for discharge. Late recovery is the return of the preoperative physiological state.

While criteria for early recovery are fairly standard from patient-to-patient, the duration of intermediate recovery and treatment received during intermediate recovery can vary. Following surgery, a patient may pass through multiple care units on their way to discharge. Traditionally, transfer to the PACU has been standard procedure following surgery but bypass of the PACU (known as a fast-track protocol) for patients following certain minor surgeries is becoming more common. Decreasing the time patients spend in the hospital can decrease stress and financial burden for patients, families and healthcare providers. However, addressing these concerns must be balanced with an understanding that postoperative cognitive impairments are currently underdiagnosed and can be indicative of long-term problems.

Given the general interest in decreasing the time that patients spend in the hospital, it is tempting to opt for anesthetic protocols that hasten emergence in an attempt to decrease the time to discharge. Our results highlight the need to treat the emergence and recovery from anesthesia as distinct clinical endpoints. A test of sensorimotor function appears to be a reliable marker for identifying delays in the recovery from anesthesia in rodents. Inclusion of sensorimotor stimulus discrimination tasks in the postoperative screening of patients may prove beneficial for non-invasive assessment of function related to cortical integration where EEG recordings are not possible.

5.10 Future Directions

General anesthesia has been described as a “stress test” for the brain. Neurologically and cognitively healthy patients appear to tolerate general anesthesia well and recover without ill effects. Special considerations must be given to individuals during early development and advanced age, especially in aged individuals with neurodegeneration, neuroinflammation, or damage to the cerebrovasculature/BBB. In children less than 3 years old, multiple exposures to general anesthesia has been linked with increased risk for development of ADHD^[317, 318]. As mentioned, aging predisposes surgical patients to POD. The etiology of both of these conditions have been linked to brain regions important for attention and awareness, including posterior cingulate cortex and other regions within the default mode network^[319-321]. In both groups, it is difficult to differentiate between the influence of anesthesia and the surgery itself on the postoperative outcomes. The 2015 National Anesthesia Clinical Outcomes Registry reported that approximately 1/3rd of the uses of general anesthesia now take place outside of the operating room, with colonoscopy being the most common non-OR procedure performed with general anesthesia. Many of these procedures can be completed with light sedation rather than surgical anesthesia. In practice, sedation during colonoscopies may in fact be more comparable with surgical anesthesia than expected, as reviews of BIS-guided anesthesia during colonoscopy have shown average anesthetic BIS index of approximately 58-59, and ranging from 22 to 88^[322, 323]. Non-OR procedures could provide a venue for the study of general anesthesia as a “stress test” in humans without the additional stress of surgery.

Numerous studies have used the adhesive removal test following focal brain damage, however, there has not been a clearly defined brain region or collection of brain regions identified that contribute to sensory deficits on the task. Whole brain infarct size appears to be

the measure best correlated with sensory dysfunction on the task^[294]. The return of pre-anesthesia levels of cortical sensorimotor integration may influence the latency to investigate the sticky dot, but this hypothesis needs to be tested. The Wada test has been used in humans to anesthetize each hemisphere of the brain independently for the evaluation of lateralization of brain functions in epilepsy patients prior to ablative surgeries^[324]. Hemispheric drug delivery methods are also available in rodents. A rodent version of the Wada test may provide an opportunity to rigorously test for brain activity correlated with successful completion of the sticky dot test in rats.

In humans, preoperative and postoperative physical activity appears to be an important factor in postoperative recovery and cognitive health. Increasing postoperative physical activity has been demonstrated to decrease overall hospital length of stay^[325]. Preoperative exercise capacity measured on a six-minute walking test (6MWT) has been identified as a predictor for POD^[230]. Ogawa et al. found that patients that were unable to walk further than 345 meters during 6MWT prior to cardiac surgery. Our experiments did not demonstrate that improved recovery from anesthesia was reliant on BDNF signaling through TrkB receptors. Previous research has demonstrated beneficial effects of BDNF on cognitive health without directly demonstrating TrkB receptor activation. While BDNF does not cross the BBB, a number of studies have demonstrated correlations between serum BDNF levels and cognitive performance or severity of symptoms in behavioral disorders^[326]. Significant decreases in serum BDNF levels during surgery have been associated with POD risk^[327] and decreased postoperative serum BDNF levels have been associated with POCD^[328]. Increased serum BDNF levels have also been correlated parietal cortex activity during a sensory integration task^[329].

Isoflurane has been shown in cell culture and in rodents to upregulate caspase 3 activity and amyloid- β , providing a potential explanation for anesthetic neurotoxicity. BDNF may be

beneficial to counteract both of these processes and limit neuron loss due to anesthesia. Increased BDNF-TrkB signaling can decrease neuron apoptosis by downregulating the activity of caspase 3. BDNF also appears to limit amyloid- β production by promoting the processing of APP into soluble proteins by increasing the activity of α -secretase^[330]. BDNF also affects glutamatergic and GABAergic signaling. BDNF appears to increase NMDA receptor activity and decrease GABA_AR activation^[331]. These effects are thought to increase the likelihood of long-term potentiation needed for synaptogenesis. However, modulation of both neurotransmitter pathways is dependent on TrkB receptor activation. BDNF also binds with p75 receptors, but this interaction is thought to primarily lead to apoptosis and therefore increased BDNF-p75 signaling is unlikely to underlie the beneficial effects of exercise. If the benefits of exercise are mediated by BDNF signaling it is likely to occur through a mechanism involving BDNF binding to TrkB receptors. BDNF-TrkB interactions can be limited in rodent studies via administration of TrkB receptor antagonists, such as ANA-12. Whether exercise hastens recovery through a mechanism dependent on BDNF-TrkB interactions could be investigated in future experiments via administration of ANA-12 prior to treadmill exercise.

Chapter 6 - Appendix

Appendix 1 – Immunohistochemistry Image Analysis

Automated image analysis techniques are available that can be used to quickly quantify staining properties within an a region of interest (ROI) in a scanned brain slice image. When images are scanned, the image information is stored with numerical values that describe each pixel's color. More specifically, color is represented by quantifying a pixel's hue, saturation and value. Positive pixel count analysis creates a threshold for the combined hue, saturation and intensity ranges that qualifies each image pixel as positive or negative for defined characteristics. In these experiments, positive pixel count analysis was used to compare the levels of amyloid- β and GFAP between WT and TgF344-AD rats.

A1.1 Hue, Saturation and Value

For our experiments, we imported Brightfield images to Qupath and image colors in 8-bit depth with red, green and blue (RGB) values. With 8-bit depth, each pixel represents the value of red, green or blue on a continuum from 0 to 255. Each pixel in the raw image represents a summation of the RGB values (demonstrated in Figure A1-1).

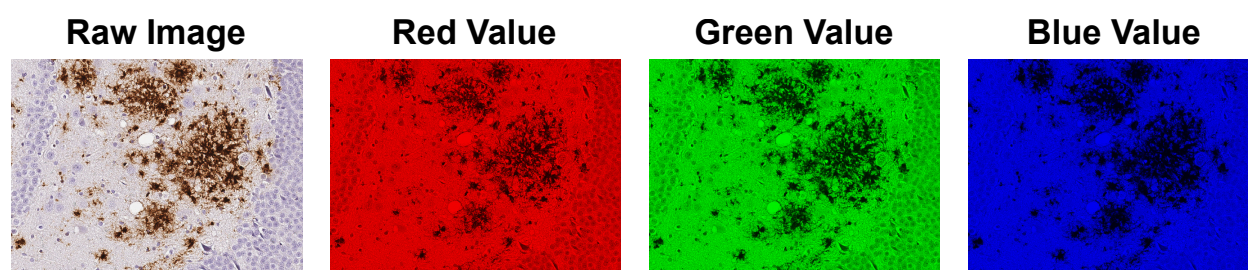


Figure A1-1: Comparison of the raw image with the RGB values from each color component

With 8-bit depth, each pixel represents the value of red, green or blue on a continuum from 0 to 255. Values closer to 0 appear darker. Values closer to 255 appear brighter.

We used positive pixel count analysis for our stain quantification. This technique is primarily based on quantification of the pixel value. Qupath analyses images by segregating stains and background based on their hue and saturation. These concepts are represented graphically in Figure A1-2. Value describes how light or dark the pixel appears. Maximum RGB values (255, 255, 255) appear as pure white and minimum RGB values (0,0,0) appear as pure black. Brightfield images are backlit with a white light, so all image backgrounds are pure white.

Hue describes the actual color of the pixel created by the combination of red, green and blue components. Saturation describes the purity of the color. In Figure A1.2a, colors with higher saturation (ex/ pure red, pure green, pure blue) are found towards the outside of the graph, and as colors fade and mix saturation drops.

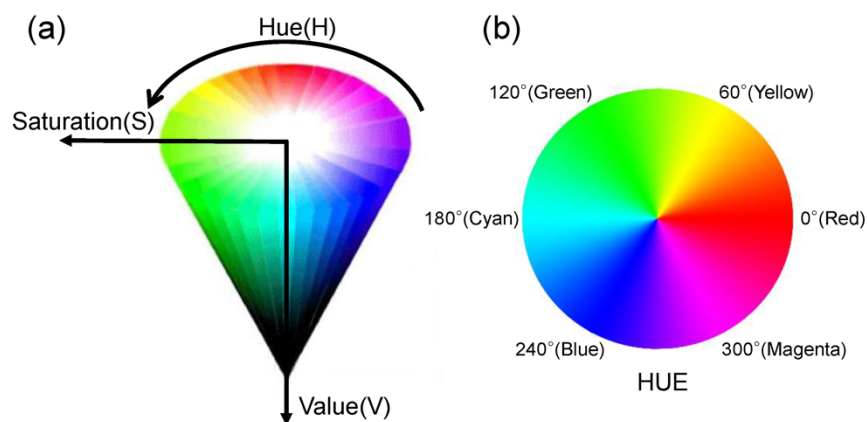


Figure A1-2: Representation of the complete reproducible color spectrum in 8-bit depth, RGB color

A) Quantification of the hue, saturation and value can be used to recreate real world colors digitally. Qupath primarily uses differences in the pixel hue and saturation to identify different stains in the image (and the image background). Qupath primarily uses pixel value for quantification of the stained area when using positive pixel count analysis. B) Normalized hues that can be recreated by mixing red, green and blue pixel content. Reproduced from Min, K.-P.; Kim, G.-W. Photo-Rheological Fluid-Based Colorimetric Ultraviolet Light Intensity Sensor. *Sensors* **2019**, *19*, 1128^[332]. This image

was made available with permissions through Creative Commons Attribution License 4.0.

A1.2 Positive Pixel Count Analysis

DAB staining was performed on brain slices for the presence of amyloid- β (antibody: 4G8) and astrocyte activity (antibody: GFAP). DAB is colocalized to a protein of interest using primary and secondary antibodies. The presence of a protein of interest is then confirmed by reacting DAB with horseradish peroxidase and hydrogen peroxide. This reaction oxidizes DAB and creates a dark brown stain. Surrounding tissue is counterstained with hematoxylin, which develops as a light blue stain. Automated image analysis takes advantage of the difference in hues between these two stains to identify tissue from background and DAB staining within the tissue.

The raw image taken from a stained brain slice results in image pixels with colors formed from overlapping of the image background, the stain of interest and a counterstain for surrounding tissue. This decreases pixel saturation and makes it harder to identify distinct stains. Qupath uses a color deconvolution algorithm based on RGB component subtraction to create alternative color channels for DAB, Hemotoxylin, and a residual channel^[333]. Examples of the stain channels for DAB staining in Qupath are represented in Figure A1-3.

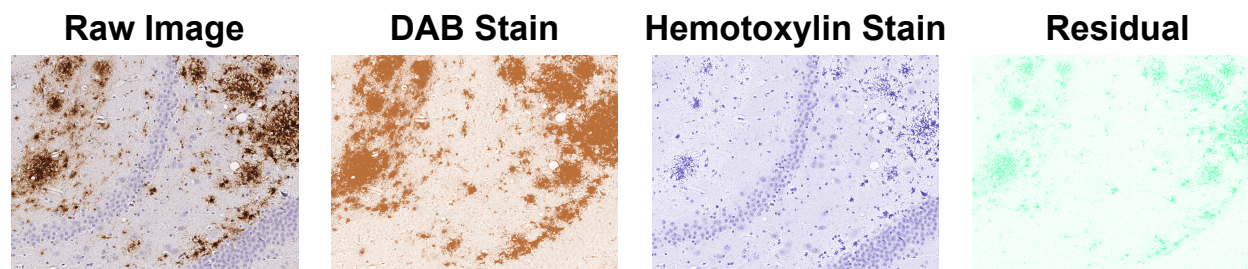


Figure A1-3: Comparison of the raw image with the channels for stain identification within Qupath

Positive pixel count analysis computes the ratio of stained pixels to counterstained pixels within a defined ROI. ROIs were drawn using anatomical identification from the Paxinos and Watson rat brain atlas^[334]. The manual inputs for the positive pixel count analysis are included in Table A1-1. To increase computational speed, images were downsampled by a factor of 4 and smoothed by a Gaussian function ($\sigma=2 \mu\text{m}$). Qupath was able to process all images with an acceptable stain identification when these performance parameters were used.

Table A1-1: Qupath Positive Pixel Count Analysis Inputs

Category	Input
Downsample Factor	4.0
Gaussian σ	2 μm
Hematoxylin Input ('Negative')	0.05 OD Units
DAB Input ('Postive')	0.4 OD Units

Our images for analysis were Brightfield images, so the color of each pixel was used to quantify the amount of light that is blocked by stained tissue. We quantified the value of each pixel

color on a scale from 0 (perfect staining, full light absorbance by DAB or hematoxylin) to 255 (pure white, no light absorbance). For a 2-D image, the optical density (OD) of each pixel is directly comparable to absorbance, and could be computed using the following equation:

Equation A1-1

$$\text{OD} = -\log_{10}\left(\frac{I}{I_{max}}\right)$$

Where I_{max} equals the original light intensity and I equals the measured intensity of the light after it is filtered by the brain slice and stains. The expression $\frac{I}{I_{max}}$ is also known as the transmittance.

In this case, transmittance is a ratio of light that passes through brain slice and stains.

The hematoxylin stain channel was used to determine the area of the ROI for positive pixel count analysis. In pixels where the light transmittance is very high, there is likely no brain tissue present (due to variations in the tissue slicing or manual drawing of the ROIs). A negative threshold of 0.05 OD units (which corresponds to a transmittance above 89%) was chosen because it successfully excluded portions of the image containing only background from the ROI. The DAB stain channel was used to determine the total number of positive pixels within the ROI. A positive threshold of 0.4 OD units (which corresponds to a transmittance below 39%) was chosen to reduce the false positive rate by including only pixels where there was considerable DAB staining. The resulting positive pixel percentage is calculated by dividing the downsampled total positive pixel count by the downsampled total ROI pixel count. The image threshold parameters are visualized in Figure A1-4. An example of the ROI and positive pixel identification is included in Figure A1-5.

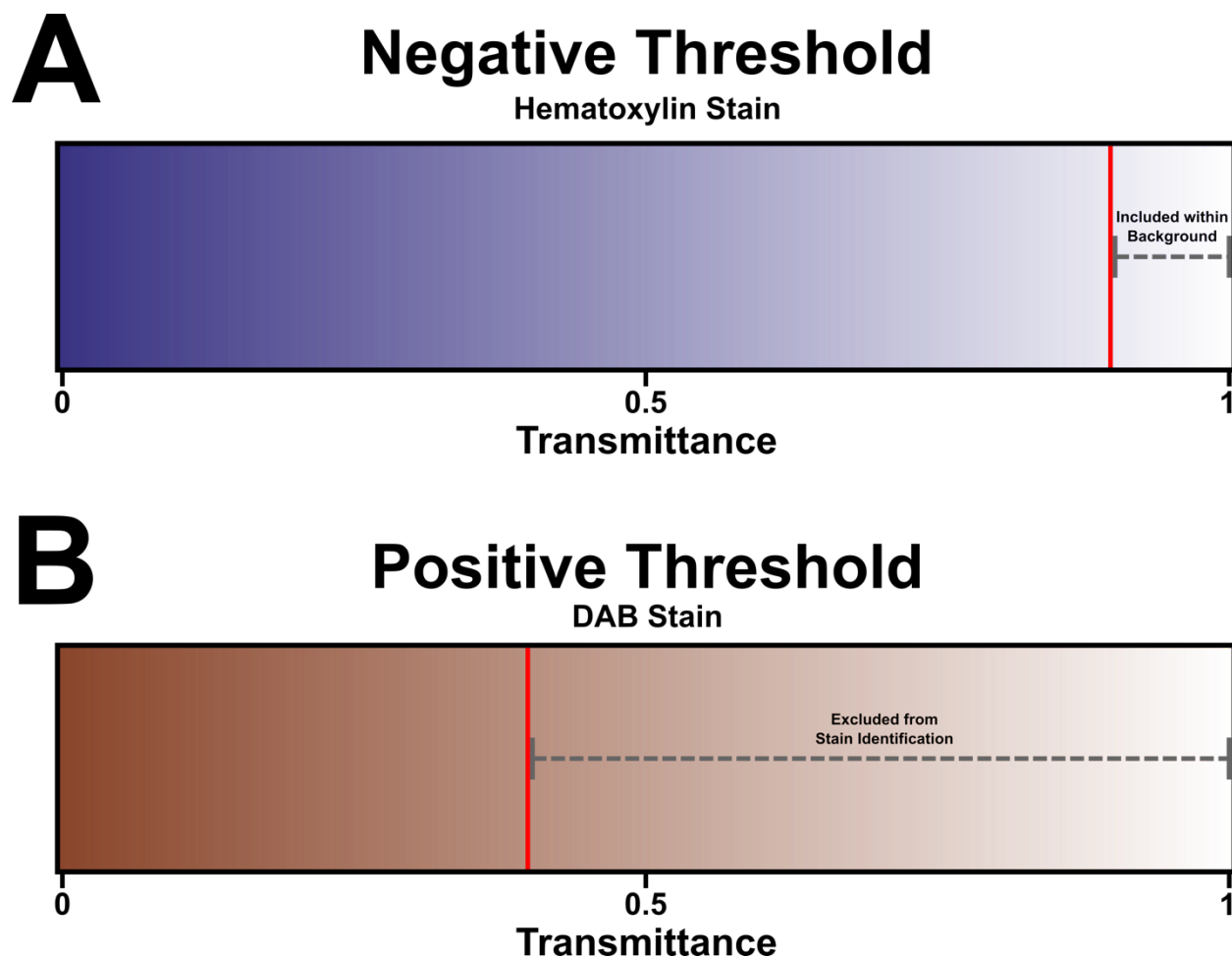


Figure A1-4: Visualization of the light transmittance gradients for both the hematoxylin and DAB stains

A) The hematoxylin stain was used to set the negative threshold for including pixels within the ROI. Pixels with a transmittance greater than 0.89 were excluded from the ROI. These pixels were unlikely to contain brain tissue. B) The DAB stain was used to set the positive threshold for identifying pixels that stained positive for amyloid- β or GFAP. Only pixels with a transmittance below 0.4 were included in the positive pixel count.

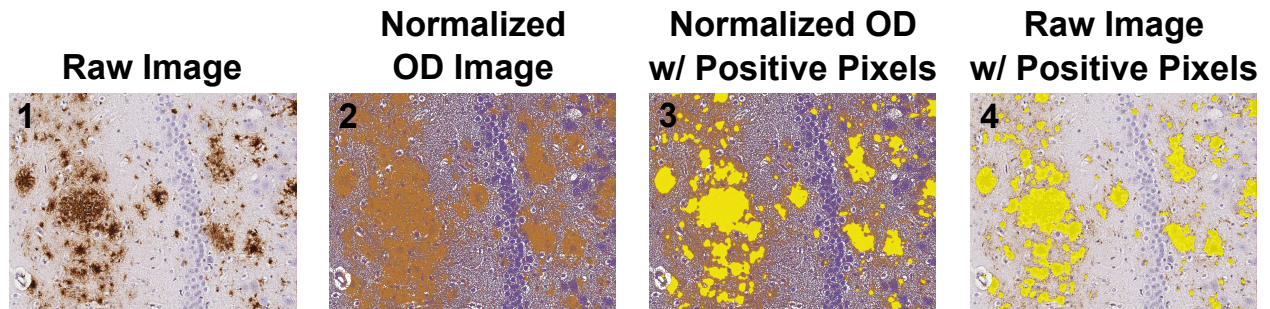


Figure A1-5: A step-by-step visualization of the positive pixel count analysis within Qupath

Panel 1 contains a raw image with DAB staining for amyloid- β . Panel 2 contains a normalized OD image where all pixel colors are rounded to the hue of the nearest stain (light transmittance = 0) or to the background (light transmittance = 1). Panel 3 shows the positive pixel identification within the normalized OD image, demonstrating how the OD thresholding affects the pixel selection. Panel 4 shows the positive pixels overlaid on the original raw image.

Appendix 2 – Extended Burst Suppression Analysis Methods

Burst suppression describes a pattern of EEG where high-amplitude, low-frequency EEG voltage changes (bursts) are followed by nearly flat EEG voltage readings (suppression). Burst suppression appears during physiological states where cortical activation is severely decreased. It has been recorded during general anesthesia, coma and hypothermia. Burst suppression always occurs following loss of consciousness and during administration of anesthesia it represents a transitional pattern between slow-wave anesthesia and a completely isoelectric EEG signal. Burst suppression is thus referred to as a “deeply” anesthetized state and often considered excessive for the purposes of surgical anesthesia.

Increasing the stimulus that causes burst suppression (for example, the dose of a general anesthetic drug) will reduce the number of observed bursts and increase the duration of the suppressions. For this reason, the burst suppression ratio (BSR, as shown in Equation A2.1) has been useful as a measurement for the depth of anesthesia:

Equation A2.1

$$BSR = \frac{T_{Supp}}{T_{Epoch}}$$

Where T_{supp} is suppression time and T_{Epoch} is the total time of the analysis window. Non-zero values of BSR can be used as a screen for the appearance of burst suppression during general anesthesia and higher BSR values are indicative of more suppression of cortical activity. BSR is used clinically to guide surgical anesthesia. Although the exact algorithms for computing consciousness monitor values are proprietary and therefore not publicly known, published results suggest that BSRs above 40% are the sole determinant of the BIS monitor values below 30^[160],

^{335]}. This appendix will cover the methods used for analysis of the EEG recordings for quantification of the burst suppression ratio.

A2.1 – EEG Acquisition

The rodent EEG recordings used for this analysis were performed in anesthetized rats within a grounded faraday cage to reduce electrical noise from the environment. The sampling rate for recording was 256Hz. There were minimal movement artifacts due to the use of anesthesia. Artifacts were still removed from the signal for any samples where the voltage readings were more extreme than ± 1 mV. As a result, the amount of noise present in raw recordings was minor and denoising protocols (outlined in Appendix 3) were used to maximize the signal-to-noise ratio prior to determining the BSR from each recording.

A2.2 – BSR Analysis

Following denoising and artifact removal, the recording is converted to a binary time series where suppression periods are assigned an arbitrary value of 1 and bursts are assigned an arbitrary value of 0. First the filtered EEG recordings were replotted based on the absolute value of the voltage readings. For the cortical electrode, suppressions of cortical activity were judged to be periods where the recorded voltage changes did not rise above 30-38 μ V. For the hippocampal electrode, suppressions of cortical activity were judged to be periods where the recorded voltage changes did not rise above 35-44 μ V. By convention, these thresholds are set by eye on the filtered EEG. For subdural EEG recordings in rats receiving sevoflurane, these voltage thresholds are comparably low, a benefit of high signal-to-noise ratio in the majority of our recordings.

The binary time series denoting bursts and suppressions was then simplified to remove suppressions with durations less than 0.5 seconds. These periods where cortical voltage readings were below threshold for less than 0.5 seconds were converted to burst periods.

The BSRs were then computed for the entire 15 minutes of EEG recording at each dose of sevoflurane. T_{Epoch} was set to 15 seconds for our analysis. We used a sliding analysis window with a 14-second overlap between consecutive epochs to create a second-by-second BSR vector with 885 total data points for each recording. The middle 600 data points (representing BSRs between minutes 2.5-12.5 during the full 15 minute EEG recording) were included to create the continuous BSR series for each rat. Figures A2-1 & A2-2 display the mean continuous BSRs for each group at each concentration of sevoflurane.

Cortical Electrode

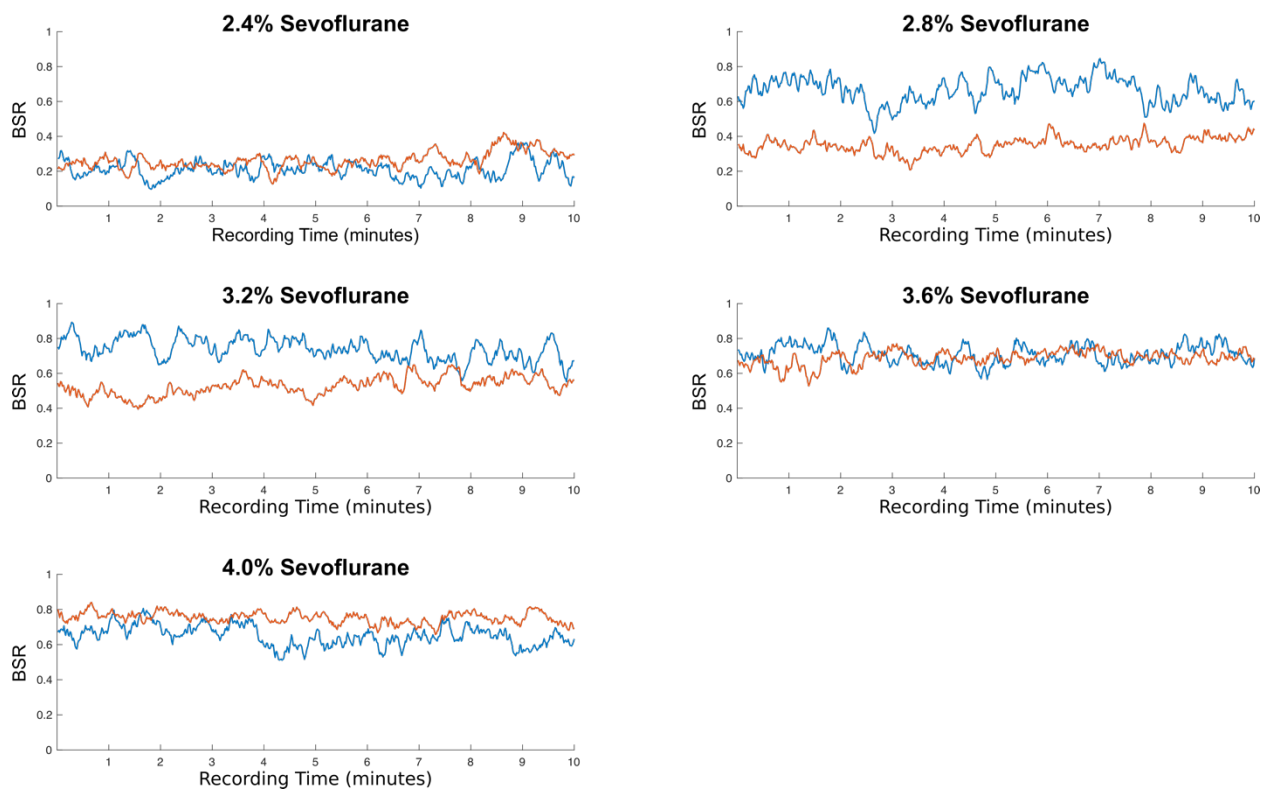


Figure A2-1: Continuous Burst Suppression Ratios calculated from the cortical electrode

Burst Suppression Ratios (BSR) plotted in one second intervals throughout 10 minutes of EEG recording from the cortical electrode. The mean BSR from wild type rats is displayed in blue and mean BSR from TgF344-AD rats are displayed in orange.

Hippocampal Electrode

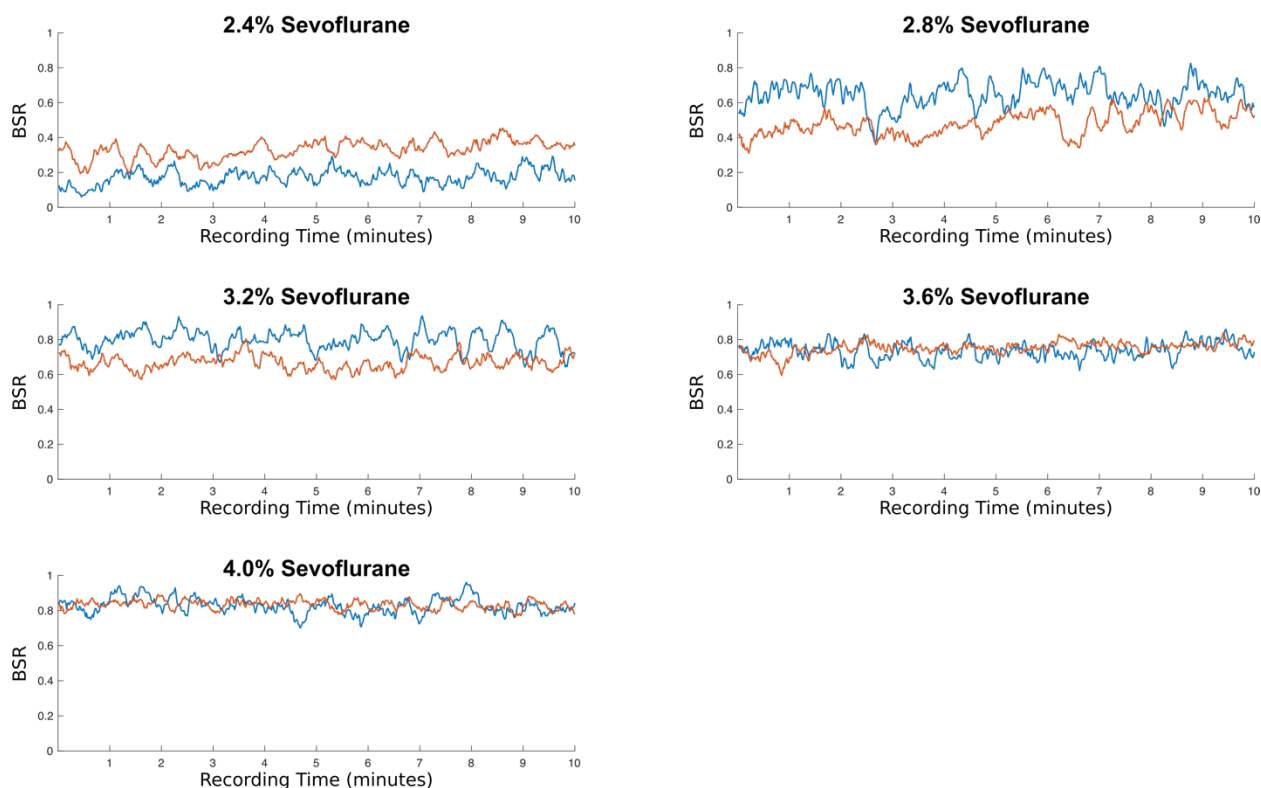


Figure A2-2: Continuous Burst Suppression Ratios calculated from the Hippocampal electrode

Burst Suppression Ratios (BSR) plotted in one second intervals throughout 10 minutes of EEG recording from the hippocampal electrode. The mean BSR from wild type rats is displayed in blue and the mean BSR from TgF344-AD rats is displayed in orange.

Following 15-minutes to equilibrate to each dose of sevoflurane, the BSRs are stable over each 10 minute recording. As a result, analysis of the BSR differences between groups and between concentrations was completed by reducing the continuous BSRs to a single mean BSR for each rat at each sevoflurane concentration.

Appendix 3 – Extended EEG Recording Denoising Methods

Wavelets are oscillatory functions which typically begin at zero, increase and decrease in a characteristic “wave”, and then settle at zero. Wavelets are useful for digital signal processing because they can be used to analyze a signal in both frequency and time. We chose to use the “wdenoise” (wavelet denoising) function in MATLAB to remove unnecessary noise from the EEG recordings, resulting in improved signal-to-noise ratio.

Different wavelet functions can be used for the purposes of signal analysis. Selection of an inappropriate Mother Wavelet Function (MWT) can bias the results of signal analysis. To determine an appropriate MWT for subdural EEG recordings in rats, we analyzed the results of signal denoising using 25 different potential MWTs (order 1-10 Symlet wavelets, order 1-10 Daubechies wavelets, & order 1-5 Coiflet wavelets). Our selection of an appropriate MWT for each electrode was based on protocol previously published in Al-Qazzaz et al. 2015^[336] and Akkar & Jasim 2017^[337]. Consistent with these two approaches, we used five levels of signal decomposition and a soft SURE threshold for elimination of noise in the EEG signal at each level. Figure A3-1 displays an example of the optimal wavelet chosen for the cortical electrode EEG recordings, demonstrating the improvement in the signal-to-noise ratio after wavelet denoising.

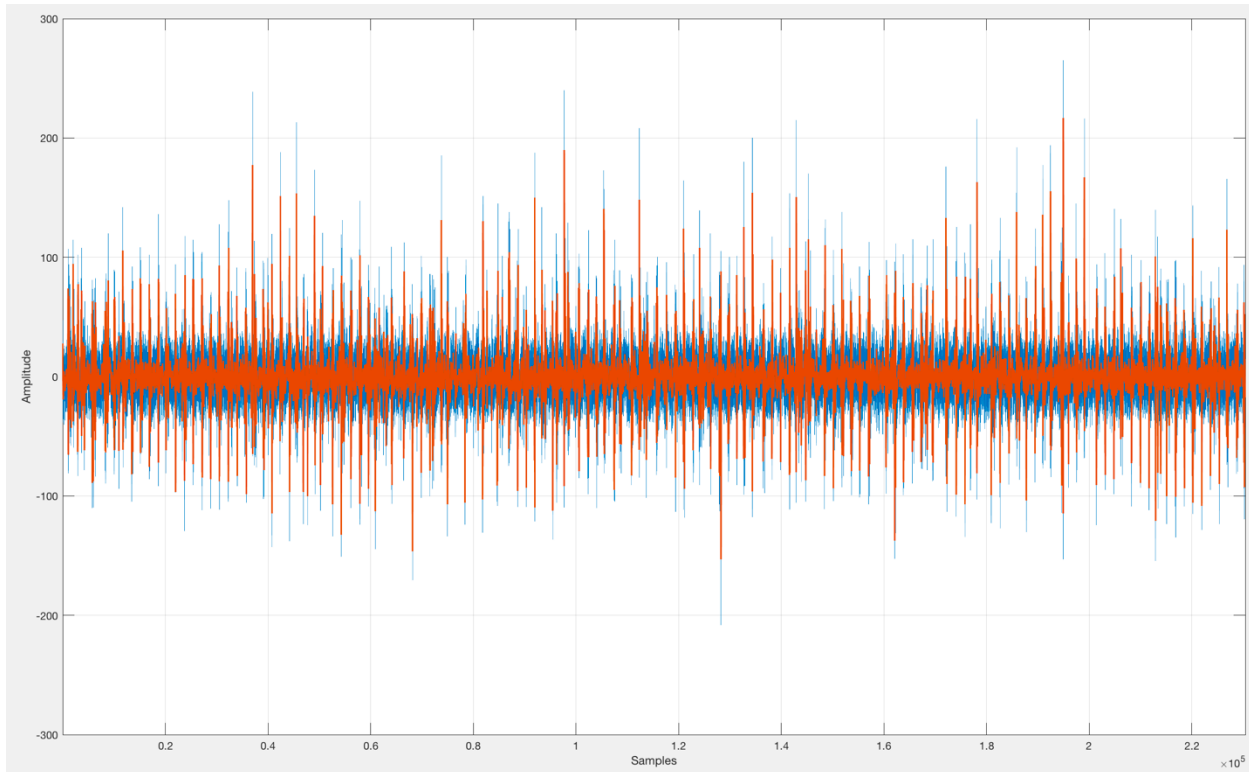


Figure A3-1: Comparison of denoised EEG with raw EEG trace

The raw, unfiltered EEG signal is plotted in blue. The same EEG recording following wavelet denoising is overlaid above in orange. Wavelet denoising improves signal-to-noise ratio, which is important for calculation of the burst suppression ratio.

A3.1 – MWT Selection Methods

For each wild type rat, 60-seconds of continuous, artifact-free, raw EEG were identified for analysis. The selected raw EEG segments were divided into sixty, 1-second epochs (256 samples). Each raw epoch was denoised using the “wdenoise” MATLAB function. The correlation coefficient between the denoised epoch and the raw epoch was computed using the “xcorr” function in MATLAB with zero phase shift.

This analysis was completed for all 60 epochs from the EEG recording for each wild type rat. This process was then repeated for each of the 25 potential MWTs and summarized for each rat by computing the mean correlation coefficient from all 60 epochs. The performance of the

MWTs was then compared by computing the mean and standard deviation of the correlation coefficients computed for each MWT between all of the rats on study.

Figures A3-2 & A3-3 summarize the results of wavelet denoising with each of the MWTs on the cortical and hippocampal electrodes respectively. Most wavelets performed equally well for denoising of the EEG recordings. Ultimately, the tenth order Daubechies wavelet was chosen to denoise the cortical electrode recordings and the fourth order Symlet wavelet was chosen to denoise the hippocampal electrode recordings. Figure A3-4 compares wavelet denoising to denoising with a 60Hz Notch filter and a 0.1-50Hz bandpass filter.

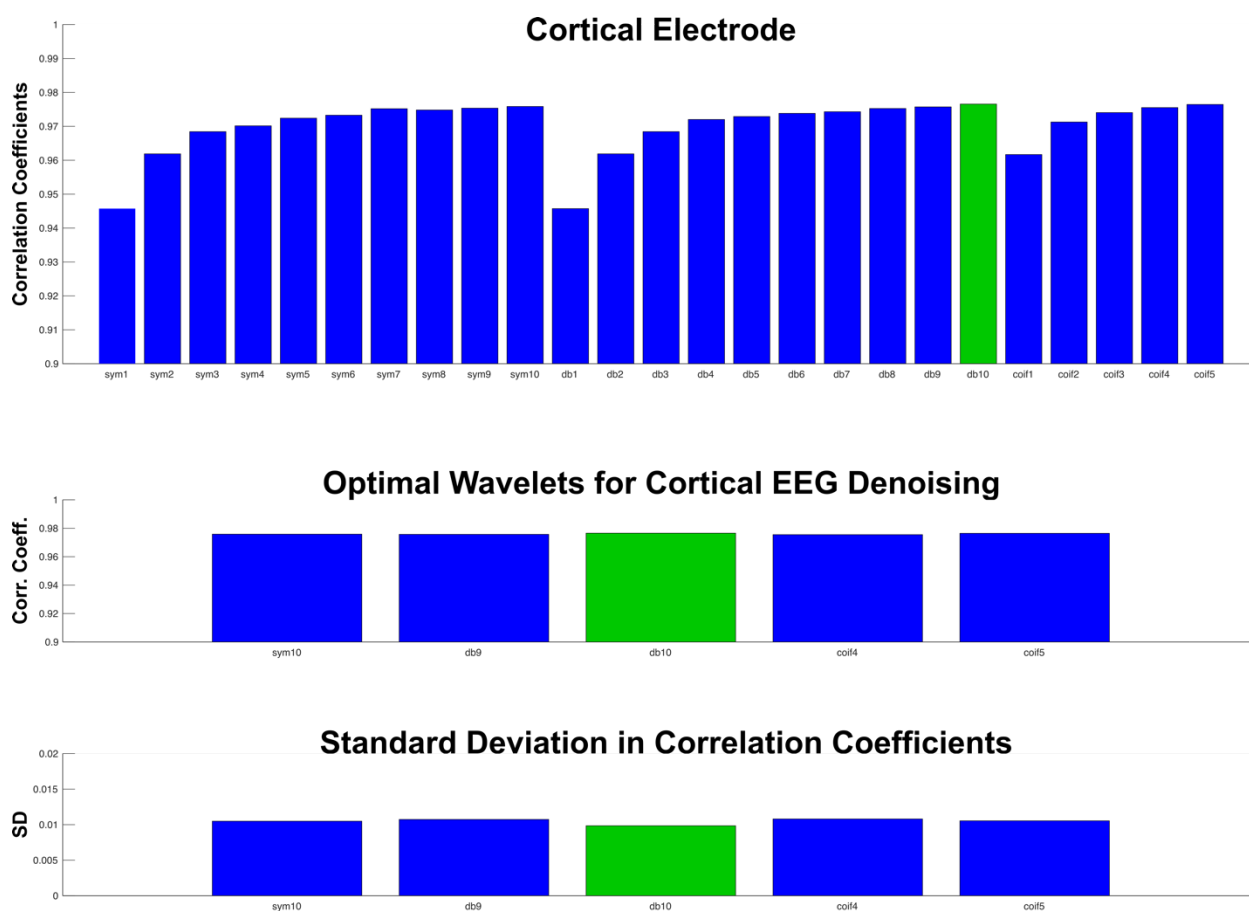


Figure A3-2: Selection of db10 wavelet for denoising of EEG recorded from the Cortical electrode

Correlation coefficients computed by cross correlation of the raw EEG signal from the cortical electrode with the corresponding denoised EEG signal with a zero phase shift. Top: The correlation coefficients for denoised signals computed from Symlet wavelets (orders 1-10), Daubechies wavelets (orders 1-10), and Coiflet wavelets (orders 1-5). All denoised signals have correlation coefficients above $r=0.95$ when compared with the raw signal, except those computed with the order 1 Symlet wavelet and the order 1 Daubechies wavelet. Middle: Comparison of the correlation coefficients for the five wavelets with highest group mean values. Bottom: Comparison of the standard deviations in the correlation coefficient for each of the wavelets included in “Optimal Wavelets” comparison. The order 10 Daubechies wavelet was chosen for denoising based on the high mean correlation coefficient between the raw EEG signal and the denoised EEG signal, plus the lower standard deviation in correlation coefficients across all recordings.

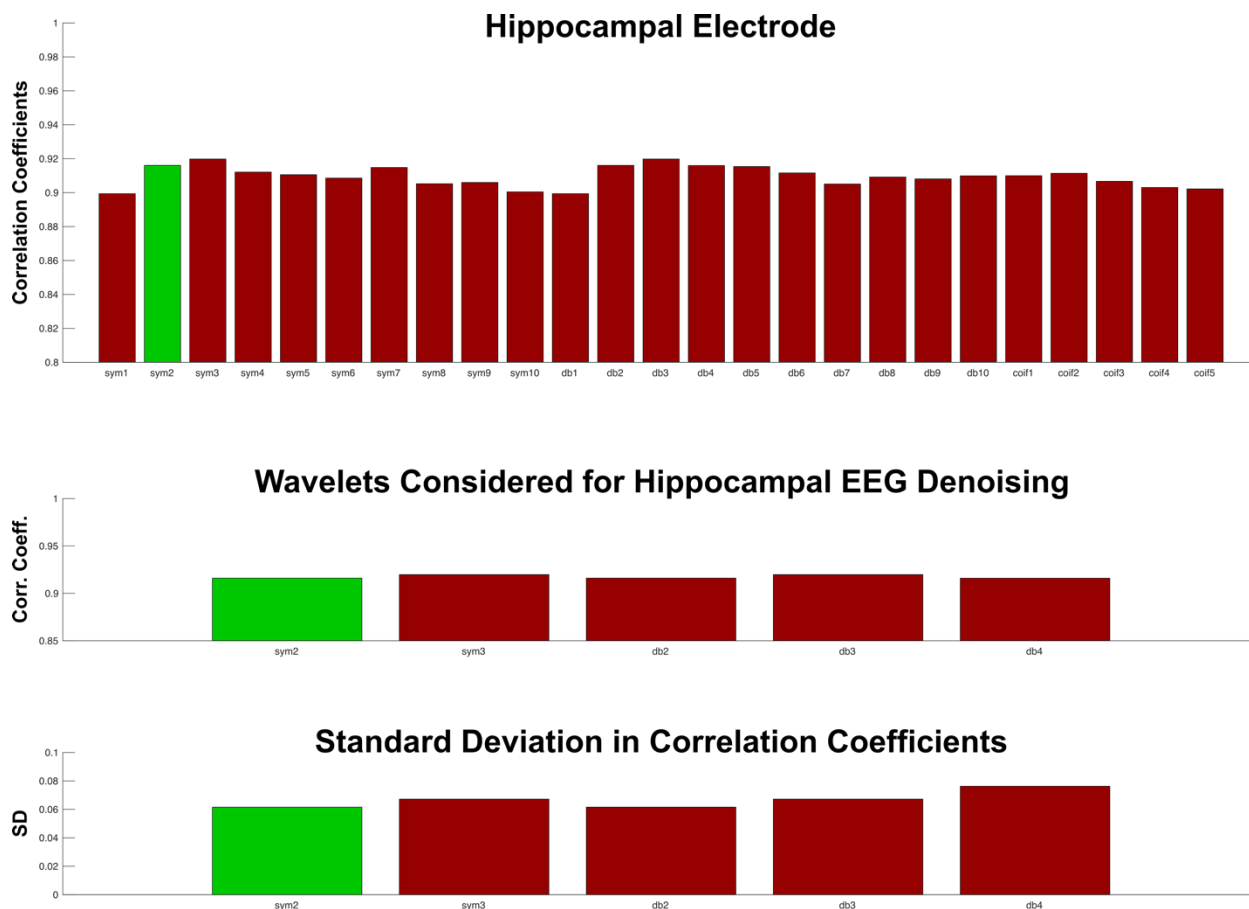


Figure A3-3: Selection of sym2 wavelet for denoising of EEG recorded from the Hippocampal electrode

Correlation coefficients computed by cross correlation of the raw EEG signal from the hippocampal electrode with the corresponding denoised EEG signal with a zero phase shift. Top: The correlation coefficients for denoised signals computed from Symlet wavelets (orders 1-10), Daubechies wavelets (orders 1-10), and Coiflet wavelets (orders 1-5). Middle: Comparison of the correlation coefficients for the five wavelets with highest group mean values. Bottom: Comparison of the standard deviations in the correlation coefficient for each of the wavelets included in “Optimal Wavelets” comparison. The order 2 Symlet wavelet was chosen for denoising based on the relatively high mean correlation coefficient between the raw EEG signal and the denoised EEG signal, plus the lower standard deviation in correlation coefficients across all recordings.

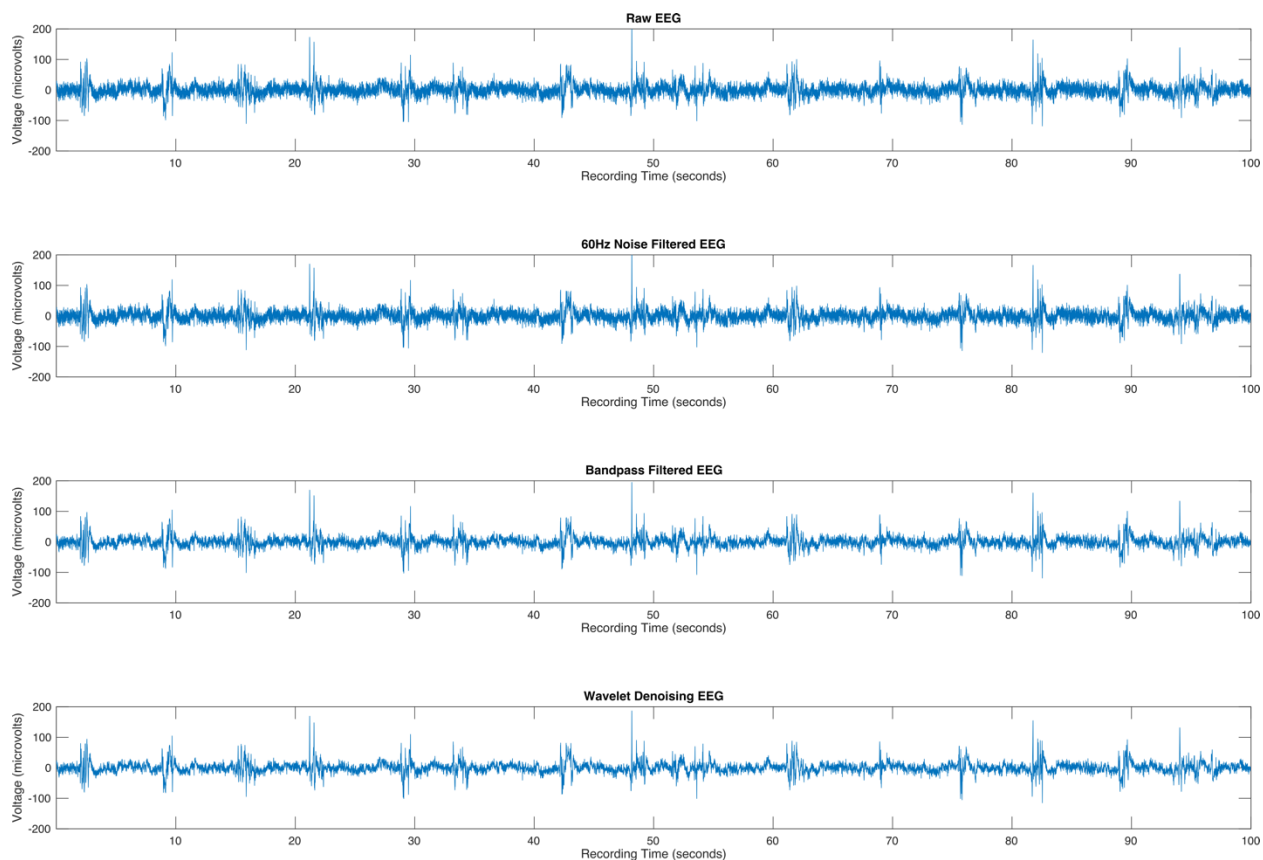


Figure A3-4: Comparison of EEG denoising strategies

Comparison of different common EEG signal denoising techniques on the same EEG recording. Top: An example of the raw EEG recording under anesthesia with burst suppression, taken from the cortical electrode. Upper Middle: Raw EEG recording with a Notch filter for 60Hz electrical noise. Lower Middle: EEG recording after applying a bandpass filter allowing frequencies between 0.1-50Hz. Bottom: EEG recording after wavelet denoising down to level 5 with a tenth order Daubechies wavelet.

Chapter 7 - References

1. Sinon, C.G., S.S. Arora, A.D. Rodriguez, and P.S. Garcia, *Special Considerations: Alzheimer's Disease*, in *Essentials of Geriatric Anesthesia*, H. Prabhakar, C. Mahajan, and I. Kapoor, Editors. 2019, CRC Press.
2. Savage, G.H., *Insanity following the Use of Anæsthetics in Operations*. British Medical Journal, 1887. **2**(1405): p. 1199-1200.
3. Batten, Charles T., M.D. and Cyril B. Courville, M.D., *MENTAL DISTURBANCES FOLLOWING NITROUS OXIDE ANESTHESIA*. Anesthesiology: The Journal of the American Society of Anesthesiologists, 1940. **1**(3): p. 261-273.
4. Eckenhoff, J.E., *Relationship of anesthesia to postoperative personality changes in children*. AMA Am J Dis Child, 1953. **86**(5): p. 587-91.
5. Bedford, P.D., *Adverse cerebral effects of anaesthesia on old people*. Lancet, 1955. **269**(6884): p. 259-63.
6. Chivukula, S., R. Grandhi, and R.M. Friedlander, *A brief history of early neuroanesthesia*. Neurosurg Focus, 2014. **36**(4): p. E2.
7. Wells, H., *A history of the discovery of the application of nitrous oxide gas, ether and other vapors, to surgical operations*. 1847, Hartford: The National Library of Medicine. 25.
8. Kavanagh, M.F., *THE ORIGIN OF THE WORD "ANESTHESIA"*. Cal West Med, 1928. **29**(1): p. 10-2.
9. Dumas, A., *The History of Anaesthesia*. J Natl Med Assoc, 1932. **24**(1): p. 6-9.
10. Civil, M., *A Hymn to the Beer Goddess and a Drinking Song*. Studies Presented to A. Leo Oppenheim, June 7, 1964, 1964: p. 67-89.
11. *Early Writing Tablet recording the Allocation of Beer*. 3100-3000 BC, British Museum: Uruk.
12. Brownstein, M.J., *A brief history of opiates, opioid peptides, and opioid receptors*. Proc Natl Acad Sci U S A, 1993. **90**(12): p. 5391-3.
13. Teall, E.K., *Medicine and Doctoring in Ancient Mesopotamia*. Grand Valley Journal of History, 2014. **3**(1).
14. Ebers, G.M., *Papyrus Ebers. Die Maasse und das Kapitel ,ber die Augenkrankheiten*. 1889, Leipzig: Hirzel.
15. Breasted, J.H., *The Edwin Smith Papyrus*. University of Chicago Press, 1930.
16. Tsai, T., J. Gadsden, and C. Connery, *Local Infiltration Anesthesia*, in *Textbook of regional anesthesia and acute pain management*. 2007, McGraw-Hill, Medical Pub. Division: New York.
17. Susruta and K. Bhishagratna, *An English translation of the Sushruta samhita, based on original Sanskrit text : Edited and published by Kaviraj Kunja Lal Bhishagratna. With a full and comprehensive introd., translation of different readings, notes, comperative views, index, glossary and plates*. 1907.
18. Chu, N.S., *[Legendary Hwa Tuo's surgery under general anesthesia in the second century China]*. Acta Neurol Taiwan, 2004. **13**(4): p. 211-6.
19. Anonymous, W.L. Idema, and S.H. West, *Records of the Three Kingdoms in Plain Language*. 2016.

20. Mair, V.H., *The Biography of Hua-t'o from the "History of the Three Kingdoms"*, in *The Columbia Anthology of Traditional Chinese Literature*, V.H. Mair, Editor. 1994, Columbia University Press. p. 688-696.
21. Hammurabi and P.S.P. Handcock, *The code of Hammurabi*. 1920.
22. al-Zahrawi, H.i.A.A.a.-Q.a., G.L. Lewis, and M.S. Spink, *On surgery and instruments*. 1973, Berkeley; Los Angeles: University of California Press.
23. Carter, A.J., *Narcosis and nightshade*. *Bmj*, 1996. **313**(7072): p. 1630-2.
24. Takrouri, M., *Surgical, medical and anesthesia in the Middle East: Notes on Ancient and medieval practice with reference to Islamic-Arabic medicine*. *The Internet Journal of Health*, 2005. **5**(1).
25. Matsuki, A. and E.K. Zsigmond, *The introduction of chloroform anesthesia in the United States*. *Anesth Analg*, 1974. **53**(1): p. 148-51.
26. Brandstater, B., E.I. Eger, 2nd, and G. Edelist, *Effects of halothane, ether and cyclopropane on respiration*. *Br J Anaesth*, 1965. **37**(12): p. 890-7.
27. Conway, C.M., *The anaesthetic ethers*. *Br J Anaesth*, 1965. **37**(9): p. 644-54.
28. Smith, G.B. and N.P. Hirsch, *Gardner Quincy Colton: pioneer of nitrous oxide anesthesia*. *Anesth Analg*, 1991. **72**(3): p. 382-91.
29. Matic, A.A., *An Anesthesiologist's Perspective on the History of Basic Airway Management: The "Progressive" Era, 1904 to 1960*. *Anesthesiology*, 2018. **128**(2): p. 254-271.
30. Ruetsch, Y.A., T. Boni, and A. Borgeat, *From cocaine to ropivacaine: the history of local anesthetic drugs*. *Curr Top Med Chem*, 2001. **1**(3): p. 175-82.
31. Bowman, W.C., *Neuromuscular block*. *Br J Pharmacol*, 2006. **147 Suppl 1**: p. S277-86.
32. Brown, B.R., Jr., I.G. Sipes, and A.M. Sagalyn, *Mechanisms of acute hepatic toxicity: chloroform, halothane, and glutathione*. *Anesthesiology*, 1974. **41**(6): p. 554-61.
33. MacDonald, A.G., *A short history of fires and explosions caused by anaesthetic agents*. *Br J Anaesth*, 1994. **72**(6): p. 710-22.
34. Eger, E.I., 2nd, L.J. Saidman, and B. Brandstater, *Minimum alveolar anesthetic concentration: a standard of anesthetic potency*. *Anesthesiology*, 1965. **26**(6): p. 756-63.
35. Eger, E.I., 2nd, *Age, minimum alveolar anesthetic concentration, and minimum alveolar anesthetic concentration-awake*. *Anesth Analg*, 2001. **93**(4): p. 947-53.
36. Schlich, T., *The history of anaesthesia and the patient-reduced to a body?* *Lancet*, 2017. **390**(10099): p. 1020-1021.
37. Nagel, T., *What is it like to be a bat?* *Philosophical Review*, 1974. **83**(October): p. 435-50.
38. Chalmers, D.J., *Facing up to the problem of consciousness*. *Journal of Consciousness Studies*, 1995. **2**(3): p. 200-19.
39. Baars, B.J., *A Cognitive Theory of Consciousness*. 1988: Cambridge University Press.
40. Tononi, G., *An information integration theory of consciousness*. *BMC Neurosci*, 2004. **5**: p. 42.
41. Dennett, D.C., *Facing up to the hard question of consciousness*. *Philos Trans R Soc Lond B Biol Sci*, 2018. **373**(1755).
42. Weisberg, J., *The Hard Problem of Consciousness*. *Internet Encyclopedia of Philosophy*.
43. Scammell, T.E., E. Arrigoni, and J.O. Lipton, *Neural Circuitry of Wakefulness and Sleep*. *Neuron*, 2017. **93**(4): p. 747-765.

44. Frith, C., R. Perry, and E. Lumer, *The neural correlates of conscious experience: an experimental framework*. Trends Cogn Sci, 1999. **3**(3): p. 105-114.
45. Crick, F. and C. Koch, *Consciousness and neuroscience*. Cereb Cortex, 1998. **8**(2): p. 97-107.
46. Suddendorf, T. and D.L. Butler, *The nature of visual self-recognition*. Trends Cogn Sci, 2013. **17**(3): p. 121-7.
47. Anderson, J.R. and G.G. Gallup, Jr., *Mirror self-recognition: a review and critique of attempts to promote and engineer self-recognition in primates*. Primates, 2015. **56**(4): p. 317-26.
48. Herman, L.M., *Body and self in dolphins*. Conscious Cogn, 2012. **21**(1): p. 526-45.
49. Butler, A.B., *Evolution of brains, cognition, and consciousness*. Brain Res Bull, 2008. **75**(2-4): p. 442-9.
50. Kanwal, J., K. Smith, J. Culbertson, and S. Kirby, *Zipf's Law of Abbreviation and the Principle of Least Effort: Language users optimise a miniature lexicon for efficient communication*. Cognition, 2017. **165**: p. 45-52.
51. Mc, C.B., S.F. Hanser, and L.R. Doyle, *Quantitative tools for comparing animal communication systems: information theory applied to bottlenose dolphin whistle repertoires*. Anim Behav, 1999. **57**(2): p. 409-419.
52. Laureys, S., *The neural correlate of (un)awareness: lessons from the vegetative state*. Trends Cogn Sci, 2005. **9**(12): p. 556-9.
53. Franks, N.P., *General anaesthesia: from molecular targets to neuronal pathways of sleep and arousal*. Nat Rev Neurosci, 2008. **9**(5): p. 370-86.
54. McCarren, H.S., J.T. Moore, and M.B. Kelz, *Assessing changes in volatile general anesthetic sensitivity of mice after local or systemic pharmacological intervention*. J Vis Exp, 2013(80): p. e51079.
55. MacIver, M.B. and B.H. Bland, *Chaos analysis of EEG during isoflurane-induced loss of righting in rats*. Front Syst Neurosci, 2014. **8**: p. 203.
56. Franks, N.P. and W.R. Lieb, *Mechanisms of general anesthesia*. Environ Health Perspect, 1990. **87**: p. 199-205.
57. Spiegel, I., E.K. Bichler, and P.S. Garcia, *The Influence of Regional Distribution and Pharmacologic Specificity of GABAAR Subtype Expression on Anesthesia and Emergence*. Front Syst Neurosci, 2017. **11**: p. 58.
58. Chua, H.C. and M. Chebib, *GABAA Receptors and the Diversity in their Structure and Pharmacology*. Adv Pharmacol, 2017. **79**: p. 1-34.
59. Ciobanu, L., O. Reynaud, L. Uhrig, B. Jarraya, and D. Le Bihan, *Effects of Anesthetic Agents on Brain Blood Oxygenation Level Revealed with Ultra-High Field MRI*. PLOS ONE, 2012. **7**(3): p. e32645.
60. Heinke, W. and C. Schwarzbauer, *In vivo imaging of anaesthetic action in humans: approaches with positron emission tomography (PET) and functional magnetic resonance imaging (fMRI)*. Br J Anaesth, 2002. **89**(1): p. 112-22.
61. Torri, G., *Inhalation anesthetics: a review*. Minerva anesthesiologica, 2010. **76**(3): p. 215-28.
62. Riznyk, L., M. Fijalkowska, and K. Przesmycki, *Effects of thiopental and propofol on heart rate variability during fentanyl-based induction of general anesthesia*. Pharmacol Rep, 2005. **57**(1): p. 128-34.

63. Abraham, M.H., W.E. Acree, Jr., C. Mintz, and S. Payne, *Effect of anesthetic structure on inhalation anesthesia: implications for the mechanism*. J Pharm Sci, 2008. **97**(6): p. 2373-84.
64. Poon KK, W.S., *New and developing anesthesia drugs*. Expert Opinion on Pharmacotherapy, 2017. **18**(2): p. 195-204.
65. Garcia, P.S., S.E. Kolesky, and A. Jenkins, *General anesthetic actions on GABA(A) receptors*. Curr Neuropharmacol, 2010. **8**(1): p. 2-9.
66. Garcia, P.S., E.W. Duggan, I.L. McCullough, S.C. Lee, and D. Fishman, *Postanesthesia Care for the Elderly Patient*. Clin Ther, 2015. **37**(12): p. 2651-65.
67. Lotfy, A.O., A.K. Amir-Jahed, and P. Moarefi, *Anesthesia with ketamine: indications, advantages, and shortcomings*. Anesth Analg, 1970. **49**(6): p. 969-74.
68. Abu-Shahwan, I. and K. Chowdary, *Ketamine is effective in decreasing the incidence of emergence agitation in children undergoing dental repair under sevoflurane general anesthesia*. Paediatr Anaesth, 2007. **17**(9): p. 846-50.
69. Pai, A. and M. Heining, *Ketamine*. BJA Education, 2007. **7**(2): p. 59-63.
70. Maksimow, A., M. Sarkela, J.W. Langsjo, et al., *Increase in high frequency EEG activity explains the poor performance of EEG spectral entropy monitor during S-ketamine anesthesia*. Clin Neurophysiol, 2006. **117**(8): p. 1660-8.
71. Hambrecht-Wiedbusch, V.S., D. Li, and G.A. Mashour, *Paradoxical Emergence: Administration of Subanesthetic Ketamine during Isoflurane Anesthesia Induces Burst Suppression but Accelerates Recovery*. Anesthesiology, 2017. **126**(3): p. 482-494.
72. Craven, R., *Ketamine*. Anaesthesia, 2007. **62**(s1): p. 48-53.
73. Kurdi, M.S., K.A. Theerth, and R.S. Deva, *Ketamine: Current applications in anesthesia, pain, and critical care*. Anesth Essays Res, 2014. **8**(3): p. 283-90.
74. Hagihira, S., *Changes in the electroencephalogram during anaesthesia and their physiological basis*. British Journal of Anaesthesia, 2015. **115**: p. i27-i31.
75. Mashour, G.A., *Consciousness, anesthesia, and neural synchrony*. Anesthesiology, 2013. **119**(1): p. 7-9.
76. Li, D., L.J. Voss, J.W. Sleight, and X. Li, *Effects of volatile anesthetic agents on cerebral cortical synchronization in sheep*. Anesthesiology, 2013. **119**(1): p. 81-8.
77. Shannon, C.E., *A Mathematical Theory of Communication*. Bell System Technical Journal, 1948. **27**(3): p. 379-423.
78. Hajat, Z., N. Ahmad, and J. Andrzejowski, *The role and limitations of EEG-based depth of anaesthesia monitoring in theatres and intensive care*. Anaesthesia, 2017. **72**(S1): p. 38-47.
79. Kenny, J.D., M.B. Westover, S. Ching, E.N. Brown, and K. Solt, *Propofol and sevoflurane induce distinct burst suppression patterns in rats*. Front Syst Neurosci, 2014. **8**: p. 237.
80. Kroeger, D. and F. Amzica, *Hypersensitivity of the anesthesia-induced comatose brain*. J Neurosci, 2007. **27**(39): p. 10597-607.
81. Ching, S., P.L. Purdon, S. Vijayan, N.J. Kopell, and E.N. Brown, *A neurophysiological-metabolic model for burst suppression*. Proc Natl Acad Sci U S A, 2012. **109**(8): p. 3095-100.
82. Japaridze, N., M. Muthuraman, C. Reinicke, et al., *Neuronal Networks during Burst Suppression as Revealed by Source Analysis*. PLoS One, 2015. **10**(4): p. e0123807.

83. Kelz, M.B., P.S. Garcia, G.A. Mashour, and K. Solt, *Escape From Oblivion: Neural Mechanisms of Emergence From General Anesthesia*. *Anesth Analg*, 2019. **128**(4): p. 726-736.
84. Pani, N., P.A. Dongare, and R.K. Mishra, *Reversal agents in anaesthesia and critical care*. *Indian J Anaesth*, 2015. **59**(10): p. 664-9.
85. Rye, D.B., D.L. Bliwise, K. Parker, et al., *Modulation of vigilance in the primary hypersomnias by endogenous enhancement of GABAA receptors*. *Sci Transl Med*, 2012. **4**(161): p. 161ra151.
86. Safavynia, S.A., G. Keating, I. Spiegel, et al., *Effects of gamma-Aminobutyric Acid Type A Receptor Modulation by Flumazenil on Emergence from General Anesthesia*. *Anesthesiology*, 2016. **125**(1): p. 147-58.
87. Mees, L., J. Fidler, M. Kreuzer, et al., *Faster emergence behavior from ketamine/xylazine anesthesia with atipamezole versus yohimbine*. *PLoS One*, 2018. **13**(10): p. e0199087.
88. Solt, K., C.J. Van Dort, J.J. Chemali, et al., *Electrical stimulation of the ventral tegmental area induces reanimation from general anesthesia*. *Anesthesiology*, 2014. **121**(2): p. 311-9.
89. Taylor, N.E., C.J. Van Dort, J.D. Kenny, et al., *Optogenetic activation of dopamine neurons in the ventral tegmental area induces reanimation from general anesthesia*. *Proc Natl Acad Sci U S A*, 2016. **113**(45): p. 12826-12831.
90. Alkire, M.T., J.R. McReynolds, E.L. Hahn, and A.N. Trivedi, *Thalamic microinjection of nicotine reverses sevoflurane-induced loss of righting reflex in the rat*. *Anesthesiology*, 2007. **107**(2): p. 264-72.
91. Meuret, P., S.B. Backman, V. Bonhomme, G. Plourde, and P. Fiset, *Physostigmine reverses propofol-induced unconsciousness and attenuation of the auditory steady state response and bispectral index in human volunteers*. *Anesthesiology*, 2000. **93**(3): p. 708-17.
92. Plourde, G., D. Chartrand, P. Fiset, S. Font, and S.B. Backman, *Antagonism of sevoflurane anaesthesia by physostigmine: effects on the auditory steady-state response and bispectral index*. *Br J Anaesth*, 2003. **91**(4): p. 583-6.
93. Mansouri, M.T., J.A. Fidler, Q.C. Meng, R.G. Eckenhoff, and P.S. Garcia, *Sex effects on behavioral markers of emergence from propofol and isoflurane anesthesia in rats*. *Behav Brain Res*, 2019. **367**: p. 59-67.
94. *Diagnostic and statistical manual of mental disorders : DSM-5*, ed. A. American Psychiatric and D.S.M.T.F. American Psychiatric Association. 2013, Arlington, VA: American Psychiatric Association.
95. Peterson, J.F., B.T. Pun, R.S. Dittus, et al., *Delirium and its motoric subtypes: a study of 614 critically ill patients*. *J Am Geriatr Soc*, 2006. **54**(3): p. 479-84.
96. Vljakovic, G.P. and R.P. Sindjelic, *Emergence delirium in children: many questions, few answers*. *Anesth Analg*, 2007. **104**(1): p. 84-91.
97. Kim, H.J., D.K. Kim, H.Y. Kim, J.K. Kim, and S.W. Choi, *Risk factors of emergence agitation in adults undergoing general anesthesia for nasal surgery*. *Clin Exp Otorhinolaryngol*, 2015. **8**(1): p. 46-51.
98. Foesel, T. and H.J. Reisch, *Postoperative behavioural changes in children: comparison between halothane and sevoflurane*. *Paediatr Anaesth*, 2001. **11**(6): p. 719-23.

99. Evered, L., B. Silbert, D.S. Knopman, et al., *Recommendations for the nomenclature of cognitive change associated with anaesthesia and surgery*; 2018. *British Journal of Anaesthesia*, 2018. **121**(5): p. 1005-1012.
100. Safavynia, S.A., S. Arora, K.O. Pryor, and P.S. Garcia, *An update on postoperative delirium: Clinical features, neuropathogenesis, and perioperative management*. *Curr Anesthesiol Rep*, 2018. **8**(3): p. 252-262.
101. Hernandez, B.A., H. Lindroth, P. Rowley, et al., *Post-anaesthesia care unit delirium: incidence, risk factors and associated adverse outcomes*. *BJA: British Journal of Anaesthesia*, 2017. **119**(2): p. 288-290.
102. Card, E., P. Pandharipande, C. Tomes, et al., *Emergence from general anaesthesia and evolution of delirium signs in the post-anaesthesia care unit*. *Br J Anaesth*, 2015. **115**(3): p. 411-7.
103. Radtke, F.M., M. Franck, M. MacGuill, et al., *Duration of fluid fasting and choice of analgesic are modifiable factors for early postoperative delirium*. *Eur J Anaesthesiol*, 2010. **27**(5): p. 411-6.
104. Xara, D., A. Silva, J. Mendonca, and F. Abelha, *Inadequate emergence after anaesthesia: emergence delirium and hypoactive emergence in the Postanaesthesia Care Unit*. *J Clin Anesth*, 2013. **25**(6): p. 439-46.
105. Neufeld, K.J., J.M. Leoutsakos, F.E. Sieber, et al., *Outcomes of early delirium diagnosis after general anesthesia in the elderly*. *Anesth Analg*, 2013. **117**(2): p. 471-8.
106. Sharma, P.T., F.E. Sieber, K.J. Zakriya, et al., *Recovery Room Delirium Predicts Postoperative Delirium After Hip-Fracture Repair*. *Anesth Analg*, 2005. **101**(4): p. 1215-1220.
107. Hesse, S., M. Kreuzer, D. Hight, et al., *Association of electroencephalogram trajectories during emergence from anaesthesia with delirium in the postanaesthesia care unit: an early sign of postoperative complications*. *Br J Anaesth*, 2019. **122**(5): p. 622-634.
108. Yang, E., M. Kreuzer, S. Hesse, et al., *Infrared pupillometry helps to detect and predict delirium in the post-anaesthesia care unit*. *J Clin Monit Comput*, 2018. **32**(2): p. 359-368.
109. Hight, D.F., J. Sleight, J.D. Winders, et al., *Inattentive Delirium vs. Disorganized Thinking: A New Axis to Subcategorize PACU Delirium*. *Front Syst Neurosci*, 2018. **12**: p. 22.
110. Palanca, B.J.A., T.S. Wildes, Y.S. Ju, S. Ching, and M.S. Avidan, *Electroencephalography and delirium in the postoperative period*. *Br J Anaesth*, 2017. **119**(2): p. 294-307.
111. Choi, S.H., H. Lee, T.S. Chung, et al., *Neural network functional connectivity during and after an episode of delirium*. *Am J Psychiatry*, 2012. **169**(5): p. 498-507.
112. Kelly, A.M.C., L.Q. Uddin, B.B. Biswal, F.X. Castellanos, and M.P. Milham, *Competition between functional brain networks mediates behavioral variability*. *NeuroImage*, 2008. **39**(1): p. 527-537.
113. Castellanos, F.X., D.S. Margulies, C. Kelly, et al., *Cingulate-precuneus interactions: a new locus of dysfunction in adult attention-deficit/hyperactivity disorder*. *Biological psychiatry*, 2008. **63**(3): p. 332-337.
114. Safavynia, S.A. and P.A. Goldstein, *The Role of Neuroinflammation in Postoperative Cognitive Dysfunction: Moving From Hypothesis to Treatment*. *Front Psychiatry*, 2018. **9**: p. 752.

115. Steinmetz, J., K.B. Christensen, T. Lund, et al., *Long-term consequences of postoperative cognitive dysfunction*. *Anesthesiology*, 2009. **110**(3): p. 548-55.
116. Culley, D.J., M. Baxter, R. Yukhananov, and G. Crosby, *The memory effects of general anesthesia persist for weeks in young and aged rats*. *Anesth Analg*, 2003. **96**(4): p. 1004-9, table of contents.
117. Culley, D.J., M.G. Baxter, C.A. Crosby, R. Yukhananov, and G. Crosby, *Impaired acquisition of spatial memory 2 weeks after isoflurane and isoflurane-nitrous oxide anesthesia in aged rats*. *Anesth Analg*, 2004. **99**(5): p. 1393-7; table of contents.
118. Crosby, C., D.J. Culley, M.G. Baxter, R. Yukhananov, and G. Crosby, *Spatial memory performance 2 weeks after general anesthesia in adult rats*. *Anesth Analg*, 2005. **101**(5): p. 1389-92.
119. Culley, D.J., M.G. Baxter, R. Yukhananov, and G. Crosby, *Long-term impairment of acquisition of a spatial memory task following isoflurane-nitrous oxide anesthesia in rats*. *Anesthesiology*, 2004. **100**(2): p. 309-14.
120. Rasmussen, L.S., T. Johnson, H.M. Kuipers, et al., *Does anaesthesia cause postoperative cognitive dysfunction? A randomised study of regional versus general anaesthesia in 438 elderly patients*. *Acta Anaesthesiol Scand*, 2003. **47**(3): p. 260-6.
121. Moller, J.T., P. Cluitmans, L.S. Rasmussen, et al., *Long-term postoperative cognitive dysfunction in the elderly ISPOCDI study. ISPOCD investigators. International Study of Post-Operative Cognitive Dysfunction*. *Lancet*, 1998. **351**(9106): p. 857-61.
122. Johnson, T., T. Monk, L.S. Rasmussen, et al., *Postoperative cognitive dysfunction in middle-aged patients*. *Anesthesiology*, 2002. **96**(6): p. 1351-7.
123. Mashour, G.A., D.T. Woodrum, and M.S. Avidan, *Neurological complications of surgery and anaesthesia*. *Br J Anaesth*, 2015. **114**(2): p. 194-203.
124. Orser, B.A., C.D. Mazer, and A.J. Baker, *Awareness during anesthesia*. *Cmaj*, 2008. **178**(2): p. 185-8.
125. Mashour, G.A., M.D., Ph.D., B.A. Orser, M.D., Ph.D., and M.S. Avidan, M.B., B.Ch., *Intraoperative Awareness: From Neurobiology to Clinical Practice*. *Anesthesiology: The Journal of the American Society of Anesthesiologists*, 2011. **114**(5): p. 1218-1233.
126. McCleane, G.J. and R. Cooper, *The nature of pre-operative anxiety*. *Anaesthesia*, 1990. **45**(2): p. 153-5.
127. Bowman, A.M., *The relationship of anxiety to development of postoperative delirium*. *J Gerontol Nurs*, 1992. **18**(1): p. 24-30.
128. Folks, D.G., A.M. Freeman, 3rd, R.S. Sokol, et al., *Cognitive dysfunction after coronary artery bypass surgery: a case-controlled study*. *South Med J*, 1988. **81**(2): p. 202-6.
129. Sanders, R.D., P.P. Pandharipande, A.J. Davidson, D. Ma, and M. Maze, *Anticipating and managing postoperative delirium and cognitive decline in adults*. *BMJ*, 2011. **343**(jul20 1): p. d4331-d4331.
130. Funder, K.S., J. Steinmetz, and L.S. Rasmussen, *Methodological issues of postoperative cognitive dysfunction research*. *Semin Cardiothorac Vasc Anesth*, 2010. **14**(2): p. 119-22.
131. Zheng, X., J. Zhou, and Y. Xia, *The role of TNF-alpha in regulating ketamine-induced hippocampal neurotoxicity*. *Arch Med Sci*, 2015. **11**(6): p. 1296-302.
132. Jevtovic-Todorovic, V., R.E. Hartman, Y. Izumi, et al., *Early exposure to common anesthetic agents causes widespread neurodegeneration in the developing rat brain and persistent learning deficits*. *J Neurosci*, 2003. **23**(3): p. 876-82.

133. Loepke, A.W., G.K. Istaphanous, J.J. McAuliffe, 3rd, et al., *The effects of neonatal isoflurane exposure in mice on brain cell viability, adult behavior, learning, and memory*. *Anesth Analg*, 2009. **108**(1): p. 90-104.
134. Perouansky, M. and H.C. Hemmings, Jr., *Neurotoxicity of general anesthetics: cause for concern?* *Anesthesiology*, 2009. **111**(6): p. 1365-71.
135. Bilotta F, E.L., Gruenbaum SE, *Neurotoxicity of anesthetic drugs: an update*. *Curr Opin Anaesthesiol*, 2017. **30**(4): p. 452-457.
136. Kalkman, C.J., L. Peelen, K.G. Moons, et al., *Behavior and development in children and age at the time of first anesthetic exposure*. *Anesthesiology*, 2009. **110**(4): p. 805-12.
137. Wilder, R.T., R.P. Flick, J. Sprung, et al., *Early exposure to anesthesia and learning disabilities in a population-based birth cohort*. *Anesthesiology*, 2009. **110**(4): p. 796-804.
138. Xie, Z., D.J. Culley, Y. Dong, et al., *The common inhalation anesthetic isoflurane induces caspase activation and increases amyloid beta-protein level in vivo*. *Ann Neurol*, 2008. **64**(6): p. 618-27.
139. Xie, Z., Y. Dong, U. Maeda, et al., *The inhalation anesthetic isoflurane induces a vicious cycle of apoptosis and amyloid beta-protein accumulation*. *J Neurosci*, 2007. **27**(6): p. 1247-54.
140. Wei, H., G. Liang, H. Yang, et al., *The common inhalational anesthetic isoflurane induces apoptosis via activation of inositol 1,4,5-trisphosphate receptors*. *Anesthesiology*, 2008. **108**(2): p. 251-60.
141. Eckenhoff, R.G. and K.F. Laudansky, *Anesthesia, surgery, illness and Alzheimer's disease*. *Prog Neuropsychopharmacol Biol Psychiatry*, 2013. **47**: p. 162-6.
142. Maldonado, J.R., *Neuropathogenesis of delirium: review of current etiologic theories and common pathways*. *The American journal of geriatric psychiatry : official journal of the American Association for Geriatric Psychiatry*, 2013. **21**(12): p. 1190-1222.
143. Thal, S.C., C. Luh, E.V. Schaible, et al., *Volatile anesthetics influence blood-brain barrier integrity by modulation of tight junction protein expression in traumatic brain injury*. *PLoS One*, 2012. **7**(12): p. e50752.
144. Tetrault, S., O. Chever, A. Sik, and F. Amzica, *Opening of the blood-brain barrier during isoflurane anaesthesia*. *Eur J Neurosci*, 2008. **28**(7): p. 1330-41.
145. Chan, M.T., B.C. Cheng, T.M. Lee, and T. Gin, *BIS-guided anesthesia decreases postoperative delirium and cognitive decline*. *J Neurosurg Anesthesiol*, 2013. **25**(1): p. 33-42.
146. Hou, R., H. Wang, L. Chen, Y. Qiu, and S. Li, *POCD in patients receiving total knee replacement under deep vs light anesthesia: A randomized controlled trial*. *Brain Behav*, 2018. **8**(2): p. e00910.
147. Ballard, C., E. Jones, N. Gauge, et al., *Optimised anaesthesia to reduce post operative cognitive decline (POCD) in older patients undergoing elective surgery, a randomised controlled trial*. *PLoS One*, 2012. **7**(6): p. e37410.
148. Radtke, F.M., M. Franck, J. Lendner, et al., *Monitoring depth of anaesthesia in a randomized trial decreases the rate of postoperative delirium but not postoperative cognitive dysfunction*. *Br J Anaesth*, 2013. **110 Suppl 1**: p. i98-105.
149. Whitlock, E.L., B.A. Torres, N. Lin, et al., *Postoperative delirium in a substudy of cardiothoracic surgical patients in the BAG-RECALL clinical trial*. *Anesth Analg*, 2014. **118**(4): p. 809-17.

150. Zhou, Y., Y. Li, and K. Wang, *Bispectral Index Monitoring During Anesthesia Promotes Early Postoperative Recovery of Cognitive Function and Reduces Acute Delirium in Elderly Patients with Colon Carcinoma: A Prospective Controlled Study using the Attention Network Test*. *Med Sci Monit*, 2018. **24**: p. 7785-7793.
151. Sieber, F.E., K.J. Zakriya, A. Gottschalk, et al., *Sedation depth during spinal anesthesia and the development of postoperative delirium in elderly patients undergoing hip fracture repair*. *Mayo Clin Proc*, 2010. **85**(1): p. 18-26.
152. Brown, C.H.t., A.S. Azman, A. Gottschalk, S.C. Mears, and F.E. Sieber, *Sedation depth during spinal anesthesia and survival in elderly patients undergoing hip fracture repair*. *Anesth Analg*, 2014. **118**(5): p. 977-80.
153. Punjasawadwong, Y., N. Boonjeungmonkol, and A. Phongchiewboon, *Bispectral index for improving anaesthetic delivery and postoperative recovery*. *Cochrane Database Syst Rev*, 2007(4): p. Cd003843.
154. Chander, D., P.S. Garcia, J.N. MacColl, S. Illing, and J.W. Sleigh, *Electroencephalographic variation during end maintenance and emergence from surgical anesthesia*. *PLoS One*, 2014. **9**(9): p. e106291.
155. Dang-Vu, T.T., S.M. McKinney, O.M. Buxton, J.M. Solet, and J.M. Ellenbogen, *Spontaneous brain rhythms predict sleep stability in the face of noise*. *Curr Biol*, 2010. **20**(15): p. R626-7.
156. Espa, F., B. Ondze, P. Deglise, M. Billiard, and A. Besset, *Sleep architecture, slow wave activity, and sleep spindles in adult patients with sleepwalking and sleep terrors*. *Clinical Neurophysiology*, 2000. **111**(5): p. 929-939.
157. Howell, M.J., *Parasomnias: an updated review*. *Neurotherapeutics*, 2012. **9**(4): p. 753-75.
158. Shortal, B.P., L.B. Hickman, R.A. Mak-McCully, et al., *Duration of EEG suppression does not predict recovery time or degree of cognitive impairment after general anaesthesia in human volunteers*. *Br J Anaesth*, 2019.
159. Fritz, B.A., P.L. Kalarickal, H.R. Maybrier, et al., *Intraoperative Electroencephalogram Suppression Predicts Postoperative Delirium*. *Anesth Analg*, 2016. **122**(1): p. 234-42.
160. Bruhn, J., T.W. Bouillon, and S.L. Shafer, *Bispectral index (BIS) and burst suppression: revealing a part of the BIS algorithm*. *J Clin Monit Comput*, 2000. **16**(8): p. 593-6.
161. Deiner, S., B. Westlake, and R.P. Dutton, *Patterns of surgical care and complications in elderly adults*. *J Am Geriatr Soc*, 2014. **62**(5): p. 829-35.
162. Hornor, M.A., M. Ma, L. Zhou, et al., *Enhancing the American College of Surgeons NSQIP Surgical Risk Calculator to Predict Geriatric Outcomes*. *J Am Coll Surg*, 2019.
163. Masters, C.L., R. Bateman, K. Blennow, et al., *Alzheimer's disease*. *Nature Reviews Disease Primers*, 2015. **1**: p. 15056.
164. Bachurin, S.O., E.V. Bovina, and A.A. Ustyugov, *Drugs in Clinical Trials for Alzheimer's Disease: The Major Trends*. *Medicinal Research Reviews*, 2017. **37**(5): p. 1186-1225.
165. Govindpani, K., L.G. McNamara, N.R. Smith, et al., *Vascular Dysfunction in Alzheimer's Disease: A Prelude to the Pathological Process or a Consequence of It?* *Journal of Clinical Medicine*, 2019. **8**(5): p. 651.
166. Counts, S.E., M.D. Ikonomic, N. Mercado, I.E. Vega, and E.J. Mufson, *Biomarkers for the Early Detection and Progression of Alzheimer's Disease*. *Neurotherapeutics*, 2017. **14**(1): p. 35-53.

167. Scheltens, P., K. Blennow, M.M. Breteler, et al., *Alzheimer's disease*. Lancet, 2016. **388**(10043): p. 505-17.
168. de la Torre, J.C., *Is Alzheimer's disease a neurodegenerative or a vascular disorder? Data, dogma, and dialectics*. Lancet Neurol, 2004. **3**(3): p. 184-90.
169. Iturria-Medina, Y., R.C. Sotero, P.J. Toussaint, J.M. Mateos-Perez, and A.C. Evans, *Early role of vascular dysregulation on late-onset Alzheimer's disease based on multifactorial data-driven analysis*. Nat Commun, 2016. **7**: p. 11934.
170. Braak, H., E. Thal Dr Fau - Ghebremedhin, K. Ghebremedhin E Fau - Del Tredici, and K. Del Tredici, *Stages of the pathologic process in Alzheimer disease: age categories from 1 to 100 years*. (1554-6578 (Electronic)).
171. Hardy, J.A. and G.A. Higgins, *Alzheimer's disease: the amyloid cascade hypothesis*. Science, 1992. **256**(5054): p. 184-5.
172. Querfurth, H.W. and F.M. LaFerla, *Alzheimer's disease*. N Engl J Med, 2010. **362**(4): p. 329-44.
173. Mawuenyega, K.G., W. Sigurdson, V. Ovod, et al., *Decreased clearance of CNS beta-amyloid in Alzheimer's disease*. Science, 2010. **330**(6012): p. 1774.
174. Koh, J.Y., L.L. Yang, and C.W. Cotman, *Beta-amyloid protein increases the vulnerability of cultured cortical neurons to excitotoxic damage*. Brain Res, 1990. **533**(2): p. 315-20.
175. Mattson, M.P., B. Cheng, D. Davis, et al., *beta-Amyloid peptides destabilize calcium homeostasis and render human cortical neurons vulnerable to excitotoxicity*. J Neurosci, 1992. **12**(2): p. 376-89.
176. Pike, C.J., A.J. Walencewicz, C.G. Glabe, and C.W. Cotman, *In vitro aging of beta-amyloid protein causes peptide aggregation and neurotoxicity*. Brain Res, 1991. **563**(1-2): p. 311-4.
177. Mattson, M.P., *Antigenic changes similar to those seen in neurofibrillary tangles are elicited by glutamate and Ca²⁺ influx in cultured hippocampal neurons*. Neuron, 1990. **4**(1): p. 105-17.
178. Baudier, J. and R.D. Cole, *Phosphorylation of tau proteins to a state like that in Alzheimer's brain is catalyzed by a calcium/calmodulin-dependent kinase and modulated by phospholipids*. J Biol Chem, 1987. **262**(36): p. 17577-83.
179. Hardy, J. and D. Allsop, *Amyloid deposition as the central event in the aetiology of Alzheimer's disease*. Trends Pharmacol Sci, 1991. **12**(10): p. 383-8.
180. Selkoe, D.J., *The molecular pathology of Alzheimer's disease*. Neuron, 1991. **6**(4): p. 487-98.
181. Wu, L., P. Rosa-Neto, G.Y. Hsiung, et al., *Early-onset familial Alzheimer's disease (EOFAD)*. Can J Neurol Sci, 2012. **39**(4): p. 436-45.
182. Bateman, R.J., L.Y. Munsell, J.C. Morris, et al., *Human amyloid-beta synthesis and clearance rates as measured in cerebrospinal fluid in vivo*. Nat Med, 2006. **12**(7): p. 856-61.
183. Balin, B.J. and A.P. Hudson, *Etiology and pathogenesis of late-onset Alzheimer's disease*. Curr Allergy Asthma Rep, 2014. **14**(3): p. 417.
184. Crous-Bou, M., C. Minguillon, N. Gramunt, and J.L. Molinuevo, *Alzheimer's disease prevention: from risk factors to early intervention*. Alzheimers Res Ther, 2017. **9**(1): p. 71.

185. Shah, N.S., J.S. Vidal, K. Masaki, et al., *Midlife blood pressure, plasma beta-amyloid, and the risk for Alzheimer disease: the Honolulu Asia Aging Study*. *Hypertension*, 2012. **59**(4): p. 780-6.
186. Love, S., *Contribution of cerebral amyloid angiopathy to Alzheimer's disease*. *J Neurol Neurosurg Psychiatry*, 2004. **75**(1): p. 1-4.
187. Arvanitakis, Z., A.W. Capuano, S.E. Leurgans, D.A. Bennett, and J.A. Schneider, *Relation of cerebral vessel disease to Alzheimer's disease dementia and cognitive function in elderly people: a cross-sectional study*. *Lancet Neurol*, 2016. **15**(9): p. 934-943.
188. Ulrich, J.D. and D.M. Holtzman, *TREM2 Function in Alzheimer's Disease and Neurodegeneration*. *ACS Chem Neurosci*, 2016. **7**(4): p. 420-7.
189. Zhao, N., C.C. Liu, W. Qiao, and G. Bu, *Apolipoprotein E, Receptors, and Modulation of Alzheimer's Disease*. *Biol Psychiatry*, 2018. **83**(4): p. 347-357.
190. Zhao, Y., X. Wu, X. Li, et al., *TREM2 Is a Receptor for beta-Amyloid that Mediates Microglial Function*. *Neuron*, 2018. **97**(5): p. 1023-1031.e7.
191. de la Torre, J.C. and T. Mussivan, *Can disturbed brain microcirculation cause Alzheimer's disease?* *Neurological Research*, 1993. **15**(3): p. 146-153.
192. de la Torre, J., *The Vascular Hypothesis of Alzheimer's Disease: A Key to Preclinical Prediction of Dementia Using Neuroimaging*. *J Alzheimers Dis*, 2018. **63**(1): p. 35-52.
193. de la Torre, J.C., *Impaired brain microcirculation may trigger Alzheimer's disease*. *Neurosci Biobehav Rev*, 1994. **18**(3): p. 397-401.
194. Tarasoff-Conway, J.M., R.O. Carare, R.S. Osorio, et al., *Clearance systems in the brain-implications for Alzheimer disease*. *Nat Rev Neurol*, 2015. **11**(8): p. 457-70.
195. Fountain, J.H. and S.L. Lappin, *Physiology, Renin Angiotensin System*, in *StatPearls*. 2019, StatPearls Publishing
StatPearls Publishing LLC.: Treasure Island (FL).
196. Hajjar, I. and K. Rodgers, *Do angiotensin receptor blockers prevent Alzheimer's disease?* *Curr Opin Cardiol*, 2013. **28**(4): p. 417-25.
197. Zhu, D., J. Shi, Y. Zhang, et al., *Central angiotensin II stimulation promotes beta amyloid production in Sprague Dawley rats*. *PLoS One*, 2011. **6**(1): p. e16037.
198. Hardy, J. and D.J. Selkoe, *The amyloid hypothesis of Alzheimer's disease: progress and problems on the road to therapeutics*. *Science*, 2002. **297**(5580): p. 353-6.
199. Benicky, J., E. Sanchez-Lemus, M. Honda, et al., *Angiotensin II AT1 receptor blockade ameliorates brain inflammation*. *Neuropsychopharmacology*, 2011. **36**(4): p. 857-70.
200. Koh, K.K., M.J. Quon, S.H. Han, et al., *Anti-inflammatory and metabolic effects of candesartan in hypertensive patients*. *Int J Cardiol*, 2006. **108**(1): p. 96-100.
201. Gong, X., H. Hu, Y. Qiao, et al., *The Involvement of Renin-Angiotensin System in Lipopolysaccharide-Induced Behavioral Changes, Neuroinflammation, and Disturbed Insulin Signaling*. *Front Pharmacol*, 2019. **10**: p. 318.
202. Trigiani, L.J., J. Royea, M. Lacalle-Aurioles, X.K. Tong, and E. Hamel, *Pleiotropic Benefits of the Angiotensin Receptor Blocker Candesartan in a Mouse Model of Alzheimer Disease*. *Hypertension*, 2018. **72**(5): p. 1217-1226.
203. Bulsara, K.G. and A.N. Makaryus, *Candesartan*, in *StatPearls*. 2019, StatPearls Publishing
StatPearls Publishing LLC.: Treasure Island (FL).

204. Hajjar, I., L. Brown, W.J. Mack, and H. Chui, *Impact of Angiotensin receptor blockers on Alzheimer disease neuropathology in a large brain autopsy series*. Arch Neurol, 2012. **69**(12): p. 1632-8.
205. Wharton, W., F.C. Goldstein, L. Zhao, et al., *Modulation of Renin-Angiotensin System May Slow Conversion from Mild Cognitive Impairment to Alzheimer's Disease*. J Am Geriatr Soc, 2015. **63**(9): p. 1749-56.
206. Cohen, R.M., K. Rezai-Zadeh, T.M. Weitz, et al., *A transgenic Alzheimer rat with plaques, tau pathology, behavioral impairment, oligomeric abeta, and frank neuronal loss*. J Neurosci, 2013. **33**(15): p. 6245-56.
207. Voorhees, J.R., M.T. Remy, C.M. Erickson, et al., *Occupational-like organophosphate exposure disrupts microglia and accelerates deficits in a rat model of Alzheimer's disease*. NPJ Aging Mech Dis, 2019. **5**: p. 3.
208. Hughes, R.N., *The value of spontaneous alternation behavior (SAB) as a test of retention in pharmacological investigations of memory*. Neurosci Biobehav Rev, 2004. **28**(5): p. 497-505.
209. Holcomb, L.A., M.N. Gordon, P. Jantzen, et al., *Behavioral changes in transgenic mice expressing both amyloid precursor protein and presenilin-1 mutations: lack of association with amyloid deposits*. Behav Genet, 1999. **29**(3): p. 177-85.
210. Douglas, R.J., *Spontaneous Alternation Behavior and the Brain*, in *Spontaneous Alternation Behavior*. 1989, Springer: New York, NY.
211. Ennaceur, A. and J. Delacour, *A new one-trial test for neurobiological studies of memory in rats. I: Behavioral data*. Behav Brain Res, 1988. **31**(1): p. 47-59.
212. Hammond, R.S., L.E. Tull, and R.W. Stackman, *On the delay-dependent involvement of the hippocampus in object recognition memory*. Neurobiol Learn Mem, 2004. **82**(1): p. 26-34.
213. Rustay, N.R., E.A. Cronin, P. Curzon, et al., *Mice expressing the Swedish APP mutation on a 129 genetic background demonstrate consistent behavioral deficits and pathological markers of Alzheimer's disease*. Brain Res, 2010. **1311**: p. 136-47.
214. Miedel, C.J., J.M. Patton, A.N. Miedel, E.S. Miedel, and J.M. Levenson, *Assessment of Spontaneous Alternation, Novel Object Recognition and Limb Claspings in Transgenic Mouse Models of Amyloid-beta and Tau Neuropathology*. J Vis Exp, 2017(123).
215. Penley, S.C., C.M. Gaudet, and S.W. Threlkeld, *Use of an eight-arm radial water maze to assess working and reference memory following neonatal brain injury*. J Vis Exp, 2013(82): p. 50940.
216. Bankhead, P., M.B. Loughrey, J.A. Fernandez, et al., *QuPath: Open source software for digital pathology image analysis*. Sci Rep, 2017. **7**(1): p. 16878.
217. Joo, I.L., A.Y. Lai, P. Bazzigaluppi, et al., *Early neurovascular dysfunction in a transgenic rat model of Alzheimer's disease*. Sci Rep, 2017. **7**: p. 46427.
218. Anckaerts, C., I. Blockx, P. Summer, et al., *Early functional connectivity deficits and progressive microstructural alterations in the TgF344-AD rat model of Alzheimer's Disease: A longitudinal MRI study*. Neurobiol Dis, 2019. **124**: p. 93-107.
219. Berkowitz, L.E., R.E. Harvey, E. Drake, S.M. Thompson, and B.J. Clark, *Progressive impairment of directional and spatially precise trajectories by TgF344-Alzheimer's disease rats in the Morris Water Task*. Sci Rep, 2018. **8**(1): p. 16153.

220. Rorabaugh, J.M., T. Chalermphanupap, C.A. Botz-Zapp, et al., *Chemogenetic locus coeruleus activation restores reversal learning in a rat model of Alzheimer's disease*. *Brain*, 2017. **140**(11): p. 3023-3038.
221. Heneka, M.T., M.J. Carson, J. El Khoury, et al., *Neuroinflammation in Alzheimer's disease*. *Lancet Neurol*, 2015. **14**(4): p. 388-405.
222. Torika, N., K. Asraf, R.N. Apte, and S. Fleisher-Berkovich, *Candesartan ameliorates brain inflammation associated with Alzheimer's disease*. *CNS Neurosci Ther*, 2018. **24**(3): p. 231-242.
223. Vehmas, A.K., C.H. Kawas, W.F. Stewart, and J.C. Troncoso, *Immune reactive cells in senile plaques and cognitive decline in Alzheimer's disease*. *Neurobiol Aging*, 2003. **24**(2): p. 321-31.
224. Kamphuis, W., J. Middeldorp, L. Kooijman, et al., *Glial fibrillary acidic protein isoform expression in plaque related astrogliosis in Alzheimer's disease*. *Neurobiol Aging*, 2014. **35**(3): p. 492-510.
225. Nichols, N.R., J.R. Day, N.J. Laping, S.A. Johnson, and C.E. Finch, *GFAP mRNA increases with age in rat and human brain*. *Neurobiol Aging*, 1993. **14**(5): p. 421-9.
226. Monk, T.G., B.C. Weldon, C.W. Garvan, et al., *Predictors of cognitive dysfunction after major noncardiac surgery*. *Anesthesiology*, 2008. **108**(1): p. 18-30.
227. Kazmierski, J., A. Banys, J. Latek, et al., *Mild cognitive impairment with associated inflammatory and cortisol alterations as independent risk factor for postoperative delirium*. *Dement Geriatr Cogn Disord*, 2014. **38**(1-2): p. 65-78.
228. Feinkohl, I., G. Winterer, and T. Pischon, *Diabetes is associated with risk of postoperative cognitive dysfunction: A meta-analysis*. *Diabetes Metab Res Rev*, 2017. **33**(5).
229. Radtke, F.M., M. Franck, L. Hagemann, et al., *Risk factors for inadequate emergence after anesthesia: emergence delirium and hypoactive emergence*. *Minerva anesthesiologica*, 2010. **76**(6): p. 394-403.
230. Ogawa, M., K.P. Izawa, S. Satomi-Kobayashi, et al., *Preoperative exercise capacity is associated with the prevalence of postoperative delirium in elective cardiac surgery*. *Aging Clin Exp Res*, 2018. **30**(1): p. 27-34.
231. Hebert, L.E., J. Weuve, P.A. Scherr, and D.A. Evans, *Alzheimer disease in the United States (2010-2050) estimated using the 2010 census*. *Neurology*, 2013. **80**(19): p. 1778-83.
232. Hirtz, D., D.J. Thurman, K. Gwinn-Hardy, et al., *How common are the "common" neurologic disorders?* *Neurology*, 2007. **68**(5): p. 326-37.
233. Prince, M., R. Bryce, E. Albanese, et al., *The global prevalence of dementia: a systematic review and metaanalysis*. *Alzheimers Dement*, 2013. **9**(1): p. 63-75.e2.
234. Silbert, B., L. Evered, D.A. Scott, and P. Maruff, *Anesthesiology must play a greater role in patients with Alzheimer's disease*. *Anesth Analg*, 2011. **112**(5): p. 1242-5.
235. Arora, S.S., J.L. Gooch, and P.S. Garcia, *Postoperative cognitive dysfunction, Alzheimer's disease, and anesthesia*. *Int J Neurosci*, 2014. **124**(4): p. 236-42.
236. Chen, C.W., C.C. Lin, K.B. Chen, et al., *Increased risk of dementia in people with previous exposure to general anesthesia: a nationwide population-based case-control study*. *Alzheimers Dement*, 2014. **10**(2): p. 196-204.
237. Chen, P.L., C.W. Yang, Y.K. Tseng, et al., *Risk of dementia after anaesthesia and surgery*. *Br J Psychiatry*, 2014. **204**(3): p. 188-93.

238. Wacker, P., P.V. Nunes, H. Cabrita, and O.V. Forlenza, *Post-operative delirium is associated with poor cognitive outcome and dementia*. *Dement Geriatr Cogn Disord*, 2006. **21**(4): p. 221-7.
239. Bilotta, F., A. Doronzio, E. Stazi, et al., *Postoperative cognitive dysfunction: toward the Alzheimer's disease pathomechanism hypothesis*. *J Alzheimers Dis*, 2010. **22 Suppl 3**: p. 81-9.
240. Chemali, J.J., J.D. Kenny, O. Olutola, et al., *Ageing delays emergence from general anaesthesia in rats by increasing anaesthetic sensitivity in the brain*. *Br J Anaesth*, 2015. **115 Suppl 1**: p. i58-i65.
241. Purdon, P.L., K.J. Pavone, O. Akeju, et al., *The Ageing Brain: Age-dependent changes in the electroencephalogram during propofol and sevoflurane general anaesthesia*. *Br J Anaesth*, 2015. **115 Suppl 1**: p. i46-i57.
242. Akhtar, S. and R. Ramani, *Geriatric Pharmacology*. *Anesthesiol Clin*, 2015. **33**(3): p. 457-69.
243. Soehle, M., A. Dittmann, R.K. Ellerkmann, et al., *Intraoperative burst suppression is associated with postoperative delirium following cardiac surgery: a prospective, observational study*. *BMC Anesthesiol*, 2015. **15**: p. 61.
244. Momeni, M., S. Meyer, M.A. Docquier, et al., *Predicting postoperative delirium and postoperative cognitive decline with combined intraoperative electroencephalogram monitoring and cerebral near-infrared spectroscopy in patients undergoing cardiac interventions*. *J Clin Monit Comput*, 2019.
245. Bianchi, S.L., B.M. Caltagaron, F.M. Laferla, R.G. Eckenhoff, and M.B. Kelz, *Inhaled anesthetic potency in aged Alzheimer mice*. *Anesth Analg*, 2010. **110**(2): p. 427-30.
246. Lim, M.M., J.R. Gerstner, and D.M. Holtzman, *The sleep-wake cycle and Alzheimer's disease: what do we know?* *Neurodegener Dis Manag*, 2014. **4**(5): p. 351-62.
247. Wang, J., Y. Fang, X. Wang, et al., *Enhanced Gamma Activity and Cross-Frequency Interaction of Resting-State Electroencephalographic Oscillations in Patients with Alzheimer's Disease*. *Front Aging Neurosci*, 2017. **9**: p. 243.
248. Basar, E., B. Femir, D.D. Emek-Savas, B. Guntekin, and G.G. Yener, *Increased long distance event-related gamma band connectivity in Alzheimer's disease*. *Neuroimage Clin*, 2017. **14**: p. 580-590.
249. Garcia-Rill, E., S. Mahaffey, J.R. Hyde, and F.J. Urbano, *Bottom-up gamma maintenance in various disorders*. *Neurobiol Dis*, 2019. **128**.
250. Eckenhoff, R.G., J.S. Johansson, H. Wei, et al., *Inhaled anesthetic enhancement of amyloid-beta oligomerization and cytotoxicity*. *Anesthesiology*, 2004. **101**(3): p. 703-9.
251. Xie, Z., Y. Dong, U. Maeda, et al., *The common inhalation anesthetic isoflurane induces apoptosis and increases amyloid beta protein levels*. *Anesthesiology*, 2006. **104**(5): p. 988-94.
252. Dong, Y., G. Zhang, B. Zhang, et al., *The common inhalational anesthetic sevoflurane induces apoptosis and increases beta-amyloid protein levels*. *Arch Neurol*, 2009. **66**(5): p. 620-31.
253. Lu, Y., X. Wu, Y. Dong, et al., *Anesthetic sevoflurane causes neurotoxicity differently in neonatal naive and Alzheimer disease transgenic mice*. *Anesthesiology*, 2010. **112**(6): p. 1404-16.

254. Tian, Y., K.Y. Chen, L.D. Liu, et al., *Sevoflurane Exacerbates Cognitive Impairment Induced by Abeta 1-40 in Rats through Initiating Neurotoxicity, Neuroinflammation, and Neuronal Apoptosis in Rat Hippocampus*. *Mediators Inflamm*, 2018. **2018**: p. 3802324.
255. Liao, W.T., X.Y. Xiao, Y. Zhu, and S.P. Zhou, *The effect of celastrol on learning and memory in diabetic rats after sevoflurane inhalation*. *Arch Med Sci*, 2018. **14**(2): p. 370-380.
256. Kang, F., C. Tang, M. Han, et al., *Effects of Dexmedetomidine-Isoflurane versus Isoflurane Anesthesia on Brain Injury After Cardiac Valve Replacement Surgery*. *J Cardiothorac Vasc Anesth*, 2018. **32**(4): p. 1581-1586.
257. Aust, J.B., W. Henderson, S. Khuri, and C.P. Page, *The impact of operative complexity on patient risk factors*. *Ann Surg*, 2005. **241**(6): p. 1024-7; discussion 1027-8.
258. Story, D.A., *Postoperative mortality and complications*. *Best Pract Res Clin Anaesthesiol*, 2011. **25**(3): p. 319-27.
259. Sarwar, N., P. Gao, S.R. Seshasai, et al., *Diabetes mellitus, fasting blood glucose concentration, and risk of vascular disease: a collaborative meta-analysis of 102 prospective studies*. *Lancet*, 2010. **375**(9733): p. 2215-22.
260. Selvin, E., C.M. Parrinello, D.B. Sacks, and J. Coresh, *Trends in prevalence and control of diabetes in the United States, 1988-1994 and 1999-2010*. *Ann Intern Med*, 2014. **160**(8): p. 517-25.
261. Gaspar, J.M., F.I. Baptista, M.P. Macedo, and A.F. Ambrosio, *Inside the Diabetic Brain: Role of Different Players Involved in Cognitive Decline*. *ACS Chem Neurosci*, 2016. **7**(2): p. 131-42.
262. Luchsinger, J.A., *Type 2 diabetes and cognitive impairment: linking mechanisms*. *J Alzheimers Dis*, 2012. **30 Suppl 2**: p. S185-98.
263. Thourani, V.H., W.S. Weintraub, B. Stein, et al., *Influence of diabetes mellitus on early and late outcome after coronary artery bypass grafting*. *Ann Thorac Surg*, 1999. **67**(4): p. 1045-52.
264. Notzold, A., K. Michel, A.A. Khattab, H.H. Sievers, and M. Huppe, *Diabetes mellitus increases adverse neurocognitive outcome after coronary artery bypass grafting surgery*. *Thorac Cardiovasc Surg*, 2006. **54**(5): p. 307-12.
265. Wang, C.G., Y.F. Qin, X. Wan, et al., *Incidence and risk factors of postoperative delirium in the elderly patients with hip fracture*. *J Orthop Surg Res*, 2018. **13**(1): p. 186.
266. Mason, S.E., A. Noel-Storr, and C.W. Ritchie, *The impact of general and regional anesthesia on the incidence of post-operative cognitive dysfunction and post-operative delirium: a systematic review with meta-analysis*. *J Alzheimers Dis*, 2010. **22 Suppl 3**: p. 67-79.
267. Kong, F., S. Chen, Y. Cheng, et al., *Minocycline attenuates cognitive impairment induced by isoflurane anesthesia in aged rats*. *PLoS One*, 2013. **8**(4): p. e61385.
268. Yang, C., B. Zhu, J. Ding, and Z.G. Wang, *Isoflurane anesthesia aggravates cognitive impairment in streptozotocin-induced diabetic rats*. *Int J Clin Exp Med*, 2014. **7**(4): p. 903-10.
269. Feng, X., Y. Uchida, L. Koch, et al., *Exercise Prevents Enhanced Postoperative Neuroinflammation and Cognitive Decline and Rectifies the Gut Microbiome in a Rat Model of Metabolic Syndrome*. *Front Immunol*, 2017. **8**: p. 1768.
270. Dall, T.M., S.E. Mann, Y. Zhang, et al., *Distinguishing the economic costs associated with type 1 and type 2 diabetes*. *Popul Health Manag*, 2009. **12**(2): p. 103-10.

271. Anthony, M. and F. Lin, *A Systematic Review for Functional Neuroimaging Studies of Cognitive Reserve Across the Cognitive Aging Spectrum*. Arch Clin Neuropsychol, 2018. **33**(8): p. 937-948.
272. Berger, M., J.W. Nadler, J. Browndyke, et al., *Postoperative Cognitive Dysfunction: Minding the Gaps in Our Knowledge of a Common Postoperative Complication in the Elderly*. Anesthesiol Clin, 2015. **33**(3): p. 517-50.
273. Cheng, S.T., *Cognitive Reserve and the Prevention of Dementia: the Role of Physical and Cognitive Activities*. Curr Psychiatry Rep, 2016. **18**(9): p. 85.
274. Hamer, M. and Y. Chida, *Physical activity and risk of neurodegenerative disease: a systematic review of prospective evidence*. Psychol Med, 2009. **39**(1): p. 3-11.
275. Boraxbekk, C.J., A. Salami, A. Wahlin, and L. Nyberg, *Physical activity over a decade modifies age-related decline in perfusion, gray matter volume, and functional connectivity of the posterior default-mode network-A multimodal approach*. Neuroimage, 2016. **131**: p. 133-41.
276. Thomas, D.E., E.J. Elliott, and G.A. Naughton, *Exercise for type 2 diabetes mellitus*. Cochrane Database Syst Rev, 2006(3): p. Cd002968.
277. Alkadhi, K.A., *Exercise as a Positive Modulator of Brain Function*. Mol Neurobiol, 2018. **55**(4): p. 3112-3130.
278. Goto, Y., M. Kakizaki, and N. Masaki, *Spontaneous Diabetes Produced by Selective Breeding of Normal Wistar Rats*. Proceedings of the Japan Academy, 1975. **51**(1): p. 80-85.
279. Goto, Y. and M. Kakizaki, *The Spontaneous-Diabetes Rat: A Model of Noninsulin Dependent Diabetes Mellitus*. Proceedings of the Japan Academy, Series B, 1981. **57**(10): p. 381-384.
280. Sena, C.M., C. Barosa, E. Nunes, R. Seica, and J.G. Jones, *Sources of endogenous glucose production in the Goto-Kakizaki diabetic rat*. Diabetes Metab, 2007. **33**(4): p. 296-302.
281. Allen, R.S., A.M. Hanif, M.A. Gogniat, et al., *TrkB signalling pathway mediates the protective effects of exercise in the diabetic rat retina*. Eur J Neurosci, 2018. **47**(10): p. 1254-1265.
282. Keith, D. and A. El-Husseini, *Excitation Control: Balancing PSD-95 Function at the Synapse*. Front Mol Neurosci, 2008. **1**: p. 4.
283. Allen, R.S., A. Feola, C.T. Motz, et al., *Retinal Deficits Precede Cognitive and Motor Deficits in a Rat Model of Type II Diabetes*. Invest Ophthalmol Vis Sci, 2019. **60**(1): p. 123-133.
284. Misal, U.S., S.A. Joshi, and M.M. Shaikh, *Delayed recovery from anesthesia: A postgraduate educational review*. Anesth Essays Res, 2016. **10**(2): p. 164-72.
285. Guenther, U., L. Riedel, and F.M. Radtke, *Patients prone for postoperative delirium: preoperative assessment, perioperative prophylaxis, postoperative treatment*. Curr Opin Anaesthesiol, 2016. **29**(3): p. 384-90.
286. Gourgouvelis, J., P. Yielder, S.T. Clarke, H. Behbahani, and B. Murphy, *You can't fix what isn't broken: eight weeks of exercise do not substantially change cognitive function and biochemical markers in young and healthy adults*. PeerJ, 2018. **6**: p. e4675.
287. Sengupta, P., *The Laboratory Rat: Relating Its Age With Human's*. Int J Prev Med, 2013. **4**(6): p. 624-30.

288. Krenk, L., L.S. Rasmussen, and H. Kehlet, *Delirium in the fast-track surgery setting*. Best Pract Res Clin Anaesthesiol, 2012. **26**(3): p. 345-53.
289. Krenk, L., H. Kehlet, T. Baek Hansen, et al., *Cognitive dysfunction after fast-track hip and knee replacement*. Anesth Analg, 2014. **118**(5): p. 1034-40.
290. Yoshii, A. and M. Constantine-Paton, *Postsynaptic localization of PSD-95 is regulated by all three pathways downstream of TrkB signaling*. Front Synaptic Neurosci, 2014. **6**: p. 6.
291. Shih, P.C., Y.R. Yang, and R.Y. Wang, *Effects of exercise intensity on spatial memory performance and hippocampal synaptic plasticity in transient brain ischemic rats*. PLoS One, 2013. **8**(10): p. e78163.
292. Lee, C.C., C.C. Huang, M.Y. Wu, and K.S. Hsu, *Insulin stimulates postsynaptic density-95 protein translation via the phosphoinositide 3-kinase-Akt-mammalian target of rapamycin signaling pathway*. J Biol Chem, 2005. **280**(18): p. 18543-50.
293. Jack, C.R., Jr., D.S. Knopman, W.J. Jagust, et al., *Tracking pathophysiological processes in Alzheimer's disease: an updated hypothetical model of dynamic biomarkers*. Lancet Neurol, 2013. **12**(2): p. 207-16.
294. T, B.V.a.F., *A Master Key to Assess Stroke Consequences Across Species: The Adhesive Removal Test*, in *Advances in the Preclinical Study of Ischemic Stroke*, M. Balestrino, Editor. 2012, IntechOpen: IntechOpen.
295. Vallar, G. and D. Perani, *The anatomy of unilateral neglect after right-hemisphere stroke lesions. A clinical/CT-scan correlation study in man*. Neuropsychologia, 1986. **24**(5): p. 609-22.
296. Hillis, A.E., M. Newhart, J. Heidler, et al., *Anatomy of spatial attention: insights from perfusion imaging and hemispatial neglect in acute stroke*. J Neurosci, 2005. **25**(12): p. 3161-7.
297. Husain, M. and C. Kennard, *Visual neglect associated with frontal lobe infarction*. J Neurol, 1996. **243**(9): p. 652-7.
298. Hurford, P., A.Y. Stringer, and B. Jann, *Neuropharmacologic treatment of hemineglect: a case report comparing bromocriptine and methylphenidate*. Arch Phys Med Rehabil, 1998. **79**(3): p. 346-9.
299. Malhotra, P.A., A.D. Parton, R. Greenwood, and M. Husain, *Noradrenergic modulation of space exploration in visual neglect*. Ann Neurol, 2006. **59**(1): p. 186-90.
300. Friedman, E.B., Y. Sun, J.T. Moore, et al., *A conserved behavioral state barrier impedes transitions between anesthetic-induced unconsciousness and wakefulness: evidence for neural inertia*. PLoS One, 2010. **5**(7): p. e11903.
301. Joiner, W.J., E.B. Friedman, H.T. Hung, et al., *Genetic and anatomical basis of the barrier separating wakefulness and anesthetic-induced unresponsiveness*. PLoS Genet, 2013. **9**(9): p. e1003605.
302. Voss, L.J., M. Brock, C. Carlsson, et al., *Investigating paradoxical hysteresis effects in the mouse neocortical slice model*. Eur J Pharmacol, 2012. **675**(1-3): p. 26-31.
303. Warnaby, C.E., J.W. Sleight, D. Hight, S. Jbabdi, and I. Tracey, *Investigation of Slow-wave Activity Saturation during Surgical Anesthesia Reveals a Signature of Neural Inertia in Humans*. Anesthesiology, 2017. **127**(4): p. 645-657.
304. Jeong, J., *EEG dynamics in patients with Alzheimer's disease*. Clinical neurophysiology, 2004. **115**(7): p. 1490-1505.

305. Rudnicka, A.R., C.M. Nightingale, A.S. Donin, et al., *Sleep Duration and Risk of Type 2 Diabetes*. Pediatrics, 2017. **140**(3).
306. Zhang, J., Y. Zhu, G. Zhan, et al., *Extended wakefulness: compromised metabolics in and degeneration of locus ceruleus neurons*. J Neurosci, 2014. **34**(12): p. 4418-31.
307. Broussard, J. and M.J. Brady, *The impact of sleep disturbances on adipocyte function and lipid metabolism*. Best Pract Res Clin Endocrinol Metab, 2010. **24**(5): p. 763-73.
308. Gotoh, M., C. Li, M. Yatoh, et al., *Hypothalamic monoamine metabolism is different between the diabetic GK (Goto-Kakizaki) rats and streptozotocin-induced diabetic rats*. Brain Res, 2006. **1073-1074**: p. 497-501.
309. Petrisic, M.S., S.J. Augood, and R.J. Bicknell, *Monoamine transporter gene expression in the central nervous system in diabetes mellitus*. J Neurochem, 1997. **68**(6): p. 2435-41.
310. Chen, X., C.D. Nelson, X. Li, et al., *PSD-95 is required to sustain the molecular organization of the postsynaptic density*. J Neurosci, 2011. **31**(17): p. 6329-38.
311. Zhang, C., Y. Zhang, Y. Shen, et al., *Anesthesia/Surgery Induces Cognitive Impairment in Female Alzheimer's Disease Transgenic Mice*. J Alzheimers Dis, 2017. **57**(2): p. 505-518.
312. Ling, Y.Z., W. Ma, L. Yu, Y. Zhang, and Q.S. Liang, *Decreased PSD95 expression in medial prefrontal cortex (mPFC) was associated with cognitive impairment induced by sevoflurane anesthesia*. J Zhejiang Univ Sci B, 2015. **16**(9): p. 763-71.
313. Li, X., X. Run, Z. Wei, et al., *Intranasal Insulin Prevents Anesthesia-induced Cognitive Impairments in Aged Mice*. Curr Alzheimer Res, 2019. **16**(1): p. 8-18.
314. Tao, Y.X. and R.A. Johns, *Effect of the deficiency of spinal PSD-95/SAP90 on the minimum alveolar anesthetic concentration of isoflurane in rats*. Anesthesiology, 2001. **94**(6): p. 1010-5.
315. Li, C., M. Schaefer, C. Gray, et al., *Sensitivity to isoflurane anesthesia increases in autism spectrum disorder Shank3(+/-) mutant mouse model*. Neurotoxicol Teratol, 2017. **60**: p. 69-74.
316. Tao, F. and R.A. Johns, *Effect of disrupting N-methyl-D-aspartate receptor-postsynaptic density protein-95 interactions on the threshold for halothane anesthesia in mice*. Anesthesiology, 2008. **108**(5): p. 882-7.
317. Hu, D., R.P. Flick, M.J. Zaccariello, et al., *Association between Exposure of Young Children to Procedures Requiring General Anesthesia and Learning and Behavioral Outcomes in a Population-based Birth Cohort*. Anesthesiology, 2017. **127**(2): p. 227-240.
318. Tsai, C.J., C.T. Lee, S.H. Liang, et al., *Risk of ADHD After Multiple Exposures to General Anesthesia: A Nationwide Retrospective Cohort Study*. J Atten Disord, 2018. **22**(3): p. 229-239.
319. Oh, J., J.E. Shin, K.H. Yang, et al., *Cortical and subcortical changes in resting-state functional connectivity before and during an episode of postoperative delirium*. Aust N Z J Psychiatry, 2019: p. 4867419848826.
320. Fleischmann, R., S. Traenkner, A. Kraft, et al., *Delirium is associated with frequency band specific dysconnectivity in intrinsic connectivity networks: preliminary evidence from a large retrospective pilot case-control study*. Pilot Feasibility Stud, 2019. **5**: p. 2.
321. Gerrits, B., M.A. Vollebregt, S. Olbrich, et al., *Probing the "Default Network Interference Hypothesis" With EEG: An RDoC Approach Focused on Attention*. Clin EEG Neurosci, 2019: p. 1550059419864461.

322. Chen, S.C. and D.K. Rex, *An initial investigation of bispectral monitoring as an adjunct to nurse-administered propofol sedation for colonoscopy*. Am J Gastroenterol, 2004. **99**(6): p. 1081-6.
323. Drake, L.M., S.C. Chen, and D.K. Rex, *Efficacy of bispectral monitoring as an adjunct to nurse-administered propofol sedation for colonoscopy: a randomized controlled trial*. Am J Gastroenterol, 2006. **101**(9): p. 2003-7.
324. Wada, J. and T. Rasmussen, *Intracarotid injection of sodium amytal for the lateralization of cerebral speech dominance*. 1960. J Neurosurg, 2007. **106**(6): p. 1117-33.
325. Abeles, A., R.M. Kwasnicki, C. Pettengell, J. Murphy, and A. Darzi, *The relationship between physical activity and post-operative length of hospital stay: A systematic review*. Int J Surg, 2017. **44**: p. 295-302.
326. Castren, E. and T. Rantamaki, *The role of BDNF and its receptors in depression and antidepressant drug action: Reactivation of developmental plasticity*. Dev Neurobiol, 2010. **70**(5): p. 289-97.
327. Wyrobek, J., A. LaFlam, L. Max, et al., *Association of intraoperative changes in brain-derived neurotrophic factor and postoperative delirium in older adults*. Br J Anaesth, 2017. **119**(2): p. 324-332.
328. Cheng, X.Q., B. Mei, Y.M. Zuo, et al., *A multicentre randomised controlled trial of the effect of intra-operative dexmedetomidine on cognitive decline after surgery*. Anaesthesia, 2019. **74**(6): p. 741-750.
329. Hiramoto, R., N. Kanayama, T. Nakao, et al., *BDNF as a possible modulator of EEG oscillatory response at the parietal cortex during visuo-tactile integration processes using a rubber hand*. Neurosci Res, 2017. **124**: p. 16-24.
330. Nigam, S.M., S. Xu, J.S. Kritikou, et al., *Exercise and BDNF reduce Abeta production by enhancing alpha-secretase processing of APP*. J Neurochem, 2017. **142**(2): p. 286-296.
331. Binder, D.K. and H.E. Scharfman, *Brain-derived neurotrophic factor*. Growth Factors, 2004. **22**(3): p. 123-31.
332. Min, K.P. and G.W. Kim, *Photo-Rheological Fluid-Based Colorimetric Ultraviolet Light Intensity Sensor*. Sensors (Basel), 2019. **19**(5).
333. Ruifrok, A.C. and D.A. Johnston, *Quantification of histochemical staining by color deconvolution*. Anal Quant Cytol Histol, 2001. **23**(4): p. 291-9.
334. Paxinos, G.a.W., Charles, *The Rat Brain in Stereotaxic Coordinates*. 6th Edition ed. 2007: Academic Press.
335. Bruhn, J., *Burst suppression ratio is the only determinant for BIS values below 30*. Can J Anaesth, 2002. **49**(7): p. 755-6; author reply 756.
336. Al-Qazzaz, N.K., S.H. Bin Mohd Ali, S.A. Ahmad, M.S. Islam, and J. Escudero, *Selection of Mother Wavelet Functions for Multi-Channel EEG Signal Analysis during a Working Memory Task*. Sensors (Basel), 2015. **15**(11): p. 29015-35.
337. Akkar HA, J.F., *Optimal Mother Wavelet Function for EEG Signal Analyze Based on Packet Wavelet Transform*. International Journal of Scientific & Engineering Research, 2017. **8**(2): p. 1222-1227.